University of Central Florida

STARS

Electronic Theses and Dissertations

2019

Biogeochemical Effects of Sea Level Rise-induced Transitions Within Coastal Wetlands

Havalend Steinmuller
University of Central Florida

BIOGEOCHEMICAL EFFECTS OF SEA LEVEL RISE-INDUCED TRANSITIONS IN
COASTAL WETLANDS

by

HAVALEND ELLEN STEINMULLER
B.S. Louisiana State University, 2013
M.S. Louisiana State University, 2015

A dissertation submitted in partial fulfillment of the requirements
for the degree of Doctor of Philosophy
in the Department of Biology
in the College of Sciences
at the University of Central Florida
Orlando, Florida

Spring Term
2019

Major Professor: Lisa G. Chambers

ABSTRACT

As sea level rise (SLR) affects coastal wetlands, ecosystem responses can include vertical accretion, landward transgression, or submergence. Sea level rise-induced transitions can alter key biogeochemical transformations within wetland soils, impacting the ability of these systems to provide ecosystem services, specifically carbon (C) storage and water quality regulation. Through a series of complementary laboratory and field-based studies, biogeochemical responses to salinity, vegetation shifts, and submergence were investigated. Changes in nutrient dynamics associated with saltwater intrusion were evaluated by artificially adding saline water to different freshwater wetland soil types, indicating that potential exports of critical nutrients (forms of nitrogen, phosphorus, and C) out of freshwater wetland soils is mediated by soil type. A controlled laboratory experiment was conducted to determine the potential degradability of C stored within submerging coastal wetland soils under both aerobic and anaerobic conditions. Under aerobic conditions, 66% more carbon dioxide was produced than under anaerobic conditions and 4x greater carbon dioxide was produced at 90-100cm depths than at the surface. At the same site, the degradability of carbon stores was examined through organic matter fractionation, stable isotopic examination, and determining the abundance of key microbial genes. Both total soil C and stores of bioavailable nutrients increased with depth, while organic matter quality decreased. Finally, the biogeochemical impacts of two separate vegetation transitions occurring co-incidentally with sea level rise were investigated: mangrove encroachment into salt marsh, and more salt- and inundation-tolerant herbaceous encroachment into herbaceous marsh. Conclusions from these studies demonstrate that vegetation transitions alter both soil nutrient storage and fast-cycling nutrient pools, indicating that biogeochemical transitions occur in advance of changes in vegetative species dominance. Results from these chapters holistically address how biogeochemical functioning, specifically nutrient cycling,

regulation of water quality, and C sequestration, within coastal wetlands responds to stressors associated with SLR.

room) to thank you for everything throughout these last four years. You have inspired me,

believed in me, encouraged me, and supported me every day, and I could never have completed

this without you.

TABLE OF CONTENTS

CHAPTER FIVE: TIPPING POINTS IN THE MANGROVE MARCH:

CHARACTERIZATION OF BIOGEOCHEMICAL CYCLING ALONG THE MANGROVE-

LIST OF FIGURES

LIST OF TABLES

CHAPTER ONE: INTRODUCTION

Wetland systems occupy the interface between terrestrial and aquatic systems and cover less than 8% of the earth's land area. Despite this small land area, wetlands are hotspots for primary productivity, biogeochemical cycling, carbon storage, and other ecosystem services (Barbier, 2011). Specifically, coastal wetlands rank among the most productive ecosystem types globally, and sequester 20-30% of the world's soil carbon (Amthor and Huston, 1998; Lal, 2007). These unique coastal systems are also home to a diverse assortment of biota, act as a buffer during storm events, and regulate hydrologic storage and flux (Barbier, 2011). While wetlands in general are threatened by drainage and increased development, coastal wetlands in particular also experience additional threats area from the coastal zone, namely through sea level rise.

Global sea level rise is currently estimated to be 3.0 ± 0.4 mm yr^{-1}, a result of melting of land ice, thermal expansion of oceans, and altered precipitation regimes (IPCC, 2014). Coastal wetlands are uniquely vulnerable to experiencing the effects of sea level rise through both their position within the coastal plain and their relatively low elevation. As a result, an estimated 22% of coastal wetlands are expected to be lost by 2100 through submergence from rising sea levels (Nicholls et al., 1999). Coastal wetlands can respond to sea level rise in one of three ways, each of which is dependent on a suite of factors, including rate of sea level rise, elevation, primary production, and extent of urban development (Kirwin and Megonigal, 2013). Wetlands that respond through vertical accretion, or "keeping pace" with sea level rise, are able to accrete both sediment and organic matter at such a rate that the elevation of the wetland platform stays within an optimal zone for marsh survival (Reed, 1990). This response usually occurs in wetlands experiencing a gradual change in sea level, coupled with a large tidal range and a high sediment

1

supply. Another type of wetland response to sea level rise is landward transgression, where wetland area gradually shifts further upland. Vegetation communities shift landward to continue to occupy their optimal niche in terms of elevation, inundation and salinity, provided there is a lack of adjacent upland development and area for the wetland to transgress (Bertness 1991; Donnelly and Bertness 2001; Morris and others 2002). High rates of sea level rise, low sediment supply, and a small tidal range catalyze the third response to sea level rise: wetland submergence, or the complete conversion of wetland habitat to open water (Baumann et al., 1984). As sea level rise continues to threaten coastal wetlands, understanding both the biogeochemical and ecosystem-level effects of these responses is critical in determining the fate of these systems, as well as predicting how the vital ecosystem services provided by these wetlands will continue to function.

The overall objective of this dissertation was, through both field-based and experimental studies, to further examine wetland submergence and transgression in response to sea level rise, specifically in an effort to understand the impacts to biogeochemical cycling (Figure 1). In order to satisfy this objective, this dissertation is divided into five research chapters, each one investigating some aspect of the biogeochemical response to sea level rise-induced wetland transitions, focusing on landward transgression and wetland submergence. The objective of the first research chapter (Chapter 2) was to experimentally determine and quantify how increasing salinity impacts the nutrient dynamics of macronutrients within different freshwater wetland types. Also utilizing an experimental approach, the goal of the second research chapter (Chapter 3) was to understand the fate of soil organic matter following coastal wetland submergence by examining potential mineralization rates of soils subjected to two separate treatments, one mimicking an intact marsh while the other mimicked submergence. Chapter 4 also focused on

wetland submergence and was aimed at understanding the degradability of sequestered carbon to sea level rise-induced mineralization by analyzing the abundance of various microbial genes, degree of decomposition, and concentrations of organic matter fractions at depth. The objectives of Chapters 5 and 6 were to characterize biogeochemical changes across a transition in both abiotic factors and vegetation communities, therefore determining how these changes alter ecosystem services. Chapter 5 focuses on the transition between mangroves and salt marsh grasses (woody-herbaceous transition) while Chapter 6 focuses on an herbaceous-herbaceous transition zone. As a whole, these dissertation chapters close critical knowledge gaps concerning the biogeochemical and ecosystem-level changes associated with sea level rise in coastal wetlands, which is summarized within Chapter 7.
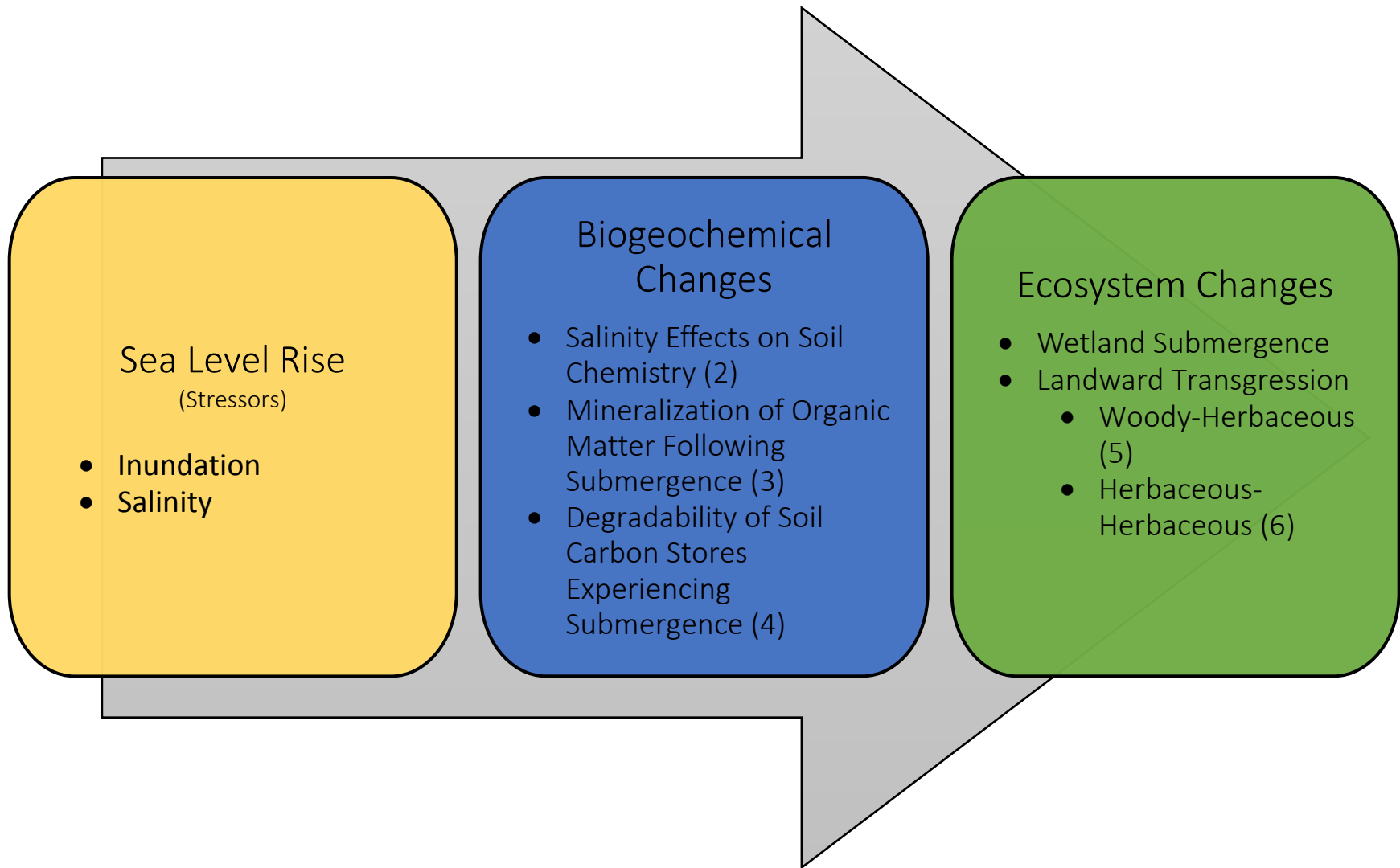
Figure 1: Conceptual model of dissertation outline, beginning as sea level rise stressors that progress into biogeochemical changes, and culminate in ecosystem change. Numbers in parenthesis correspond to dissertation chapter numbers.

CHAPTER TWO: CAN SALTWATER INTRUSION ACCELERATE NUTRIENT EXPORT FROM FRESHWATER WETLAND SOILS? AN EXPERIMENTAL APPROACH

Abstract

Coastal wetlands are vulnerable to saltwater intrusion, which may alter soil biogeochemical processes, lead to the export of nutrients into the coastal zone, and contribute to eutrophication. Using intact soil cores from three different freshwater wetlands and subjecting them to control (0), 5, or 15 parts per thousand (ppt) seawater treatments, we investigated how different wetland soils (bayhead swamp, cypress dome, and mineral marsh) and salinities alter the export of soil nutrients (soluble reactive phosphorus, SRP; ammonium, NH_4^+; and dissolved organic carbon, DOC), as well as microbial biomass C and greenhouse gas emissions. The highest salinity treatment increased carbon dioxide production by 30% with no change in methane production. Porewater NH_4^+ concentrations averaged 8x higher than the control in the 15 ppt treatment, and 5x greater than the control in the 5 ppt treatment, with a ~1 week lag period between porewater accumulation of NH_4^+ and export into the surrounding water; the magnitude of NH_4^+ export was mediated by wetland soil type. SRP concentrations averaged 8x higher and 3.5x higher in the cypress dome and bayhead swamp 15 ppt treatments, respectively, than in their controls, though no effect was observed within the mineral marsh. Dissolved organic C concentrations differed by wetland soil type but were unaffected by salinity treatment. This study demonstrates that saltwater intrusion could catalyze a rapid export of nutrients from freshwater wetland soils into the coastal zone, though nutrient export varies by wetland soil type.

Introduction

Global sea level is rising at a rate of 3.2 ± 0.4 mm yr^{-1} and is estimated to result in a roughly 1-meter increase by 2100 (Church et al. 2015, IPCC, 201), which has implications for the salinization of coastal and inland landscapes. Specifically, the low-lying coastal plain is particularly vulnerable to this amplified rate of sea level rise, including tidal freshwater coastal wetlands that occupy the terrestrial interface between the coastal ocean and upland areas, and developed under conditions of low salinity and minimal tidal inundation. As one of the most productive ecosystem types on the planet, coastal wetlands provide critical habitat for wetland biota, regulate water quality, sequester carbon, and act as a buffer during storm events (Barbier et al. 2011). Sea level rise is estimated to result in the loss of 20-30% of the global extent of coastal wetlands and their critical services by 2100 (Nicholls et al., 1999). In response to sea level rise, coastal wetlands may transgress landward: brackish marshes become more saline and inundated, and saltwater intrudes into tidal freshwater wetlands (Neubauer and Craft, 2009). Saltwater intrusion can have effects on all components of the wetland, including shifting vegetation communities, loss of habitats, changes in the microbial consortia, and disruptions to biogeochemical cycles (Herbert et al., 2015).

Sea level rise has sparked a variety of research addressing the effects of saltwater intrusion on the cycling of carbon (C), nitrogen (N), and phosphorus (P) in coastal wetlands. Many of these studies have been controlled laboratory experiments that subjected soils from either tidally-influenced freshwater or brackish wetlands to increases in inundation and/or seawater (i.e., Chambers et al. 2011, 2013, 2014; Weston et al. 2006, 2011; Jun et al. 2013; Marton et al. 2012; van Dijk et al. 2015). It is important to note the difference between increases in salinity (i.e. salts, such as NaCl) and saltwater intrusion, which contains sulfate, a terminal electron acceptor.

6

For ease of understanding, 'salinity' will henceforth refer to the influx of seawater containing sulfate. Previous short-term experiments suggest that subjecting soils to seawater can affect both abiotic and biotic drivers of biogeochemical cycling within freshwater wetlands. Abiotic effects result from the influx of high concentrations of ions brought into the system by saline water: Na^+, Cl^-, SO_4^{2-}, Mg^{2+}, Ca^{2+}, and K^+. On a timescale of hours to days, these ions have the potential to disrupt the chemical equilibrium of the system, alter the solubility of minerals and gases, and promote flocculation of particles (Stumm and Morgan 1996, Sholkovitz 1976, Gardner et al. 1991). Biotic effects often result from abiotic changes, and can include microbial responses, such as increased respiration due to the influx of bioavailable nutrients or terminal electron acceptors, as well as vegetation response, such as landward transgression of saline-tolerant communities (i.e. Chambers et al., 2013a; b). Microbiota are also affected by the osmotic stress associated with increased ionic concentrations and respond with decreased respiration rates and decreased microbial diversity (Baldwin et al. 2006).

Despite the amount of literature available on the effects of saltwater intrusion on wetland soils, there are still conflicting reports regarding respiration and C mineralization, largely because of differences in experimental design (i.e. salinity regimes) and the time-scale of the experiments (i.e. Chambers et al. 2011, 2013, 2014; Weston et al. 2006, 2011;. The majority of studies have shown increases in CO_2 production with the influx of seawater into either tidally-influenced freshwater wetlands or brackish wetlands (Chambers et al. 2011, 2014; Weston et al. 2006, 2011; Marton et al. 2012). Saltwater intrusion into freshwater wetlands increases the availability of sulfate, an abundant ion in seawater that serves as a terminal electron acceptor during anaerobic microbial respiration. The influx of sulfate poises the redox potential of soils to thermodynamically favor sulfate reduction over other respiration pathways and therefore

increases CO_2 production (Reddy and DeLaune, 2008). Tidal freshwater wetlands are known to be sources of methane (CH_4), a greenhouse gas with 25x the radiative forcing potential of CO_2, due to high electron pressure and available organic matter (IPCC, 2014). Most studies report that with an influx of seawater, brackish or tidal freshwater wetlands produce less CH_4 due to shifting respiration pathways, though the magnitude of the salinity change, and time-scale of the experiment, can alter the effect (Chambers et al. 2011, 2014; Weston et al. 2006; Poffenbarger et al. 2011; Neubauer et al. 2013; Marton et al. 2012). However, in one tidal laboratory study with increased salinity (5 ppt), Weston et al. (2011) observed an increase in CH_4 emissions from tidal freshwater marsh soil cores over a 1-year period.

Dissolved organic carbon (DOC) is another C loss pathway that may be affected by increased salinity. Studies indicate DOC concentrations may be unaffected by changes in salinity (Weston et al. 2014, Weston et al. 2006) or decreased with elevated salinity (Chambers et al. 2013, Ardon et al. 2016). Salts can stimulate flocculation of DOC, resulting in the transformation of DOC into particulate organic C (Ardon et al. 2016). Clearly, the effects of increasing salinity on C loss (CO_2, CH_4, and DOC) in wetland soils have yet to be fully understood, and most likely depends on other factors, such as soil type, salinity concentration, substrate quality, dominant vegetation, hydrologic fluctuations, and nutrient availability.

Increases in salinity can also have implications for changes in phosphorus cycling. Phosphorus cycling is regulated by adsorption/desorption, flocculation/dissolution, and ionic exchange (Reddy et al. 1999). Phosphorus availability is highly influenced by the pH of the system; increases in salt concentrations or influx of seawater can decrease pH (Weston et al. 2006, Chambers et al. 2011). Moreover, increases in sulfate concentrations in the water column can lead to the dissolution of minerals containing iron (Fe), and the subsequent release of P

bound to Fe. In a laboratory study coupled with a field component, Jun et al. (2013) documented

decreases in P concentrations via promotion of sorption after a 2-3 ppt salinity increase in a tidal

freshwater floodplain forest after ~ 1 week. Similar results were reported by Weston et al.

(2006), during which freshwater wetland sediments were subjected to a 10 ppt increase in

salinity that resulted in an initial decrease in HPO_4^{2-} porewater concentrations, followed by a

subsequent increase after 15 days, indicating that the duration of saltwater intrusion has

ramifications for phosphorus availability. In contrast, exposure of a tidal freshwater marsh to a 5

ppt increase in salinity over 1 year resulted in no significant change to phosphate concentrations

(Weston et al. 2011), while a laboratory study investigating salinity pulses on freshwater,

brackish, and salt marshes documented greater soluble reactive P (SRP) release within the

freshwater and brackish marshes (Chambers et al. 2013).

The most well documented effect of increasing salinity on wetland soils may be the near

immediate liberation of ammonium (NH_4^+) from the soil and into the porewater. Ammonium is

the most prevalent species of N in anaerobic environments and adheres to the soil cation

exchange complex (CEC). NH_4^+ is stripped from the CEC within hours and replaced with

divalent or monovalent ions present in seawater with the influx of ions from increased salinity.

(Rysgaard et al. 1991, Seitzinger et al. 1999, Weston et al. 2006, Ardón et al. 2013, Jun et al.

2013). What remains unknown is how salinity and wetland soil type impact how much of this

NH_4^+ is subsequently nitrified or assimilated within the soil, versus how much diffuses into the

surrounding surface water and is exported from the system.

This study seeks to quantify the effects of seawater intrusion on the export of bioavailable

nutrients (DOC, SRP, and NH_4^+) and production of greenhouse gases in three different types of

freshwater wetland soils of varying physiochemical properties, specifically organic matter

content. If nutrients released into the porewater through the biotic and abiotic processes described above are released into the surrounding water column, and subsequently the coastal zone (facilitated by tidal flow), there could be far-reaching ecosystem-level implications. Increases in N and P can reduce limitations on phytoplankton growth in the coastal ocean and contribute to harmful algal blooms and associated hypoxia (Turner and Allan, 1982).

Methods

Experimental Design

In order to understand the effects of salinity on nutrient dynamics, we selected sites at three different types of freshwater wetlands in east-central Florida: a cypress dome (28°36'30.4" N, 81°11'57.16"W), bayhead swamp (28°36'22.95"N, 81°12'6.77"W), and mineral marsh (28°35'30.40"N, 81°10'46.88"W). Site selection was based on obtaining a varying range of soil organic matter. Soils at the cypress dome site were classified as Sanibel muck (Histic Humaquepts) and had a 10cm overlying water column. Dominant vegetation was *Taxodium distichum.* Soils at the bayhead swamp site were within the same taxonomic classification, and though there was no overlying water column, soils were saturated. Dominant vegetation species were *Persea palustris* and *Myrica cerifera*. Dominant vegetation at the mineral marsh site was *Eleocharis spp.*, and a 10 cm water column overlayed Basinger fine sand soils (Spodic Psammaquents). Intact cores were collected in 25 cm long X 10 cm wide PVC tubes, each with nine holes (1/2 inch diameter) pre-drilled at randomly spaced intervals around the tube. Cores were collected to a depth of 15 cm using the push coring method. Immediately after removal from the natural environment, cores were wrapped in cling wrap to prevent water drainage through the holes and to preserve anaerobic conditions, then plugged at the bottom with a mechanical stopper. Twelve field-replicate cores from each site were placed on ice and transported back to the laboratory. Once the intact soil cores arrived at the lab, they were sorted

by site and flooded with a 5 cm water column for a 24-hour acclimation period before the start of the experiment.

Prior to beginning the experiment, water was obtained from Lake Claire (28°36'27.53" N, 81°12'9.71" W), a shallow lake located in close proximity to the three wetland sites and fed by the same surface and groundwater as the sampling sites. Water from the lake was pumped through series of 10, 5, and 1 μm filters to remove particulates and stored in five (5) 20-L Nalgene carboys prior to addition to the soil cores. The two salinity treatments (5 and 15 ppt) were created by adding TropicMarin sea salt (Tropic Marin; Wartenburg, Germany) to the water stored in the carboys to obtain the appropriate salinity, and then the solution was mixed for ten minutes.

All cores were placed in an individual water bath comprised of a larger PVC tube (15.24 cm diameter) with a water-tight cap at the bottom. A ¼ inch pumice air stone was then inserted into each core at a depth of 10 cm and attached to a 15 cm long silicon tube connected to a 20 mL syringe to obtain porewater samples (Figure 2). The individual water baths were filled with water of an appropriate salinity treatment and a 5 cm water column was maintained above the soil surface. Each salinity treatment included four replicates from each site (bayhead swamp, cypress dome, mineral marsh). Over a three-week period, the water bath was drained and replaced weekly with filtered water from the nearby lake at the appropriate salinity for the treatment.

Nutrient Sampling

Porewater samples were collected via the airstone connected to a 20 mL syringe 7 times over the course of the three-week experiment, and 8 times from the surrounding water bath (Table 1).
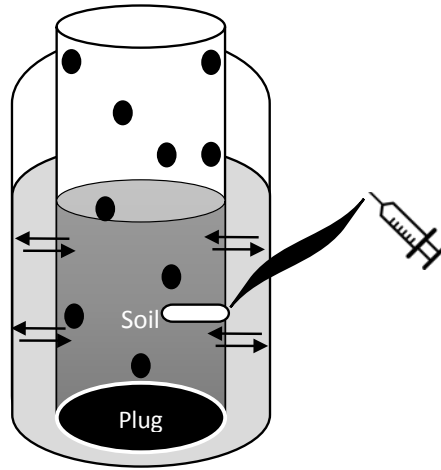
Figure 2: Diagram of core setup. Each soil core had nine 127 mm holes drilled at random into the core tube and was contained within a capped 15.24 cm polyvinyl chloride water bath. A 6.36 mm long air stone was inserted into the cores at a depth of 10 cm.

Table 1: Timeline for each sampling and water change that took place over the course of the experiment.

Day	Sampling
1	Porewater and leachate
2	Porewater and leachate
4	Porewater, change water
5	Leachate
7	Porewater and leachate
11	Porewater, change water
12	Leachate
14	Porewater and leachate
18	Porewater, change water
19	Leachate
21	Porewater and leachate

Twenty mL of water was extracted, immediately filtered through a Supor 0.45 μM filter, and acidified with distilled, deionized (DDI) H_2SO_4 to a pH < 2. Temperature, pH, and conductivity measurements were obtained immediately prior to each sampling event over the course of the experiment using an Accumet bench top pH probe (Accumet XL200, ThermoFisher Scientific, Waltham, MA, USA). After each sampling, filtered lake water of the appropriate salinity was added to the water bath to maintain a constant water column height of 5 cm above the soil surface.

The surrounding water column, porewater, and filtered Lake Claire water samples were analyzed for dissolved organic carbon (DOC) on a Shimadzu TOC-L Analyzer (Kyoto, Japan). Samples were analyzed for ammonium-N (NH_4^+-N) and SRP on a SEAL AQ2 Automated Discrete Analyzer (Seal Analytical, Mequon, WI) using EPA Methods 350.1 Rev. 2 and 365.1 Rev. 2, respectively (USEPA, 1993). Samples were also analyzed for NO_x (nitrate + nitrite) on the Seal AQ2 using EPA Method 353.1 Rev. 2.0 (USEPA, 1993), but concentrations were consistently below the detection limit (0.003 mg NO_x L^{-1}) and are therefore not discussed.

Soil Physiochemical Properties

At the end of the laboratory experiment, soils were destructively sampled and extruded to three depths (0-5 cm, 5-10 cm, and 10+ cm). Each sample was immediately weighed and stored at 4°C to be analyzed for physiochemical properties. Gravimetric moisture content was determined by homogenizing the field-moist soil samples and placing them in a forced air oven at 70°C for 3 days until a constant weight was achieved. Bulk density was calculated with % moisture and expressed on a dry weight basis. Dried soils were ground using a SPEX Sample Prep 8000M Mixer/Mill (Metuchen, NJ). Dried, ground subsamples were used to determine total C and N on a Vario Micro Cube CHNS Analyzer (Elementar Americas Inc., Mount Laurel, NJ).

Solid-phase total soil P analysis was performed by combusting dried subsamples at 550°C for 5 hours to determine percent organic matter via loss-on-ignition, boiling the resulting ash in 1 N HCl on a hot plate for 30 minutes, and subsequent filtration through Whatman #41 filters (Andersen, 1976). Samples were then analyzed on an AQ2 Automated Discrete Analyzer (Seal Analytical, Mequon, WI) via EPA method 365.1 Rev. 2. Extractable NH_4^+ concentrations were determined by placing 2.5g field-moist soil into a 40 mL centrifuge tube, adding 25 mL of 2 M KCl, and agitating on an orbital shaker at 100 rpm for 1 h. Samples were then centrifuged for 10 minutes at 4000 rpm and 10°C. The supernatant was filtered through Supor 0.45μM filters, acidified with DDI H_2SO_4 to a pH < 2, and analyzed for NH_4^+-N within 30 days (Roy and White, 2013).

Microbial Biomass C

Microbial biomass C (MBC) was determined via use of the chloroform-fumigation method after Vance et al. (1987). Microbial biomass C analysis was performed on the 0-5cm depth segment for each sample by weighing 2.5g field-moist soil into 40mL centrifuge tubes in duplicate. One set of samples was fumigated with chloroform for 24 h in a glass vacuum desiccator. The non-fumigated control set was extracted with 25 mL of 0.5M K_2SO_4, agitated continuously for 1 h at 100 rpm on an orbital shaker, and centrifuged for 10 minutes at 10°C and 4000 rpm. The supernatant was decanted and vacuum-filtered through Supor 0.45 μM filters. The samples were then acidified with DDI H_2SO_4 to a pH < 2 and analyzed within 30 days. Following the 24 h chloroform fumigation, the fumigate samples were analyzed in the same method as the non-fumigated samples. A Shimadzu TOC-L Analyzer (Kyoto, Japan) was used to determine non-purgeable organic carbon (NPOC) for each set of samples. Microbial biomass

C was calculated as the difference in NPOC between the fumigate samples and the non-fumigated samples.

Respiration – Carbon Dioxide and Methane

Respiration rates were obtained by weighing 7g of field-moist soil (0-5 cm) into glass serum bottles and capping them with rubber septa and aluminum crimps. Bottles were evacuated to 75cm Hg, and purged for 3 minutes with 99.99% O_2-free N_2 gas. Fifteen mL of N_2-purged site water was injected into each sample. Bottles were shaken continuously on an orbital shaker at 100 rpm and 25°C for 1 hour. Gas samples were extracted using gas-tight syringes every hour for a 4-hour period and injected into a GC-2014 Gas Chromatograph (Shimadzu Instruments, Kyoto, Japan).

Statistical Analysis

Data analysis was performed using a three-way ANOVA in R (R Foundation for Statistical Computing, Vienna, Austria) to determine effects of wetland soil type, salinity, depth, and their interactions. The Shapiro-Wilks test was utilized to determine whether the soil physiochemical data met the assumptions of normality and Levene's test was used to determine homogeneity of variance. Greenhouse gas efflux (CH_4 respiration and CO_2 respiration) and microbial biomass C data were analyzed by use of an ANOVA in R to determine the effects of wetland soil type, salinity, and the interaction between the two. These data were transformed using a square-root transformation to meet the assumption of normality (Shapiro-Wilk test). Nutrient data (both nutrient concentrations in the porewater and in the surrounding water) and environmental conditions (temperature, pH, conductivity) were analyzed in R via a repeated-measures ANOVA to determine the effects of wetland soil type, salinity, and the interaction between the two. The variable 'week' was added to account for each time the water in the

mesocosms was replenished and was treated as a covariate. The total concentration of each

nutrient within the porewater was determined by summing the average concentration of each

nutrient in the porewater at each sampling time. The total concentration of each nutrient within

the surrounding water was calculated in the same manner. To determine the percentage of each

nutrient that that was exported into the surrounding water from the porewater, the total in the

surrounding water was then divided by the total in the porewater, and the resulting decimal

multiplied by 100 to yield a percentage.

Results
Soil Physiochemical Properties

Percent moisture content and bulk density varied with the three-way interaction between

wetland soil type, salinity, and depth ($p<0.01$ and $p<0.001$, respectively). Generally, the highest

moisture content occurred in the bayhead swamp, and the lowest moisture content was found in

the mineral marsh; moisture content decreased with depth (Table 2). Moisture content was

negatively correlated to bulk density and positively correlated with total C, N, and P, and percent

organic matter (Table 3). Bulk density ranged from 1.83 ± 0.06 g cm^{-3} in the control mineral

marsh treatment at the 10+ depth interval, to 0.11 ± 0.01 g cm^{-3} in the control bayhead swamp

treatments at the 5-10 cm depth interval. Bulk density was also negatively correlated to total C,

N, and P, and percent organic matter (Table 3). The interaction between wetland soil type and

salinity influenced the pH of the water column, which varied between 7.89 ± 0.08 in the bayhead

swamp 15 ppt treatment, and 6.87 ± 0.05 the cypress dome 5 ppt treatment; increases in salinity

contributed to increases in pH. Organic matter content varied between wetland soil type

($p<0.001$), with average organic matter contents of 4.03 ± 0.83, 37.89 ± 2.99, and 82.49 ± 1.11

% within the mineral marsh, cypress dome, and bayhead swamp, respectively (Table 2).

Table 2: Control soil physiochemical properties by wetland soil type and depth. All physiochemical properties differ significantly among wetland soil types.

Wetland Soil Type	Depth (cm)	Moisture Content		Bulk Density (g cm^{-3})		% Organic Matter		Total C (g kg^{-1})		Total N (g kg^{-1})		Total P (mg kg^{-1})		Extractable NH$_4^+$ (mg L^{-1})	
		Mean	StErr	Mean	StErr	Mean	StErr	Mean	StErr	Mean	StErr	Mean	StErr	Mean	StErr
Bayhead Swamp	0-5	0.85	0.01	0.11	0.01	92.54	2.82	455.83	4.34	13.03	1.53	618.11	131.52	126.67	33.32
	5-10	0.87	0.00	0.11	0.01	85.72	2.24	443.35	11.85	12.15	0.64	510.76	17.94	117.08	23.40
	10+	0.85	0.00	0.14	0.01	75.90	4.23	417.05	11.99	13.05	0.92	525.06	54.18	107.97	40.22
Cypress Dome	0-5	0.75	0.02	0.23	0.03	47.91	4.39	250.88	25.13	9.83	1.11	352.17	35.79	60.43	4.40
	5-10	0.66	0.03	0.37	0.05	31.13	3.98	161.53	13.56	7.93	0.23	449.72	126.83	31.54	4.62
	10+	0.55	0.04	0.57	0.06	19.86	4.44	111.97	1.83	5.51	0.29	191.37	17.61	21.88	5.79
Mineral Marsh	0-5	0.37	0.02	0.75	0.03	8.31	1.42	64.78	8.29	3.58	0.60	51.63	11.22	16.81	2.05
	5-10	0.22	0.01	1.34	0.09	2.54	0.93	10.53	5.72	0.65	0.27	56.63	27.37	0.40	0.21
	10+	0.12	0.06	1.83	0.06	0.91	0.23	1.83	0.48	0.27	0.03	76.17	1.67	8.61	7.76

Table 3: Correlation table of soil physiochemical measurements. Degrees of freedom = 108, at r =0.197, p= 0.05, at r=0.256, p=0.01. Values in bold are significant.

	Extractable NH$_4^+$ (mg g^{-1})	Moisture Content (%)	Bulk Density (g cm^{-3})	Total C (g kg^{-1})	Total N (g kg^{-1})	Organic Matter (%)
Moisture Content	**0.723**					
Bulk Density	**-0.675**	**-0.960**				
Total C	**0.681**	**0.797**	**-0.751**			
Total N	**0.548**	**0.620**	**-0.588**	**0.744**		
% OM	**0.755**	**0.844**	**-0.783**	**0.928**	**0.639**	
Total P	**0.562**	**0.489**	**-0.473**	**0.538**	**0.628**	**0.592**

Organic matter content significantly decreased with depth. Percent organic matter showed a strong positive correlation with total C, N, and P, and extractable NH_4^+ concentrations (Table 3). Total C differed with wetland soil type ($p<0.001$), and ranged from 405 ± 7.99 g kg^{-1} in the bayhead swamp to 35.0 ± 10.5 kg^{-1} in the mineral marsh (Table 2). As depth increased, total C decreased ($p<0.01$). Total N varied between wetland soil type ($p<0.001$) and was highestin the bayhead swamp, at 12.3 ± 0.34 g kg^{-1}, and lowest in the mineral marsh, at 2.71 ± 1.37 g kg^{-1} (Table 2). Total P also differed by wetland soil type ($p>0.001$) in the same manner as total N: highest in the bayhead swamp and lowest in the mineral marsh (Table 2). Strong positive correlations existed between total C, N, and P (Table 3).

The interaction between wetland soil type and salinity resulted in changes in soil extractable NH_4^+ concentrations ($p<0.001$). Concentrations ranged from a high of 117.2 ± 17.4 mg g^{-1} in the bayhead swamp control treatment, to a low of 5.0 ± 1.6 mg g^{-1} in the mineral marsh 5 ppt treatment (Table 2). Extractable NH_4^+ concentrations also differed with depth ($p<0.01$), being lower in the 10+ cm depth interval (47.2 ± 8.6 mg g^{-1}) than the 0-5 cm depth interval (67.5 ± 8.2 mg g^{-1}). Extractable NH_4^+ negatively correlated to bulk density and positively correlated to moisture content, total C, N, and P (Table 3).

<div align="center">Microbial Biomass</div>

Wetland soil type significantly affected microbial biomass C (0-5 cm; $p<0.001$), specifically, the cypress dome and bayhead swamp had higher MBC than the mineral marsh ($p<0.001$; Figure 3). The lowest average MBC occurred in the mineral marsh with 258 ± 92.0 mg g^{-1}, while the highest was found within the bayhead swamp with 1807 ± 297 mg g^{-1}. The MBC in the cypress dome was 1750 ± 216 mg g^{-1}, which was not significantly different from the bayhead swamp. The main effect of salinity was also significant ($p<0.01$); average MBC was

higher (1678 ± 297 mg g^{-1}) in the 15 ppt treatment than the 5 ppt treatment (1378 ± 336 mg g^{-1}) and the control treatment (1034 ± 212 mg g^{-1}). Microbial biomass C was positively correlated with both the rate of CH_4 production and the rate of CO_2 production (Table 4).

Greenhouse Gas Production

The rate of CH_4 production (0-5 cm) did not differ significantly with salinity treatment but did differ by wetland soil type ($p < 0.001$, Figure 3). Average methane production in both the cypress dome (4.81 ± 1.45 µg CH_4-C g^{-1} h^{-1}) and bayhead swamp (3.50 ± 0.19 µg CH_4-C g^{-1} h^{-1}) (Figure 3). The highest rates were observed in the bayhead swamp (17.23 ± 2.37 µg CO_2-C g^{-1} h^{-1}) and lowest rates were observed within the mineral marsh (0.95 ± 0.51 µg CO_2-C g^{-1} h^{-1}). Between the 0 ppt and 15 ppt treatment, CO_2 rates changed significantly ($p < 0.05$), ranging from an average of 11.46 ± 3.59 µg CO_2-C g^{-1} h^{-1} in the 15 ppt treatment to 6.86 ± 2.02 µg CO_2-C g^{-1} h^{-1} in the 0 ppt treatment.

Nutrient Export

Porewater Nutrients

Porewater NH_4^+ concentrations differed with the interaction between wetland soil type and salinity treatment ($p < 0.001$, Figure 4a). In all three wetland soil types, the 15 ppt salinity treatment contained the highest average porewater NH_4^+ concentration (2.43 ± 0.33 to 2.99 ± 0.40 mg L^{-1}), followed by the 5 ppt treatment (1.16 ± 0.17 to 2.27 ± 0.26 mg L^{-1}), both of which were always significantly greater than the control (0 ppt; 0.25 ± 0.02 to 0.44 ± 0.07 mg L^{-1}). Specifically, the average porewater NH_4^+ concentrations in the 15 ppt treatment ranged from 5x (bayhead swamp) to 12x (cypress dome) greater than the control, while the 5 ppt treatment ranged from 2x (bayhead swamp) to 9x (cypress dome) greater than the control. Generally, NH_4^+ concentrations in the porewater increased with increasing salinity almost immediately (i.e., within 1 day after salinity addition), reaching a peak in week 3.
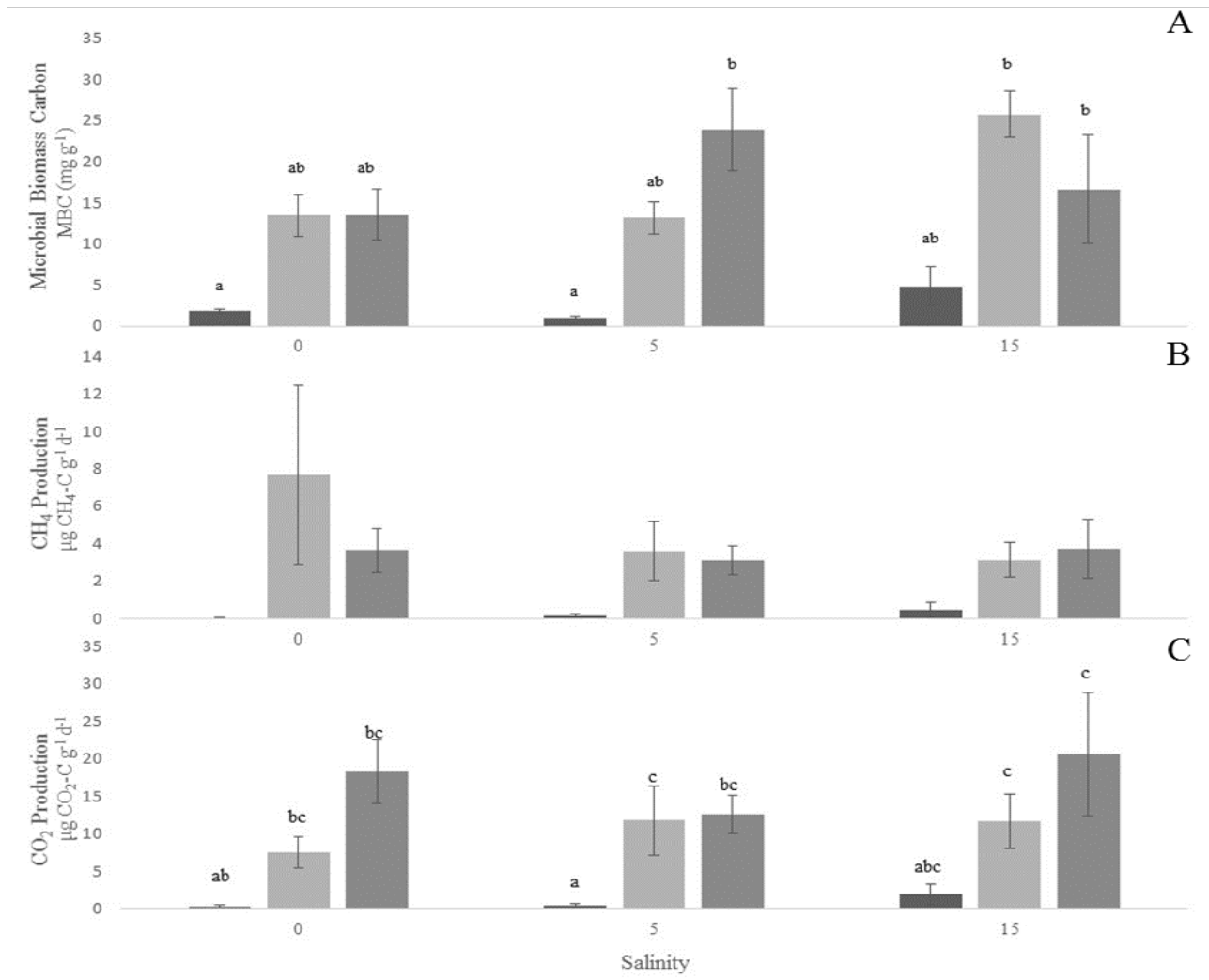
Figure 3: Microbial biomass C (A), CH$_4$ production (B), and CO$_2$ production (C) with regards to salinity and wetland soil type. Data are shown as mean ± standard error (n=4). Letters denote significant differences among wetland soil types (from left to right: bayhead swamp, cypress dome, mineral marsh) and salinity treatments.

Concentrations of SRP in the porewater differed with the interaction between wetland soil type and salinity (p<0.001), ranging from a high of 0.42 ± 0.11 mg L^{-1} in the 15 ppt mineral marsh to a low of 0.018 ± 0.001 mg L^{-1} in the 15 ppt bayhead swamp (Figure 4b). Both the cypress dome and mineral marsh showed a similar pattern of increasing SRP with increasing salinity, with the highest concentrations seen in the mineral marsh. In contrast, the bayhead swamp had the lowest porewater SRP in the 15 ppt treatment, but the effect of salinity was not significantly different than the control. Porewater SRP was not significantly correlated with week.

Dissolved organic carbon concentrations in the porewater changed with the interaction between wetland soil type and salinity (p<0.001), ranging from 29.16 ± 2.08 mg L^{-1} in the cypress dome 15 ppt treatment, to 15.39 ± 0.706 mg L^{-1} in the bayhead swamp 15 ppt treatment (Figure 4c). In the bayhead swamp, DOC concentrations were highest within the control treatment, and decreased slightly with increasing salinity. However, in both the cypress dome and mineral marsh wetland soil types, the 15 ppt treatment had the greatest average DOC concentrations. Overall, the concentration of DOC in the porewater was greatest in the control treatments in week 1, and gradually decreased until week 3.

Water Column Nutrients

Salinity had a significant effect on water column NH_4^+ concentrations within the surrounding water bath (p<0.001, Figure 5a). Concentrations of NH_4^+ in the 15 ppt treatment ranged from 4x (bayhead swamp) to 8.7x (cypress dome) greater than the controls, while the 5 ppt treatment ranged from 2.7x (bayhead swamp) to 5.3x (cypress dome) greater than the controls. Time also affected NH_4^+ export into the water column, with the highest concentrations observed between weeks 1 and 2 of the 3-week study in both the 15 and 5ppt treatments. Over the course of the experiment, the highest percentage of total NH_4^+ that was exported from the

porewater into the surrounding water column was seen in the 5 ppt bayhead swamp treatment (95%), while the lowest export was observed within the 5 ppt mineral marsh treatment (32%, Table 5). With the exception of the bayhead swamp, the percentage of porewater that was exported into the surrounding water was highest in the 15 ppt salinity treatment.

Soluble reactive phosphorus in the water column varied with the interaction between salinity and wetland soil type ($p < 0.01$, Figure 5b). The greatest average water column SRP concentrations were observed in the 15 ppt cypress dome treatment, 0.20 ± 0.12 mg L^{-1}, and the lowest in the 5 ppt cypress dome treatment, 0.01 ± 0.002 mg L^{-1}. The concentration of SRP averaged 8x higher and 3.5x higher in the cypress dome and bayhead swamp 15 ppt treatments, respectively, than in their respective controls. In the mineral marsh, neither salinity treatment differed significantly from the control. Export of SRP out of the porewater and into the surrounding water was highest in the bayhead swamp 15 ppt treatment (103%), and lowest within the 15 ppt cypress dome treatment (2%, Table 5). Week was not a significant control on SRP concentrations.

Concentrations of DOC in the water column around the soil cores varied between wetland soil type ($p < 0.01$, Figure 5c), with the highest average concentrations observed in the cypress dome (21.71 ± 2.41 mg L^{-1}) and lowest average concentrations found in the bayhead swamp (15.87 ± 1.54 mg L^{-1}). Time (week) was also a significant control on water column DOC concentrations, though that effect was considered an artifact of the experimental design and treated as a covariate (see discussion). DOC in the water column was highest during the first week, and then decreased during week 2. After week 2, the DOC concentrations were stable for the remainder of the experiment.
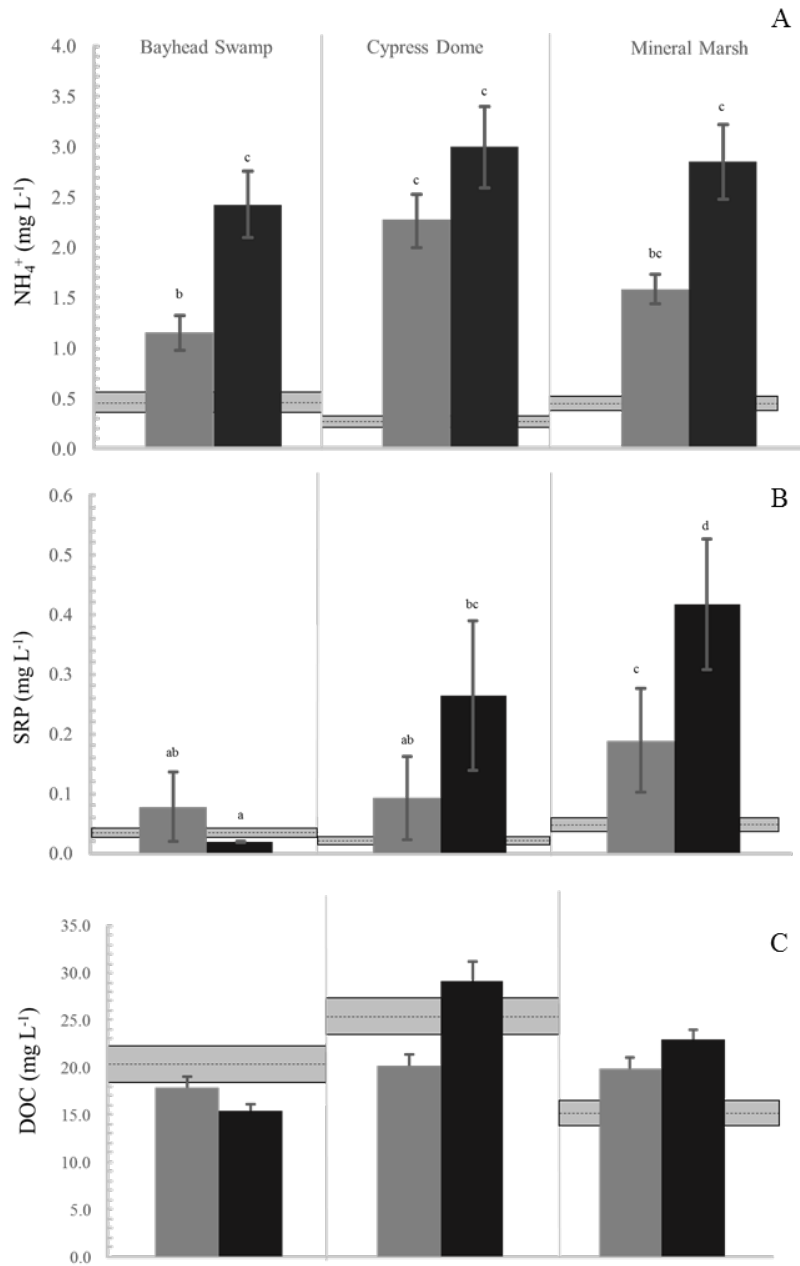
Figure 4: Average NH_4^+ (A), soluble reactive P (SRP) (B), and dissolved organic C (DOC) (C)

concentrations in the porewater by both salinity and wetland soil type. Letters denote significance.

Control treatments ± 1 SE are denoted by horizontal bars. Gray vertical bars indicate the mean and SE of

the 5 ppt treatment, and black vertical bars indicate the mean and SE of the 15 ppt treatment.
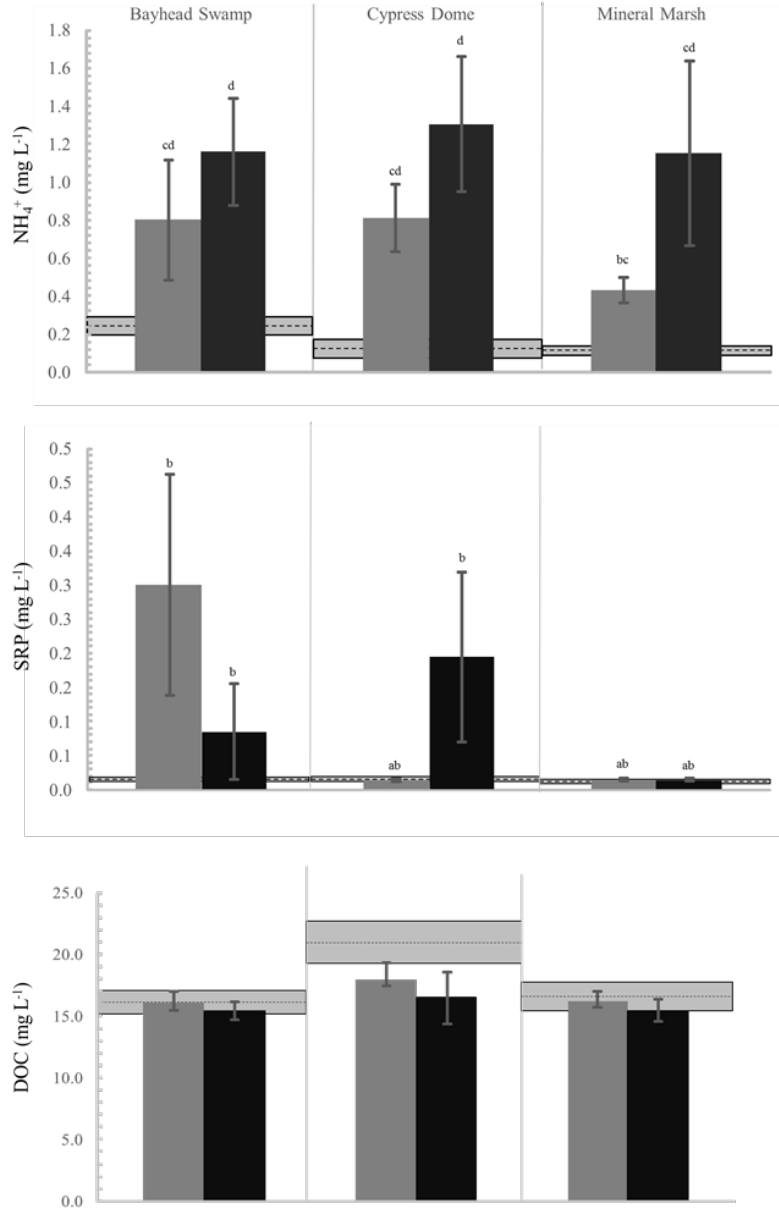
Figure 5: Average NH$_4^+$ (A), soluble reactive P (SRP) (B), and dissolved organic C (DOC) (C) concentrations in the surrounding water by both salinity and wetland soil type. Letters denote significance. Control treatments ± 1 SE are denoted by horizontal bars. Gray vertical bars indicate the mean and SE of the 5-parts per thousand (ppt) treatment, and black vertical bars indicate the mean and SE of the 15-ppt treatment.

Table 4: Correlation table of microbial biomass C and greenhouse gas analyses. Degrees of freedom = 35, alpha = 0.05, r =0.283. Values in bold are significant.

	Microbial Biomass C (mg g^{-1})	CH$_4$ Respiration (µg CH$_4$-C g^{-1} d^{-1})
Microbial C (mg g^{-1})		
CH$_4$ Respiration (µg CH$_4$-C g^{-1} d^{-1})	**0.316**	
CO$_2$ Respiration (µg CO$_2$-C g^{-1} d^{-1})	**0.512**	0.273

Table 5: Percentage of total porewater nutrients (NH4+, SRP, DOC) that was exported from the porewater to the surrounding water over the course of the experiment.

Wetland Soil Type	Salinity	% NH$_4^+$	% SRP	% DOC
Bayhead Swamp	5	94.7	82.9	82.1
	15	66.0	103.0	96.7
Cypress Dome	5	57.3	55.9	75.0
	15	84.0	2.0	26.7
Mineral Marsh	5	32.3	12.0	55.0
	15	81.0	6.6	24.3

Total export of DOC out of the porewater and into the surrounding water was highest in the 15 ppt bayhead swamp treatment (82%), and lowest within the 15 ppt mineral marsh (24%, Table 5).

<div align="center">Discussion</div>

We utilized soils from three different freshwater wetland soil types and monitored the export of nutrients from the porewater into the surrounding water column over time in an effort to more fully understand how both wetland soil type and increases in salinity (as a product of sea level rise) affect the potential export of labile soil nutrients through both horizontal flow (mimicking tidal fluctuations) and diffusion. A variety of controlled laboratory studies have been conducted to determine the short-term effects of increased salinity on freshwater wetland soils, though these studies have focused primarily on the response of the porewater nutrients to salinity changes, or how greenhouse gas production changes over time (e.g., Ardon et al. 2013, 2016; Baldwin et al. 2006; Bartlett et al. 1987; Chambers et al. 2011, 2013, 2014; Jun et al. 2013; Marton et al. 2012, Poffenbarger et al. 2011; van Dijk et al. 2015; Weston et al. 2006, 2011). Generally, these studies have been conducted on one wetland soil type, and few studies have examined how wetland soil type/organic matter content (and properties correlated to organic matter) impacts the response to increases in salinity. We found wetland soil type significantly affected how soils respond to increasing salinity, specifically export of nutrients and greenhouse gas production.

In terms of soil physiochemical parameters, the mineral marsh represented the lowest amount of elemental C, N, and P within the soil, as well as low organic matter content, low moisture content, and high bulk density, compared to the other wetland soil types. Consequently, rates of CH_4 and CO_2 production were lowest at this site due to the lack of soil

organic matter available to provide an electron donor to support high respiration rates (Reddy

and DeLaune, 2008). Likewise, microbial biomass C was also significantly lower within the

mineral marsh than in either of the other treatments. In general, the mineral marsh was observed

to have a larger particle size than the other two wetland soil types (grain size = 2.94Φ;

Steinmuller, unpublished data). The large particle size of sand promotes shorter path lengths for

oxygen diffusion and higher hydraulic conductivity, and sandy soils are thus more aerated than

organic-rich soils (Brady and Weil, 2009). Sandy soils also lack the electrochemical charges

associated with clay and organic soils that adhere nutrients to the soil.

Carbon Dynamics

Average CO_2 respiration rates generally increased with increasing salinity across all

wetland soil types. The influx of sulfate associated with elevated salinity poises the redox

potential of wetland soils to use sulfate as an alternate electron acceptor for respiration, a

pathway that is thermodynamically favored over methanogenesis, and results in an increase in

CO_2 production (Reddy and DeLaune, 2008). This finding is consistent with several previous

studies, all of which have found accelerated CO_2 respiration rates after exposing freshwater soils

to increases in seawater (Chambers et al. 2011; Weston et al. 2006, 2011; Marton et al. 2012).

Microbial biomass C was greater in the 15 ppt treatment than the other two treatments and was

significantly correlated to CO_2 production. Other studies have also found higher microbial

biomass in more saline coastal wetland soils (Chambers et al., 2013) which may be attributed to

an increasing abundance of sulfate reducers, despite the limitations imposed by the osmotic

stress associated with the influx of ions within seawater (i.e., Baldwin et al. 2006).

Previous studies have also suggested that implementation of brackish and saline salinity

regimes (> 10-18 ppt) catalyzes a decrease in CH_4 production due to competitive inhibition by

sulfate reducers (i.e. Weston et al. 2006, and Chambers et al. 2011, Neubauer et al. 2013).

However, CH_4 production was not significantly affected by changes in salinity (up to 15 ppt) in

this study. Others have found methanogenesis can occur concomitantly with sulfate reduction as

long as the methanogenic bacteria are utilizing noncompetitive substrates (i.e., substrates that are

not suitable electron donors for sulfate reduction), which may explain our findings (Capone and

Kiene, 1988). Average CH_4 production rates in the control treatments were roughly 50% lower

than CO_2 respiration rates, indicating that methanogenesis is not the dominant pathway for

respiration under ambient salinity. Roden and Wetzel (1996) concluded that sulfate reduction

and methanogenesis were responsible for 4% and 29% of mineralized C in freshwater wetlands,

respectively, while reduction of iron accounted for roughly 67%. In contrast, sulfate reduction

can constitute up to 95% of the organic C oxidation in freshwater sediments exposed to 10 ppt

seawater (Weston et al., 2006). The observed increase in CO_2 production, concomitant with no

change in CH_4 production, affects the global warming potential (GWP) of these wetlands.

Previous studies have asserted that saltwater intrusion into wetlands increase CO_2 production and

decreases CH_4 production, decreasing the net GWP of these wetlands (Chambers et al., 2011).

However, in this case, CH_4 production rates remained constant with increases in salinity while

CO_2 production rate accelerated, resulting is a net increase in the GWP of all three wetland soil

types.

The effect of salinity treatments on DOC concentrations within the porewater was

mediated by wetland soil type, as evidenced by the opposing response of DOC in the cypress

dome and mineral marsh (increasing with salinity), as compared to the bayhead swamp (a slight

decrease with salinity). In the bayhead swamp, DOC was lost via export into the surrounding

water in response to salinity, which was expected based on previous findings that soils of higher

C content release more C in response to elevated salinity levels (Marton et al. 2012). However, concentrations of DOC in the surrounding water of the bayhead swamp showed no change with salinity, despite the substantial flux of DOC from the porewater. Flocculation is likely responsible for this discrepancy- upon exposure to saline water, approximately 13% of DOC within surface waters can immediately flocculate and shift to particulate organic matter (Ardon et al. 2016). In the mineral marsh and cypress dome, the increases in porewater DOC concentrations in response to salinity could be a result of a stimulation of organic matter mineralization (i.e., Weston et al. 2011, Chambers et al. 2014). In addition, average DOC within all the treatments decreased with time over the course of the 3-week experiment, likely due to the effects of soil collection. DOC has been observed to 'leak' from wetland soil cores for several hours after coring due to the severing and death of roots, resulting in the observed decrease in labile DOC in the porewater over time (Gribsholt and Kristensen, 2002).

Nitrogen Dynamics

Ionic displacement resulting from an increase in salinity likely caused desorption of NH_4^+ from the CEC in all of the wetland soil types, and the magnitude of this process increased with salinity. Previous research has demonstrated that exchangeable NH_4^+ is liberated from the soil particles within hours due to the elevated competition for exchange sites with monovalent and divalent cations from salinity increases (i.e. Seitzinger et al. 1991, Rysgaard et al. 1991, Gardner et al. 1991). However, no previous research has characterized the export of NH_4^+ from the porewater into the surrounding water in the short term within different wetland soil types. In this study, NH_4^+ concentrations increased in the porewater within 1 day of salinity exposure, and then peaked in the surrounding surface water within the first week of the study, though the concentration of liberated NH_4^+ differed by wetland soil type. The timescale of NH_4^+ exchange

from the CEC is consistent with a similar studies that exposed wetland soils to increased salinity

treatments (Seitzinger et al., 1991; Weston et al., 2006, 2011; Jun et al., 2013; Ardón et al.,

2013). The highest percentage of export within the 5 ppt treatment was in the bayhead swamp

treatment (94.7%); which we attribute to the high organic matter content and potential for

organic N mineralization to NH_4^+. The 15 ppt treatment had a slightly reduced export of NH_4^+

out of the porewater (66-84%), but higher concentrations within the porewater, indicating that

although more NH_4^+ was present, it was more tightly held within the soil. Extractable NH_4^+

increased between the 5 ppt and 15 ppt treatments, which can be attributed to increases in

mineralization catalyzed by availability of sulfate (Noe et al. 2013; Weston et al. 2006, 2011;

Chambers et al. 2013; Ardon et al. 2016), as well as differences in liberation of NH_4^+ from the

CEC between treatments (Rysgaard et al. 1999). Extractable NH_4^+ concentrations also differed

between wetland soil types, demonstrating the importance of inherent soil physiochemical

properties in mediating the response of NH_4^+ availability to increased salinity.

<div align="center">Phosphorus Dynamics</div>

Soluble reactive phosphorus concentrations in both the porewater and surrounding water

were highly dependent on wetland soil type. In the bayhead swamp, SRP concentrations

decreased with increasing salinity, while the cypress dome and mineral marsh showed the

opposite trend in the porewater. Almost the entirety of SRP produced in the porewater was

exported into the surrounding water in the bayhead swamp (83% - 103%). The maximum

occupation of exchange sites would result in excess SRP readily exported into the surrounding

water, as evidenced by the high percentage of export. In contrast, despite the mineral marsh and

cypress dome having higher average concentrations of SRP in the porewater, the SRP appeared

to be held in the porewater more tightly, with only 2-6% of the SRP within the porewater of the

15 ppt treatments being exported into the surrounding water. This discrepancy between the concentrations in the porewater and concentrations in the surface water can be attributed to differences in soil type (Hebert et al. 2015). Both the mineral marsh and cypress dome contained more inorganic C than the bayhead swamp, and SRP exported from the porewater into the surrounding water could complex with inorganic C and form particulates that flocculate and are removed from the water column, and therefore were not detected as dissolved nutrients (Boström et al., 1988). In addition to abiotic factors such as soil type mediating SRP export into the surrounding water, the P cycle is tightly coupled to cycling of both iron and sulfur, both of which are heavily influenced by pH changes produced by an influx of seawater (Portnoy and Giblin, 1997). Seawater can catalyze a concomitant increase in both pH and concentrations of dissolved Al and Fe, which have the ability to complex with phosphate, thereby potentially altering phosphorus dynamics.

Experimental Design Considerations

We implemented a controlled laboratory experiment to isolate and quantify the changes in greenhouse gas production, MBC, and porewater and surrounding water nutrients in response to salinity. Although this approach did successfully address the study objectives, consideration should be taken when extrapolating results directly to a field setting. For example, this study only focused on the soil system—plants were excluded from the experimental cores because the nature and magnitude of their influence could not be held constant across the experimental units. However, in the field, plants are expected to play a significant role in mediating nutrient availability and exchange between porewater and surrounding water pools (Bedford et al., 1999). Likewise, phytoplankton was removed from the added surface water through filtering prior to addition to the experimental cores. Despite these limitations, this study does inform how

different freshwater wetland soil types are expected to respond in the short-term to increases in salinity, as well as the magnitude and timing of these responses. Future studies should test these conclusions under field conditions.

Conclusion

This study represents the first experimental attempt to quantify the movement of bioavailable nutrients (NH_4^+, SRP, DOC) in different wetland soil types from the porewater of freshwater wetland soils to the surrounding water column following an increase in salinity. In general, the mineral-rich soils demonstrated a smaller response to saltwater intrusion than the more organic soils when it came to nutrient release and export, presumably due to the differences in initial nutrient availability and how tightly those nutrients were held within the soil structure. Although this study only investigated short-term responses to saltwater intrusion (i.e., 3 weeks), the finding will have important implications for coastal wetland systems exposed to periodic salinity pulses and demonstrates the vulnerability of coastal zones located near coastal peatlands to salinity-induced eutrophication.

CHAPTER THREE: UNDERSTANDING THE FATE OF SOIL ORGANIC MATTER IN SUBMERGING COASTAL WETLAND SOILS: A MICROCOSM APPROACH

Abstract

Coastal wetland submergence can occur when rates of relative sea-level rise exceed that of soil elevation gain or landward transgression. In highly organic soils, the collapse of the wetland platform into open water can cause disarticulation of the soil structure, exposing previously protected anaerobic microzones to oxygenated seawater, which may accelerate mineralization rates. Nine soil cores (1 m deep) were collected from three sites within Barataria Bay, LA (USA), a region known for high rates of wetland submergence. Both the biogeochemical properties of the soils with depth were determined, as well as the impacts of the introduction of oxygenated seawater on carbon mineralization rates. Both field enzyme activity (β-glucosidase, N-acetyl-beta-D-glucosaminidase, alkaline phosphatase, β-xylosidase, and β-cellobiosidase) and microbial biomass carbon (MBC) did not significantly change with depth until 50 cm, where activity increased dramatically, then gradually decreased. Total carbon (C), total nitrogen, and percent organic matter were highest between 50 and 100 cm. Following initial biogeochemical characterization, soil microcosms were created for 11 depth segments under anaerobic conditions (mimicking an intact wetland) and aerobic conditions (mimicking a submerging wetland mixing with oxygenated water); carbon dioxide (CO_2) production was measured within the bottles over 14 days. Carbon dioxide production averaged 66% greater in the aerobic treatment than the anaerobic treatment. Both treatments exhibited a general trend of increasing CO_2 production with depth (particularly from 40-100 cm), with the difference in CO_2 production between aerobic and anaerobic treatments being 4x greater at 90-100 cm than at the soil surface (0-5 cm). The increase in C mineralization rates observed at depth was positively

correlated with indicators of greater microbial activity (i.e., higher enzyme activity and MBC) and greater nutrient availability. Study results indicate coastal wetland submergence into open water could significantly enhance CO_2 emissions, even in deep (40+ cm) soils, contrary to the typically observed pattern of soil microbial activity and soil quality decreasing with depth. These findings underline the need to analyze deeper soil samples (1+ m) in order to fully understand the implications of sea level rise on C loss from submerging coastal wetland soils.

Introduction

Coastal wetlands rank as one of the most productive ecosystem types on Earth (Amthor and Huston, 1998). High rates of primary production coupled with prevailing anaerobic conditions from tidal flooding allow salt marsh sediments to sequester 244.7 g C m^{-2} y^{-1} (Ouyang and Lee, 2014). Wetland macrophytes contain different forms of organic compounds that are deposited on the soil surface as detritus when plants senesce. These materials can contain recalcitrant lignins and tannins, but also include significant quantities of labile, low molecular weight compounds that are rapidly and preferentially degraded by microbial consortia in the surficial soil (Reddy and DeLaune, 2008; Bianchi and Canuel, 2011). The remaining recalcitrant, high molecular weight organic compounds are subsequently buried and comprise the extensive peat deposits found within many coastal wetlands (DeBusk and Reddy, 1998). These processes are the foundation of a 'decay continuum', where soil organic carbon (C) gradually becomes more refractory and recalcitrant over time (Melillo et al., 1989). Additionally, it is generally accepted that microbial processes such as decomposition decrease with depth, due to prevailing anaerobic conditions and a decrease in both the availability of labile organic compounds and electron acceptors (Gale and Gilmour, 1988; Maltby, 1988; Mendelssohn et al., 1999; Schipper and Reddy, 1995; Schipper et al., 2002; Webster and Benfield, 1986). High organic C

accumulation rates within coastal wetlands are facilitated by the burial of organic matter throughout the 'decay continuum'. For example, in coastal Louisiana salt marshes, organic C accumulation ranges from 132 g m^{-2} yr^{-1} (DeLaune and Pezeshki, 2003) to 310 g m^{-2} yr^{-1} (Hatton et al., 1983). Combined with vertical accretion rates of 0.75 – 1.35 cm yr^{-1} (Delaune et al., 1981), projected annual C accumulation in these wetlands is roughly 30 kg C m^{-2} (DeLaune and White, 2012). However, these vast pools of soil organic C, and the associated nutrients found within organic matter, may be threatened by rising sea levels.

The eustatic sea level rise rate is currently 3.4 ± 0.4 mm yr^{-1} and is expected to continue rising throughout the next century (IPCC, 2014). Coastal wetlands, which form the interface between terrestrial and marine systems, are particularly vulnerable to sea level rise. In response to the combined stressors of increased inundation and salinity, coastal wetlands respond to sea level rise in three distinct patterns: (a) by maintaining their position within the coastal landscape by accreting vertically at a rate that either matches or exceeds sea level rise, (b) transgressing landward to occupy a more conducive elevation within the coastal plain, or (c) submerging, which occurs when relative sea level rise rates exceed rates of soil surface elevation gain (Kirwan and Megonigal, 2013).

Coastal wetlands within Barataria Bay, Louisiana, USA are responding to increases in sea level predominantly via submergence, and the subsequent complete conversion of previously wetland habitat to open water (Baumann et al., 1984). Relative sea level rise rates in Barataria Bay rank among the highest in the world, averaging ~13 mm y^{-1} (Church et al., 2013). The combination of subsidence via tectonic downwarping, eustatic sea level rise, erosive processes (as high as 3-5.5 mm d^{-1} in some places, J.R. White, unpublished data), and a lack of sediment inputs, have resulted in Barataria Bay losing approximately 25.9 km^2 yr^{-1} (Penland et al., 2000).

As these wetlands are lost, 1 to 2 m of accumulated organic-rich soil also submerges (DeLaune and White, 2012). Vegetation death and wetland submergence result in a loss of soil structure, and the wetland platform collapses (DeLaune and White, 2012).

Following submergence, the accumulated soil organic matter can be either reburied within the bay or mineralized in the water column, being released as CO_2 into the atmosphere or as dissolved inorganic C within the water column. During the mineralization process, stored nutrients within the soil organic matter, such as nitrogen (N) and phosphorus (P), can also be released into the coastal zone (Bianchi et al., 2008). The high bulk density and low organic matter content of bay sediments suggest that coastal peat deposits are not reburied within the bay (Pietroski et al., 2015; White et al., 2009). Rather, as sequestered wetland soil organic materials are submerged and disarticulated in a more turbulent open water environment, the previously protected anaerobic microzones within the soil are exposed to oxygenated seawater. Under these conditions, microbial respiration is expected to increase, owing to oxygen being the most efficient and thermodynamically favored respiration pathway (Reddy and DeLaune, 2008). The addition of oxygen as an electron acceptor has been shown to catalyze increases in the mineralization of organic matter, concomitantly increasing concentrations of inorganic N and P (Bridgham et al., 1998; McLatchey and Reddy, 1998; Updegraff et al., 1995). Decomposition of organic material and the release of N and P into the water column could potentially exacerbate nutrient pollution present in deltaic Louisiana and contribute to hypoxic events (Eldridge and Morse, 2008; Bianchi et al. 2008). While studies have acknowledged the importance of inputs of terrestrial organic matter to the coastal zone (Odum, 1968), the magnitude of inputs via coastal wetland submergence has not been well studied. This study aims to understand the fate of soil organic matter, particularly C, N, and P, following sea level-rise induced coastal wetland

submergence. Specifically, the potential mineralization of organic coastal wetland soils with depth under anaerobic conditions (to mimic decomposition rates within an intact marsh), and aerobic conditions (to mimic decomposition rates within a submerging marsh subjected to oxygen-rich seawater) were investigated. We hypothesized that the exposure to oxygen-rich seawater would result in an increase in mineralization potential, concomitant with increases in other indicators of microbial biomass and activity. We expected that these changes would be mediated by depth, with the magnitude of the increase in CO_2 production due to oxygenation decreasing with depth due to the changing ratio of labile: recalcitrant C.

Methods
Study Area

Barataria Bay, a 6,333 km^2 area of shallow open water and coastal wetlands, is located immediately west of the Mississippi River delta and east of Bayou Lafourche in southeastern Louisiana (USA). Salinity concentrations in the salt marsh zone within the bay range from 6 to 22 ppt, depending on season, location, freshwater input, tidal flux, and prevailing winds (Levine et al., 2017; Rakocinski et al., 1992). Tides within the bay are generally diurnal, and average 0.3 m (Conner and Day, 1987). At the time of sampling, percent dissolved oxygen was between 79-108% saturation at 1 m depth in the water column within the bay, and averaged ~8 mg/L from March to May of 2017 (USGS Monitoring Station #07380251; USGS, 2018), representing a well oxygenated system. Hydrologic flux within the bay is dominated by tidal flushing, storm events, and wind-driven circulation, contributing to relatively high dissolved oxygen concentrations within the bay (Conner and Day, 1987). Three marshes were selected for sampling (Figure 6), based on similar hydrologic regimes, ecogeomorphic characteristics, and vegetation communities (i.e, all sites were dominated by *Spartina alterniflora*).
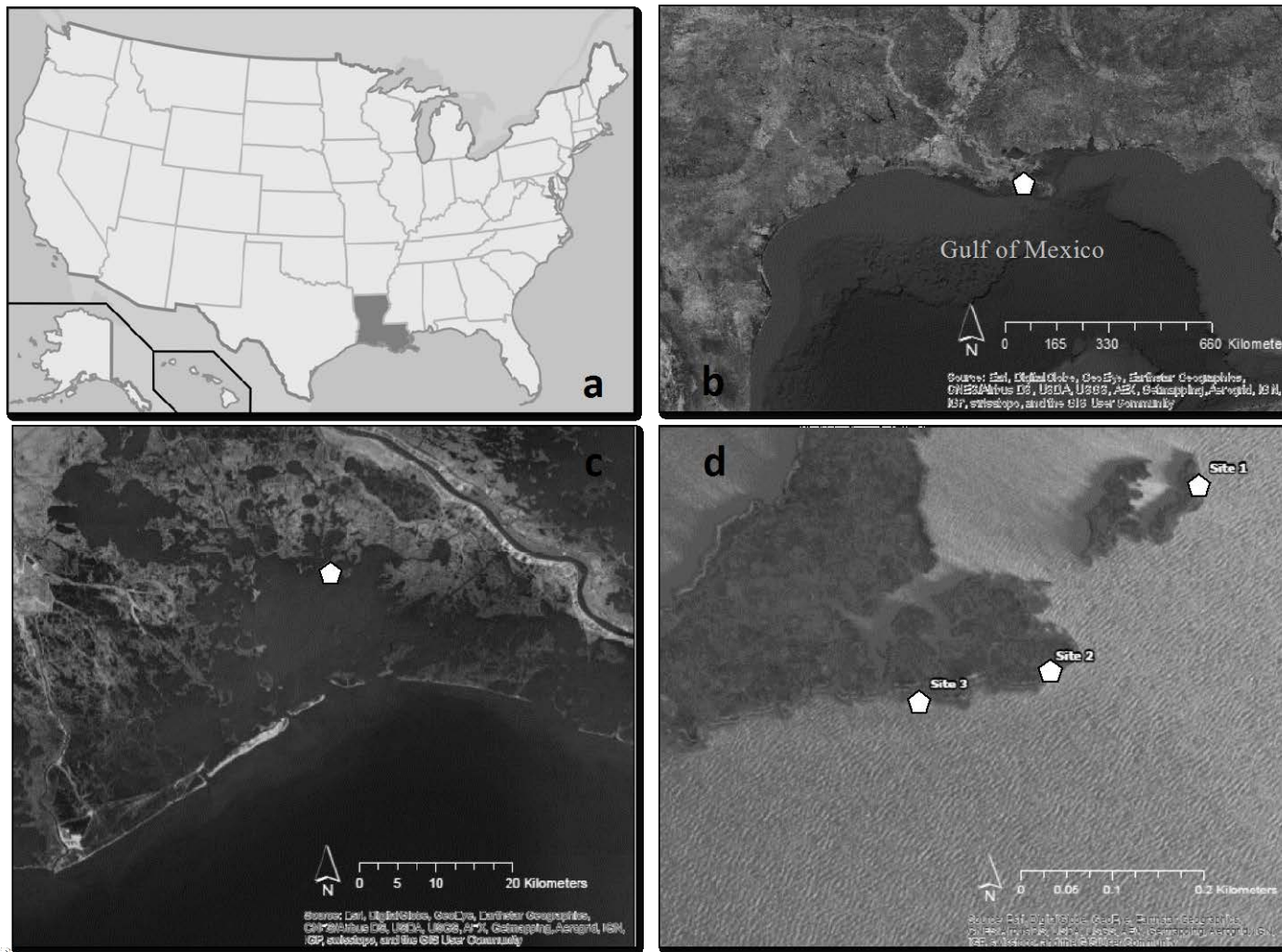
Figure 6: Map of Louisiana (highlighted) within the United States (a), map of the gulf coast of Louisiana (b), map of Barataria Bay, LA (c), and zoomed-in view of sites within the bay (b).

Soil and Water Sampling

All three sites were sampled ~2 weeks apart throughout early spring of 2017. At each of the three sites, one (1) liter of surface water was collected ~10 cm below the water surface. Three (3) soil cores were taken via the push-core method to a depth of 100 cm at each site, 1 m from the coastal edge, within the marsh platform. Each of the nine (9) cores were extruded into 11 depth segments: 0-5, 5-10, 10-20, …, 90-100 cm. Soil samples were placed in sealed polyethylene bags and placed on ice, then immediately transported to the laboratory. Soil and water samples were kept at 4°C until being shipped overnight, on ice, to University of Central Florida for analysis. Site water was filtered through Supor 0.45 µM filters upon arrival.

Soil Physiochemical Properties

Soil bulk density and moisture content were determined by drying a subsample of soil using a gravimetric oven at 70°C after 3 days or until a constant weight was achieved. Dried soils were ground using a SPEX Sample Prep 8000M Mixer/Mill (Metuchen, NJ). Dried, ground subsamples were used to determine percent organic matter using the loss-on-ignition method, where soils were burned at 550°C in a muffle furnace for a total of 3 hours. Following determination of percent organic matter, soils were digested with 50 mL of 1 N HCl at 100°C for 30 minutes, then filtered through Whatman #41 filter paper for total P analysis (Andersen, 1976). Total P content was then determined colorimetrically via an AQ2 Automated Discrete Analyzer (Seal Analytical, Mequon, WI) in accordance with EPA method 365.1 Rev. 2. Total C and N content was determined by use of a Vario Micro Cube CHNS Analyzer (Elementar Americas Inc., Mount Laurel, NJ). Soil pH was determined by creating a 1:5 slurry of soil to distilled, deionized water, and subsequent measurement using an Accument bench top pH probe (Accumet XL200, ThermoFisher Scientific, Waltham, MA, USA).

Greenhouse Gas Production

Soils were homogenized and duplicate subsamples (approximately 7 g) from each depth segment of each core were weighed into 100 mL glass serum bottles. All bottles were capped with a rubber septa and aluminum crimp and evacuated to -75 mmHg. Replicate bottles were randomly assigned to one of two treatments: anaerobic (purged with 99% O_2-free N_2 gas for 3 minutes), or aerobic (purged with Breathing Grade air containing 21% O_2 for 3 minutes). Anaerobic bottles were injected with 14 mL of filtered, N_2-purged site water, while aerobic bottles were injected with 14 mL of filtered, breathing air-purged site water. Bottles were then placed on an orbital shaker at 150 rpm and 25°C. Headspace samples were taken at 1, 2, 4, 7, 10, and 14 day time points, and injected into a GC-2014 gas chromatograph (Shimadzu Instrument, Kyoto, Japan) equipped with a flame ionization detector. Respiration rates were calculated as the change in CO_2 production over time. After each gas sample was extracted from the bottles' headspace, the bottle was purged with either 99% O_2-free N_2 gas or Breathing Grade air for 3 minutes, depending on treatment. Additionally, methane (CH_4) production was analyzed on the same instrument at the same time. However, CH_4 production was generally below detection, and thus results are not discussed.

Following the 14 day incubation, bottles were uncapped, and the remaining soil sample was placed in a 20 mL HDPE scintillation vials for analysis of extractable ammonium (NH_4^+), nitrate (NO_3^-), and soluble reactive phosphorus (SRP), microbial biomass C, and enzyme analysis.

Extractable Nutrient Analysis

Extractable nutrient analyses (DOC, NH_4^+, NO_3^-, and SRP) occurred on soils immediately after field sampling (time zero), and on soils from the bottles after the 14-day

incubation. Rates of potentially mineralizable nutrients were calculated as the extractable

nutrient concentration after the 14-day incubation minus the initial extractable nutrient

concentration, divided by the 14 days. The extraction process consisted of weighing 2.5 g of wet

soil (both from the field and from the bottle incubation) into 40 mL centrifuge tubes and adding

25 mL of 2M KCl. Samples were then shaken continuously on an orbital shaker for one hour at

25°C and 150 rpm, then centrifuged for 10 minutes at 10°C and 5000 rpm. Following the

centrifuge, samples were immediately filtered through Supor 0.45 µM filters and acidified with

double distilled H_2SO_4 to a pH of <2 for preservation. Extractable nutrients samples were then

analyzed using an AQ2 Automated Discrete Analyzer (Seal Analytical, Mequon, WI, EPA

methods 231-A Rev.0, 210-A Rev.1, and 204-A Rev.0).

Microbial Biomass Carbon

Microbial biomass C (MBC) was determined on soils both immediately after the field

sampling and soils from the bottles after the incubation period following the method outlined in

Vance et al. (1987). Duplicates of approximately 1 g dry weight of field-moist soil were weighed

into 40 mL centrifuge tubes and assigned to either a fumigate or non-fumigate treatment. The

fumigated samples were exposed to gaseous chloroform for 24 hours in a glass desiccator. After

24 hours, the samples were extracted with 25 mL of 0.5 M K_2SO_4, placed in an orbital shaker for

one hour at 25°C and 150 rpm. After incubation, samples were immediately centrifuged for 10

minutes at 10°C and 5000 rpm. The supernatant was vacuum filtered through Supor 0.45 µM

filters, acidified with double distilled H_2SO_4 for preservation, and stored at 4°C until analysis.

Non-fumigate samples were processed in the same manner, excluding the chloroform

fumigation. Dissolved organic carbon (DOC) was determined by use of a Shimadzu TOC-L

Analyzer (Kyoto, Japan). Microbial biomass C was calculated as the difference between the fumigated samples and the non-fumigated samples.

Enzyme Activity

Extracellular enzyme assays were performed to determine activity of β-glucosidase (BG), N-acetyl-beta-D-glucosaminidase (NAG), alkaline phosphatase (AP), β-xylosidase (XY), and β-cellobiosidase (CB). Similar to extractable nutrients and microbial biomass C, extracellular enzyme assays were performed on both initial soil samples after they were retrieved from the field, and soils following the bottle incubation. Assays were conducted using fluorescent substrate 4-methylumbelliferone (MUF) for standardization and fluorescently labeled MUF-specific substrates (German et al., 2011). To create a 1:100 slurry, 0.5 g of soil was added to 39 mL of autoclaved distilled deionized water and shaken continuously on an orbital shaker for 1 hour at 25°C and 150 rpm. Fluorescence was measured at excitation/emission wavelengths 360/460 on a BioTek Synergy HTX (BioTek Instruments, Inc., Winooski, VT, USA) both immediately after substrate and sample were added, and 24 hours later to determine a rate of enzyme activity.

Statistical Analysis

All statistical analysis was performed using R (R Foundation for Statistical Computing, Vienna, Austria) within RStudio (RStudio Team, 2015). Prior to determining significance, all parameters were analyzed for homogeneity of variance using Levene's test, and assumptions of normality using the Shapiro-Wilk test. If datasets were not normal, they were transformed using a logarithmic transformation to meet the assumptions of normality.

Data was separated into field characteristics (before the incubation), and experimental results (following the incubation). Field characteristics were analyzed using a linear mixed-effect

model in R with site and depth as predictor variables. 'Core' was included as a random effect to test for effects of replicate cores taken at each site. Post-hoc tests were conducted using package lsmeans via the Tukey method. Pearson product-moment correlations were also performed between all field characteristics. Significance was determined based on an alpha value of 0.05 for all tests, and adjusted with a Bonferroni correction to 0.004.

Experimental results were analyzed via a linear mixed-effect model in R with treatment, depth, the interaction between treatment and depth, and site as predictor variables. Core was again included as a random effect. The lsmeans package was used to determine post-hoc significance based on the Tukey method. Significance was determined based on an alpha value modified by a Bonferroni correction to 0.004.

Results
Field Characteristics
Physiochemical Data

Moisture content changed significantly with depth, ranging from 63.5 ± 2.0 % at the surface (0-5 cm) to 85.5 ± 0.5% at 70-80 cm and generally increasing with depth (Table 6). Moisture content was negatively correlated to bulk density, and strongly positively correlated to organic matter content, total N, total C, and extractable NO_3^- (Table 2). Moisture content was weakly correlated to NAG, AP, BG, and XY activity (Table 2). Depth was also a significant predictor variable for bulk density, ranging from 0.21 ± 0.2 g cm^{-3} at 20-30 cm to 0.07 ± 0.1 g cm^{-3} at 70-80 cm (Table 6). Organic matter content, total C and total N were all correlated to each other, and with depth (Table 6, Table 7). Within the 0-50 cm depth intervals, organic matter content averaged 19.1 ± 0.74 % (Figure 7). Deeper than 50 cm, organic matter content averaged 43.9 ± 2.3 %. Total N displayed the same trend, with lower values in the top 50 cm (4.41 ± 0.22 g kg^{-1}), and higher values in the bottom 50 cm (11.1 ± 0.59 g kg^{-1}).
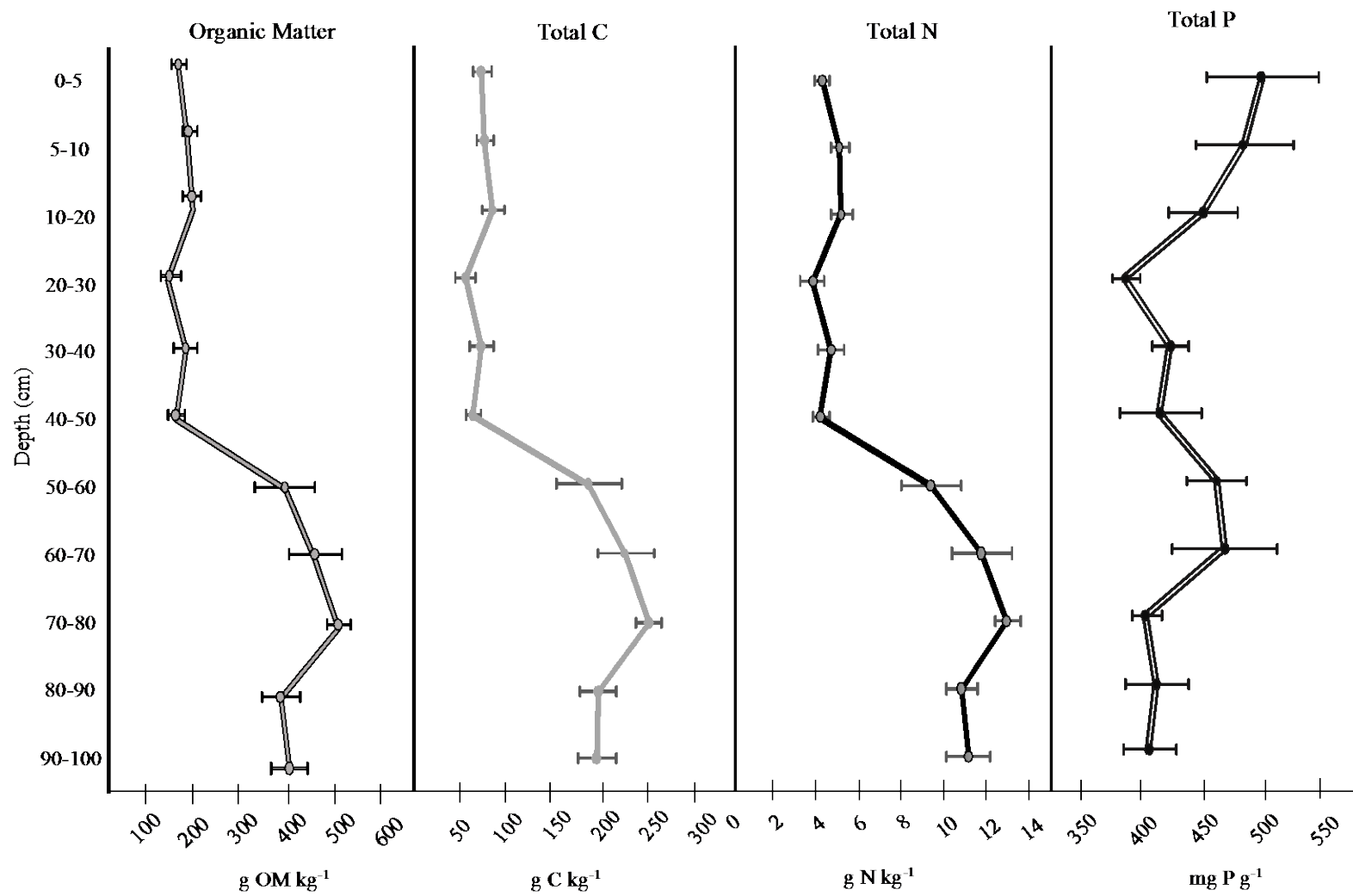
Figure 7: Organic matter, total C, total N, and total P concentrations in soil with depth. Values shown are mean ± standard error (n=9).

Table 6: p-values associated with each parameter tested using linear model. α = 0.004. Values in bold denote significance. Ext. refers to 'extractable'.

	% OM	Total C	Total N	Total P	NAG	AP	BG	XY	CB	Ext. DOC	Ext. NO_3^-	Ext. NH_4^+	MBC
					Field Characteristics								
Site	0.5426	0.6638	0.0876	**0.0276**	**<0.0001**	**0.0001**	**0.0001**	**<0.0001**	**<0.0001**	0.9679	0.5252	0.6327	0.006
Depth	**<0.0001**	**<0.0001**	**<0.0001**	0.0966	**<0.0001**	0.0131	0.0301	**0.0026**	0.2084	**0.0001**	**<0.0001**	**<0.0001**	**<0.0001**

	NAG	AP	BG	XY	CB	MBC	CO₂ Production	PMN
				Experimental Results				
Treatment	**0.0025**	0.5799	0.1494	0.0565	0.2387	0.4851	**0.0003**	**0.0001**
Depth	**<0.0001**	**<0.0001**	**<0.0001**	**0.0029**	**0.0017**	**<0.0001**	**<0.0001**	0.0205
Site	0.6569	0.9153	**<0.0001**	**<0.0001**	**<0.0001**	**0.0001**	**<0.0001**	**<0.0001**
*Treatment*Depth*	0.361	0.2974	0.285	0.8464	0.8674	0.5585	0.9245	**<0.0001**

Table 7: Correlation matrix including Pearson product-moment correlations between field characteristics. Degrees of freedom = 99. α = 0.05.

Critical value = 0.197. Values in bold are significant, while values that are bold and underlined denote strong significance (critical value > 0.8).

Ext. refers to 'extractable'.

	Moisture Content	Bulk Density	pH	%OM	TC	TN	TP	NAG	AP	BG	XY	CB	Ext. DOC	Ext. NO$_3^-$	Ext. NH$_4^+$	Ext. SRP
Bulk Density	**_-0.85_**															
pH	**0.26**	**-0.27**														
%OM	**_0.90_**	**_-0.81_**	**0.27**													
TC	**_0.91_**	**_-0.82_**	**0.29**	**_0.98_**												
TN	**_0.90_**	**_-0.84_**	**0.33**	**_0.96_**	**_0.98_**											
TP	0.05	-0.05	**-0.42**	0.05	0.07	0.05										
NAG	**0.36**	**-0.34**	0.14	**0.49**	**0.47**	**0.42**	0.19									
AP	**0.34**	**-0.32**	0.14	**0.40**	**0.41**	**0.45**	0.17	**0.52**								
BG	**0.30**	**-0.27**	0.07	**0.39**	**0.36**	**0.33**	0.19	**0.69**	**0.27**							
XY	**0.44**	**-0.36**	0.10	**0.53**	**0.51**	**0.46**	0.11	**0.75**	**0.36**	**0.69**						
CB	0.19	-0.13	-0.16	**0.25**	**0.22**	0.18	**0.27**	**0.57**	**0.20**	**0.62**	**_0.83_**					
Ext. DOC	**0.53**	**-0.45**	0.13	**0.52**	**0.54**	**0.53**	0.02	**0.23**	**0.26**	**0.23**	**0.25**	0.08				
Ext. NO$_3^-$	**_0.81_**	**-0.70**	**0.29**	**_0.82_**	**_0.83_**	**_0.84_**	0.08	**0.30**	**0.29**	0.19	**0.24**	0.01	**0.39**			
Ext. NH$_4^+$	-0.15	-0.01	0.13	-0.10	-0.09	-0.10	0.00	-0.10	-0.08	-0.12	-0.09	-0.03	-0.11	-0.13		
Ext. SRP	0.15	-0.09	-0.03	0.15	0.16	0.19	0.05	0.01	0.09	0.03	-0.01	-0.06	0.04	**0.23**	-0.18	
Microbial C	**_0.81_**	**-0.72**	**0.29**	**_0.84_**	**_0.85_**	**_0.87_**	0.13	**0.44**	**0.47**	**0.41**	**0.44**	**0.20**	**0.52**	**0.76**	-0.12	0.17

Table 8: Soil physiochemical parameters by site (averaged over depth intervals) ± standard error (n=33). Site was not a significant predictor variable for any soil physiochemical parameters.

Site	Moisture Content	Bulk Density (g cm^{-3})	pH	% Organic Matter	Total C (g kg^{-1})	Total N (g kg^{-1})	Total P (g kg^{-1})
1	0.74 ± 0.01	0.14 ± 0.01	7.10 ± 0.11	28.06 ± 2.17	135.12 ± 11.43	6.55 ± 0.52	429.75 ± 11.86
2	0.75 ± 0.02	0.14 ± 0.01	7.10 ± 0.11	32.24 ± 2.86	152.51 ± 15.74	7.62 ± 0.72	478.48 ± 23.75
3	0.73 ± 0.02	0.13 ± 0.01	7.68 ± 0.05	30.77 ± 3.40	152.16 ± 18.02	8.14 ± 0.91	430.92 ± 9.53

Similarly, total C averaged 85.0 ± 3.9 g kg^{-1} in the upper 50 cm and 220.5 ± 11.4 g kg^{-1} in the lower 50 cm. Both total C and N were significantly correlated to NAG, AP, BG, and XY activity, as well as extractable NO_3^- (Table 7). Total P was not significant with depth (Table 6). Also, site was not a significant predictor variable for any physiochemical measurement (Table 8).

Enzyme Activity

Site was a significant predictor variable for all measured enzyme activities (Table 6). N-acetyl-beta-D-glucosaminidase activity ranged from 17.7 ± 1.60 nmol MUF g^{-1} min^{-1} at site 2, and 3.18 ± 0.54 nmol MUF g^{-1} min^{-1} at site 1. The lowest enzyme activity was consistently measured within site 1. Alkaline phosphatase activity at site 1 was 2.94 ± 0.32 nmol MUF g^{-1} min^{-1}. Comparatively, XY activity was 1.69 ± 0.15 nmol MUF g^{-1} min^{-1} and CB activity was 1.54 ± 0.25 nmol MUF g^{-1} min^{-1}. The greatest AP activity was within site 3, where activity was 19.6 ± 4.64 nmol MUF g^{-1} min^{-1}. CB and XY activity were greatest within site 2. β-glucosidase activity was lowest within site 1, at 4.98 ± 0.48 nmol MUF g^{-1} min^{-1}, and greatest within site 2, at 22.61 ± 1.98 nmol MUF g^{-1} min^{-1}.

Additionally, soil depth affected all enzymes except for CB (Table 1). All enzymes showed a similar trend with depth (Figure 8). Within the top 50 cm, activity generally decreased from the surface. However, at 50-60 cm, activity increased approximately 50% compared to the 0-5 cm depth interval, then gradually decreased. N-acetyl-beta-D-glucosaminidase activity ranged from 5.69 ± 1.91 nmol MUF g^{-1} min^{-1} at 90-100 cm to 29.2 ± 7.81 nmol MUF g^{-1} min^{-1} at 50-60 cm. Alkaline phosphatase activity was lowest at the 90-100 cm depth, where activity was 6.85 ± 1.66 nmol MUF g^{-1} min^{-1}, and greatest within the 60-70 cm depth interval, where activity was 27.2 ± 13.9 nmol MUF g^{-1} min^{-1}. Activity of BG ranged from 5.22 ± 1.14 nmol MUF g^{-1} min^{-1} at 90-100 cm to 32.6 ± 13.6 nmol MUF g^{-1} min^{-1} at 50-60 cm.
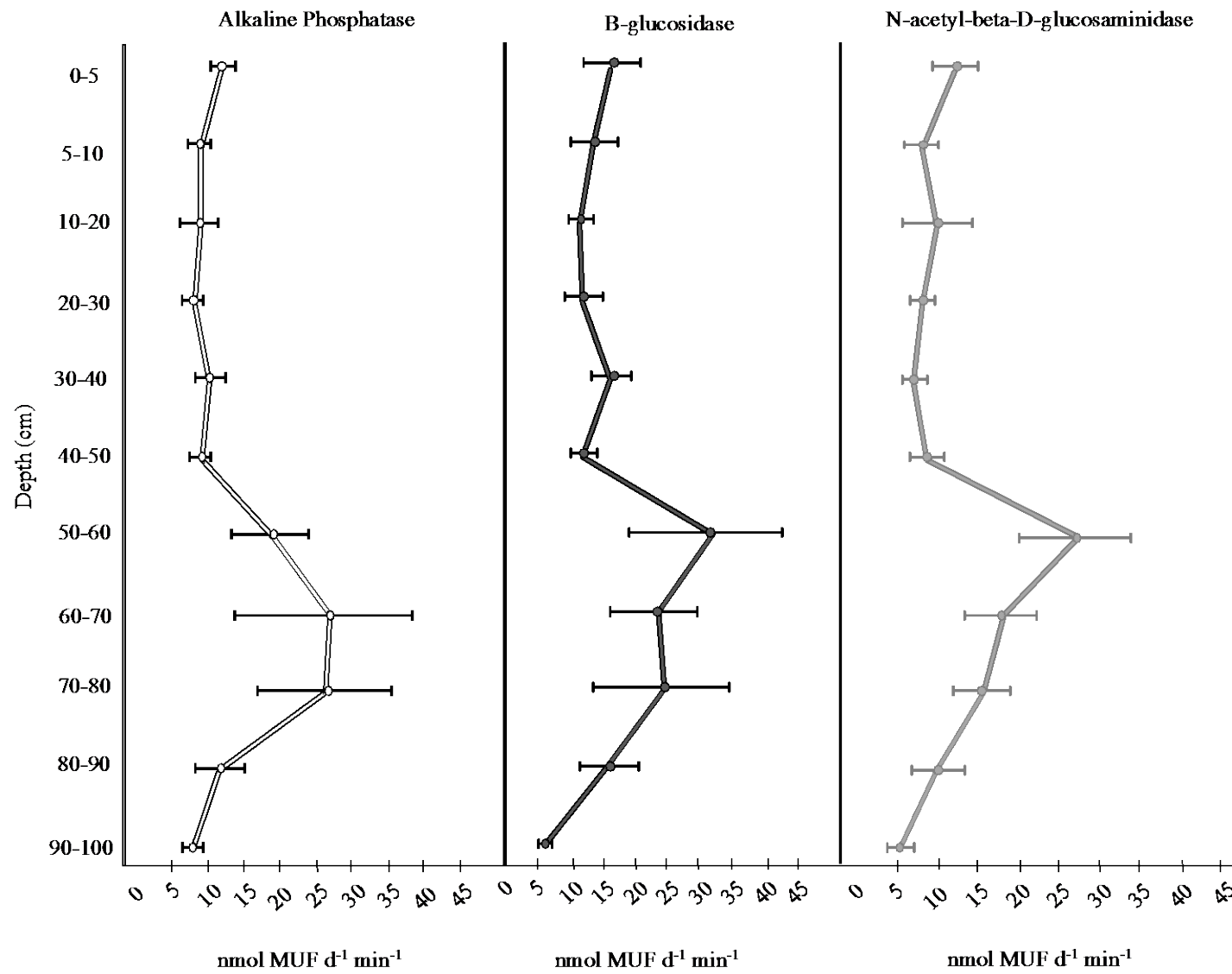
Figure 8: Initial (field) AP activity, BG activity, and NAG activity with depth. Values shown are mean ± standard error (n=9).

Xylosidase activity at the 90-100 cm depth was lowest, at 2.83 ± 0.84 nmol MUF g^{-1} min^{-1}, while the 50-60 cm depth was highest, at 8.30 ± 2.97 nmol MUF g^{-1} min^{-1}. Microbial biomass C strongly correlated with all enzyme activity (Table 7). Additionally, NAG, AP, and XY activity significantly correlated to extractable NO_3^- (Table 7). All enzyme activities were significantly correlated to each other (Table 7).

Microbial Biomass C

Microbial biomass C was significantly affected by both site and depth (Table 6). The highest MBC concentrations were found at site 3, with $5,904 \pm 630$ mg kg^{-1}, and lowest at site 1, with $4,225 \pm 279$ mg kg^{-1}. In terms of depth, MBC was generally similar from 0-5 cm to 40-50 cm, averaging $3,504 \pm 207$ mg kg^{-1} (Figure 9). Below 50 cm, MBC averaged $7,377 \pm 393$ mg kg^{-1}. Microbial biomass C was significantly correlated to both extractable NO_3^- and extractable NH_4^+ concentrations (Table 7).

Extractable Nutrients and DOC

Extractable NO_3^- displayed a similar trend to the enzyme activity and MBC data - concentrations were lowest between 0-5 cm and 40-50 cm, then increased below 50 cm (Figure 10). The lowest extractable NO_3^- concentrations were found at 40-50 cm, 1.61 ± 0.19 mg kg^{-1}, while the highest concentrations were 5.38 ± 0.17 mg kg^{-1} at the 70-80 cm depth. Though depth significantly affected extractable NO_3^- values, site was insignificant (Table 6). Extractable NH_4^+ was significant with depth (Table 6), ranging from 22.6 ± 7.89 mg kg^{-1} at the surface to 1.94 ± 0.30 mg kg^{-1} at 30-40 cm. Extractable DOC was significantly affected by depth (Table 6), and ranged from 163 ± 13.5 mg kg^{-1} at 0-5 cm to 608 ± 52.5 mg kg^{-1} at 60-70 cm. Extractable DOC exhibited a similar trend to extractable NO_3^-, enzyme activity, and MBC. Extractable SRP was consistently below detection (data not shown).
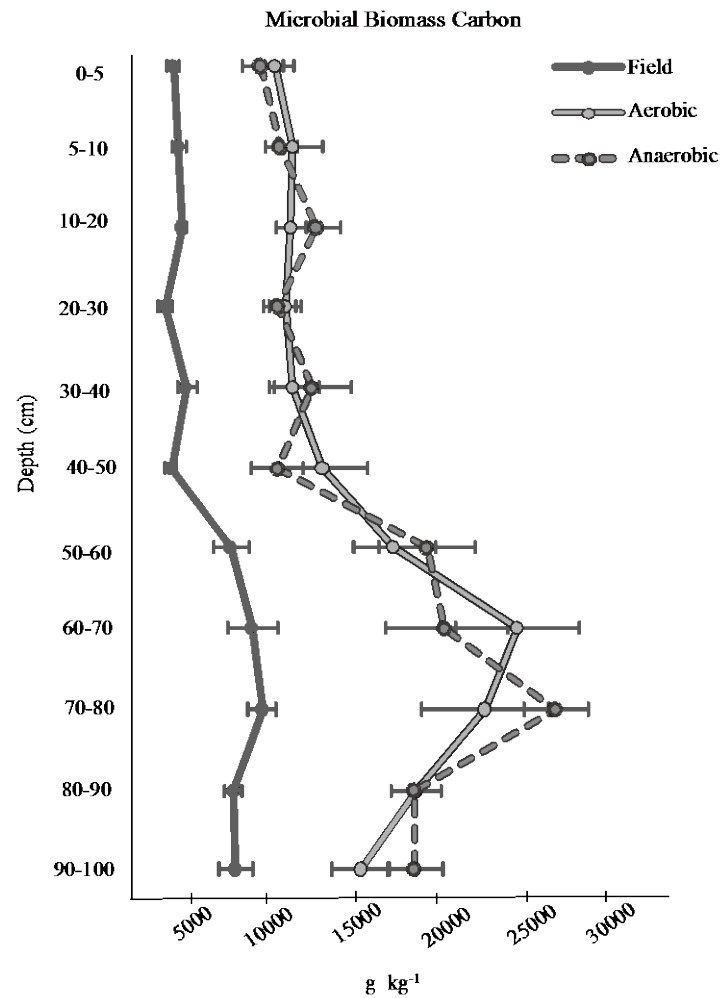
Figure 9: Initial (field) microbial biomass C, aerobic MBC, and anaerobic MBC concentrations with depth. Values shown are mean ± standard error (n=9).
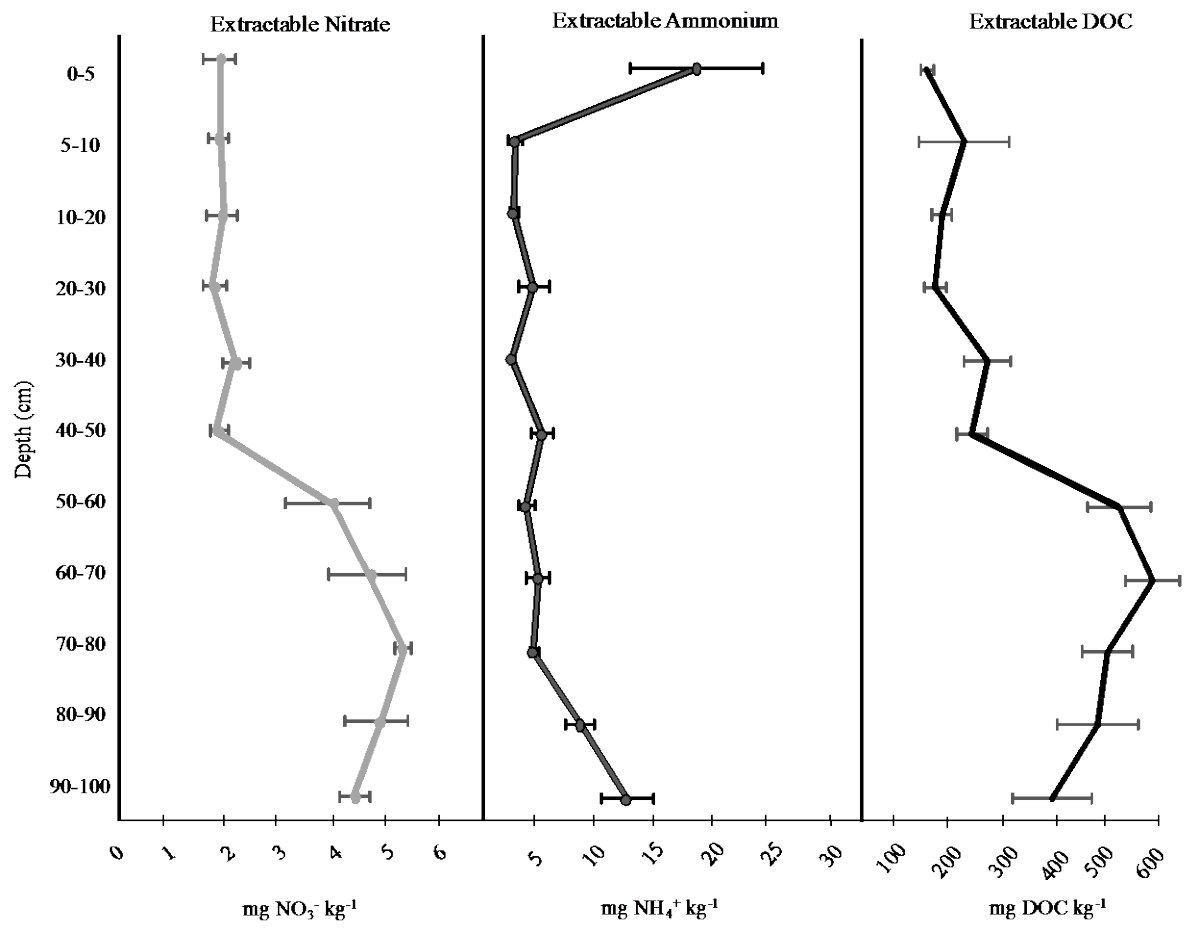
Figure 10: Initial (field) extractable nitrate, extractable ammonium, and extractable DOC concentrations with depth. Values shown are mean ± standard error (n=9).

Experimental Results

Carbon Dioxide Production

        Treatment and depth were both significant predictor variables for CO_2 production (Table 6). The anaerobic treatment was consistently lower than the aerobic treatment. To account for the effects of the bottle incubation, the difference in CO_2 production between the aerobic and anaerobic treatment was calculated. In general, the difference in CO_2 production between the two treatments increased with depth, ranging from 0.69 ± 0.20 mg CO_2-C kg^{-1} hr^{-1} within the 10-20 cm depth interval to 9.06 ± 0.97 mg CO_2-C kg^{-1} hr^{-1} within the 90-100 cm depth interval (Figure 11).
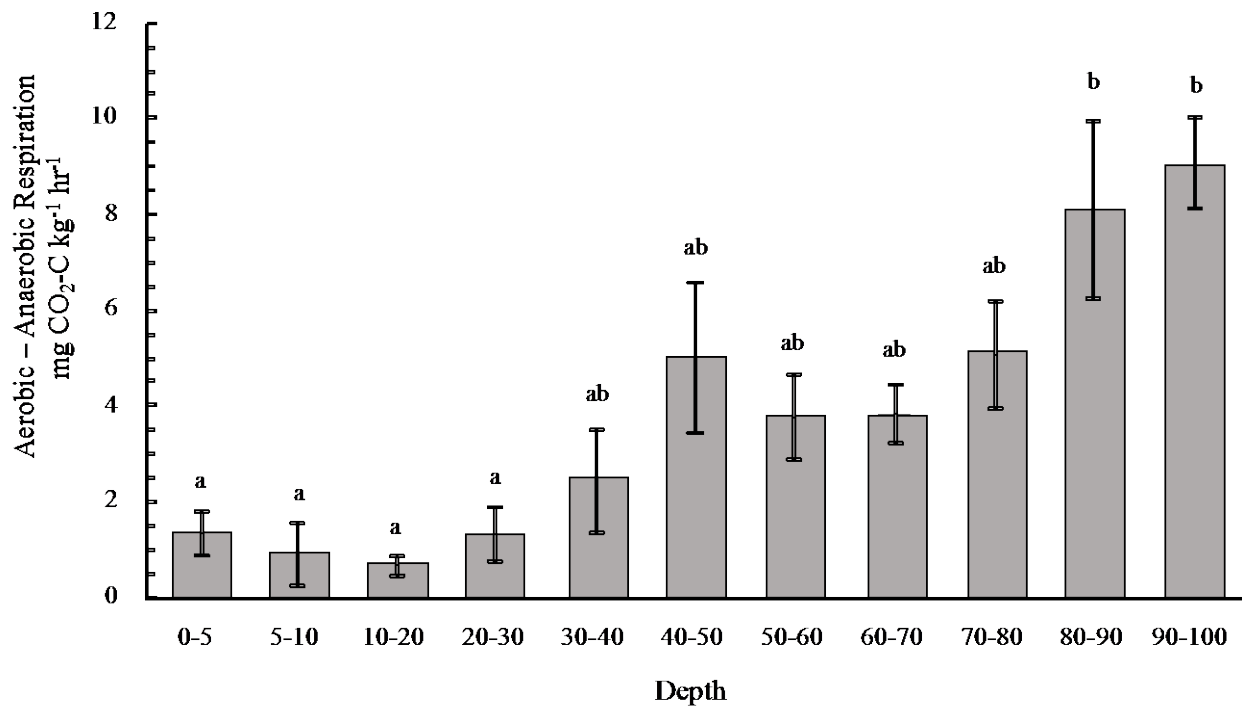
Figure 11: Difference in respiration between aerobic treatments and anaerobic treatments (aerobic respiration – anaerobic respiration) by depth. Values shown are mean ± standard error (n=9). Letters indicate significant differences between depths ($p < 0.05$).

Enzyme Activity

Treatment did not significantly affect any enzyme activity except for NAG (Table 6). N-acetyl-beta-D-glucosaminidase activity was significantly higher in the anaerobic treatment, 29.9 $\pm$ 2.47 nmol MUF g^{-1} min^{-1}, than the aerobic treatment, 21.2 $\pm$ 1.84 nmol MUF g^{-1} min^{-1}. Following the incubation, depth still significantly affected all enzyme activities (Table 6), which showed the same trend as the initial/field enzyme activities. Within the first 50 cm, NAG and AP activity averaged 16.8 $\pm$ 1.60 nmol MUF g^{-1} min^{-1} and 10.5 $\pm$ 0.47 nmol MUF g^{-1} min^{-1}, respectively. From 50-100cm, activity of NAG increased to an average of 36.1 $\pm$ 1.04 nmol MUF g^{-1} min^{-1}, while AP activity averaged 27.0 $\pm$ 0.74 nmol MUF g^{-1} min^{-1}. β-glucosidase activity ranged from 15.7 $\pm$ 2.05 nmol MUF g^{-1} min^{-1} at 90-100 cm to 41.6 $\pm$ 4.03 nmol MUF g^{-1} min^{-1} at 70-80 cm. Activity of XY was lowest at 5-10 cm, where activity averaged 3.45 $\pm$ 0.81 nmol MUF g^{-1} min^{-1}, and greatest at 50-60 cm, where activity averaged 12.9 $\pm$ 2.65 nmol MUF g^{-1} min^{-1}. CB activity ranged from 9.88 $\pm$ 1.73 nmol MUF g^{-1} min^{-1} at 60-70 cm to 3.64 $\pm$ 0.62 nmol MUF g^{-1} min^{-1} at 40-50 cm. Activity of BG, XY, and CB were significant with site (Table 1). Both XY and CB activity were greatest at site 2, while BG activity was highest within site 3.

Microbial Biomass C

Microbial biomass C was not significantly affected by treatment but was affected by both depth and site (Table 6). Within site 3, MBC was greatest, averaging 15,952 $\pm$ 1,513 mg kg^{-1}, though not significantly different from site 2. Similar to enzyme activity, MBC concentrations were lower between the surface (0-5 cm) and 50 cm, then increased roughly 2x from 50 to 100 cm.
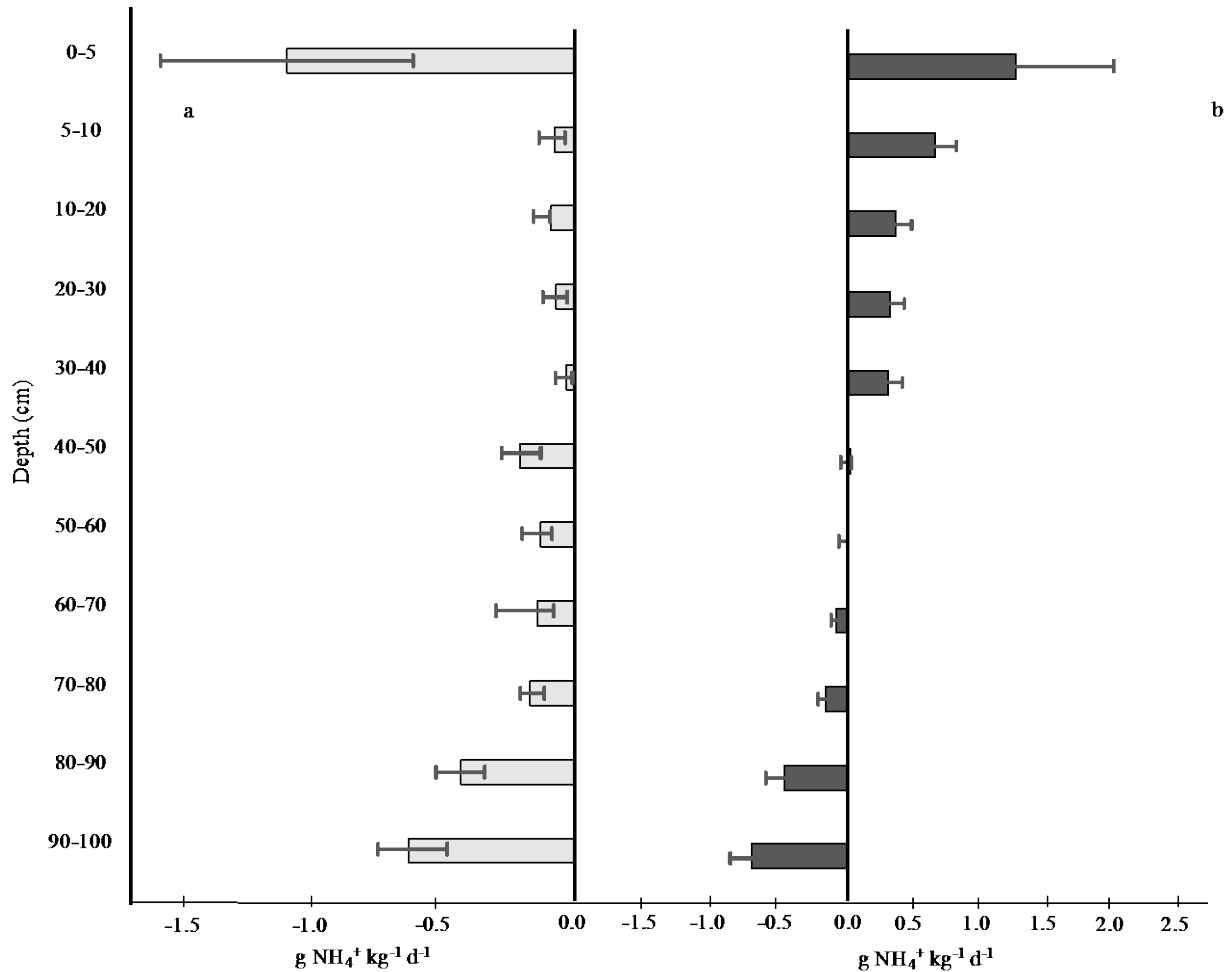
Figure 12: Rates of potential aerobic ammonium (a) and anaerobic ammonium (b) mineralization with depth. Negative rates indicate immobilization, while positive rates indicate mineralization. Values shown are mean ± standard error (n=9).

Potentially Mineralizable Nutrients

Rates of potentially mineralizable NH_4^+ (PMN) were significantly different with the interaction between treatment and depth (Table 6). Within the aerobic treatment, the rates of PMN ranged from -0.03 ± 0.03 mg NH_4^+ d^{-1} at 30-40 cm to -1.31 ± 0.49 mg NH_4^+ d^{-1} at 0-5 cm. Negative rates of PMN indicate net immobilization of NH_4^+, rather than mineralization. Within the anaerobic treatment, PMN rates were positive from 0-40 cm, and negative from 50 cm to 100

55

cm (Figure 12). Extractable SRP was generally below detection, and thus PMP rates could not be calculated.

Discussion
Field Characteristics

Soil organic matter, total C, total N, and extractable DOC all exhibited the same trend, remaining relatively consistent from 0-50 cm, and then increasing at 50 cm (Figure 7). Surprisingly, this trend is exhibited at all cores collected at all three sites, indicating that the increase in organic matter is not an isolated occurrence, but may be an artifact of the region's

history. Barataria Bay is a highly dynamic area, impacted by both anthropogenic disturbances and high-energy storm events. Prior to the early 1900s, Barataria Bay was hydrologically connected to Bayou Lafourche, which supplied freshwater to the wetlands within the bay (Conner and Day, 1987; DeLaune and Lindau, 1987). A study by DeLaune (1981) examining C isotopes present within the soil to a depth of 130 cm indicated that the current brackish marshes of Barataria Bay were once freshwater marshes, exhibiting the low $\delta^{13}C$ values associated with freshwater marsh vegetation. The hydrologic isolation of Barataria Bay from the freshwater inputs of Bayou Lafourche in 1904 altered the salinity regime of these sites, causing the marshes to become brackish (Conner and Day, 1987). The C-rich soil was then buried under a thin layer of mineral sediment, and brackish vegetation colonized the sites, leading to the deposition of less organic C into the soil matrix, likely associated with a greater tidal influence (Delaune, 1986; Reddy and DeLaune, 2008). Total phosphorus does not reflect this trend, and instead exhibits relatively stable concentrations with depth. Unlike C and N, the P cycle is tightly coupled to sorption and desorption with mineral components, flocculation and dissolution,

leaching, and uptake by macrophytes, any of which could influence total P concentrations with depth (Reddy et al., 1999).

Similarly, depth significantly impacted all measured parameters of soil microbial activity (Figures 3 and 4). It is generally accepted that the maximum amount of soil microbial activity occurs in the surficial soils (0-10 cm) or within the rhizosphere of wetlands (Brix, 1987; Reddy et al., 1989). These hot spots of microbial activity are facilitated by oxygen diffusion into the soil matrix from the atmosphere or water column, as well as oxygen leaking out of the roots of wetland macrophytes to create a 2-3 mm thick oxidized rhizosphere (Brix, 1987; Reddy and DeLaune, 2008). However, in this study, the most microbially-active soil depths in the field were between 50-100 cm, substantially deeper than expected. Microbial biomass C increased nearly 50% between the 0-5 cm and 50-60 cm depths; NAG and BG enzyme activity and CO_2 production mirrored this increase, indicating that microbial activity can be greater at these depths than has been previously documented (Blume et al., 2002; Fierer et al., 2003). The increase microbial activity at depth is likely related to both the greater quality and quantity of organic matter and associated nutrients at depth. Activity of BG at these sites was roughly 3x greater than activity reported in a similar soil at a depth of 0-5cm (Chambers et al. 2016). However, due to the small number of studies that have quantified rates of enzyme activity in brackish marsh soils, it is difficult to compare our rates to other systems.

Despite the abundance of organic matter found at depth in this study, anaerobic respiration in deep soils is typically limited by the availability of alternate electron acceptors, such as NO_3^- (Reddy and DeLaune, 2008; Figure 12). Generally, NO_3^- present at depth within brackish wetlands is consumed preferentially over sulfate and lost via denitrification, the microbially-mediated anaerobic reduction of nitrogenous oxides to nitrogen gas (Tiedje, 1982).

Denitrification rates within the brackish marsh of Barataria range from 44.6 to 2,158 μmol m^{-2} d^{-1} (Smith and DeLaune, 1983), and more specifically, the denitrification rate at one of the sampling locations was 9.3 ± 0.3 mg N_2O-N kg^{-1} h^{-1} (Pietroski et al., 2015). Though these rates would support a high removal of NO_3^-, measured extractable NO_3^- concentrations peaked between 50 -100 cm at all three sites, indicating that nitrate is not being denitrified by the resident microbiota. Extractable nitrate values ranged from 0.79 - 1.25 mg L^{-1} between 50-100cm, roughly half the concentration within the Mississippi River during spring floods (Turner and Rabalais, 1991). The presence of NO_3^-, combined with high rates of microbial activity, could indicate subsurface tidal flushing at these depths. Horizontal subsurface flow of seawater through the marsh platform has been observed within tidal marshes, and is often aerobic, contributing to the oxidation of iron within the soil matrix (Harvey et al., 1987; Huettel et al., 1998; Mann and Wetzel, 1995; Osgood, 2000; Taillefert et al., 2007). Subsurface flushing of seawater close to the marsh edge (1 m inland) could catalyze increases in CO_2 production, decreases in denitrification rates, and promote the mineralization of bioavailable N and P. Moreover, subsurface tidal flushing may also destabilize the marsh platform, accelerating marsh collapse and submergence.

CO$_2$ Production

Oxygen is an electron acceptor thermodynamically favored over all other pathways of microbial respiration. As such, the addition of oxygen to soil microcosms increased CO_2 production at all depths within all sites, relative to the anaerobic treatment. However, the difference in respiration between treatments at the 90-100 cm depth was roughly 4x greater than respiration at the soil surface (Figure 11), indicating exposure to O_2 accelerated soil respiration in deep soils to a much greater extent than in shallow soils. Though the chemical structure of

present C was not directly measured, CO_2 production within both treatments increased at depth, indicating that the available soil C was readily decomposable, regardless of oxygen availability. Similar to MBC and enzyme activity, CO_2 production may be influenced by the site history and the availability of organic matter. Taking into account soil density, the differences in potential CO_2 production rate between the surface and deeper depths becomes more striking: 8.86 µg of CO_2-C cm^{-3} h^{-1} is potentially lost within the 0-5 cm depth interval, while 95.1 µg of CO_2-C cm^{-3} h^{-1} could be lost within 90-100 cm, a 10x difference in CO_2 loss. This disparity is due to the greater density of total C present deeper within the soil profile.

<div align="center">Nitrogen and Phosphorus Mineralization Rates</div>

An increase in respiration from an influx of oxygenated seawater can potentially mineralize inorganic forms of N and P during the degradation of organic compounds. Within the aerobic treatment, all potentially mineralized NH_4^+ was converted to NO_3^-, likely through nitrification, an oxidative process. From the soil surface to 50 cm, net mineralization of NH_4^+ was positive within the anaerobic treatment, though the magnitude decreased with depth, indicating that NH_4^+ is being released with respiration (Figure 12). Immobilization, the transformation of inorganic forms of N to organic forms, was the dominant process deeper than 50 cm. Net immobilization suggests that the present N was being assimilated into the microbial biomass, which increased simultaneously to support increased decomposition of available C (Figure 4). Owing to the observed increase in CO_2 production with depth in both treatments, we expected to see a concurrent release of nutrients (McLatchey and Reddy, 1998). The net N immobilization observed may be an artifact of the experimental design, as increasing microbial biomass C during the incubation period greatly enhanced the demand for inorganic N. Potentially mineralizable P was also quantified, but SRP concentrations were generally below detection.

Site History

Variable content of soil organic matter with depth was strongly correlated with measurements of microbial activity in this study, suggesting that site history (e.g. shifts in plant litter quality and quantity, hydrology, and depositional patterns over time) impacted current ecosystem functioning. These currently brackish marshes developed above previously existing freshwater marshes through the processes of burial and accretion with time, driven by shifts in inundation and salinity regimes (Delaune, 1986). The dynamic temporal nature of coastal ecosystems and plant communities has been documented by others, which have similarly observed different soil types and plant communities with depth (Brinson et al., 2018; Hussein, 2009; Mackie et al., 2005). These shifts in dominant vegetation preserved within the coastal wetland soils continue to occur as a result of sea level rise and climatic change (e.g., mangrove encroachment into salt marshes; Kelleway et al., 2017), and can be further accelerated by anthropogenic hydrologic modifications, such as levees and freshwater diversions (Delaune, 1986; Nyman et al., 1990). Therefore, although the results of this study are specific to this region's unique site history of hydrologic isolation, similar patterns of shifting organic matter content and quality with depth can be expected in many coastal wetlands, underlining the need to sample deeper into the soil profile to fully understand the consequences of wetland erosion and submergence on stored C and nutrients.

Conclusions

In organogenic wetlands, submergence induced by sea level rise endangers the large stocks of C sequestered within coastal soil. Though the general paradigm within wetland science is that the degradability of soil organic matter decreases with depth (Gale and Gilmour, 1988; Maltby, 1988; Mendelssohn et al., 1999; Schipper and Reddy, 1995; Schipper et al., 2002; Webster and Benfield, 1986), this study challenges that assumption: increases in enzyme

activity, microbial biomass C, and CO_2 production at depth indicates the sequestered C is not particularly recalcitrant (Reddy and DeLaune, 2008; Stevenson and Cole, 1999). Our findings indicate these deeper (>50 cm) organic matter stocks can be vulnerable to mineralization, especially following wetland erosion and submergence. More specifically, aerobic conditions, which could be stimulated by the availability of dissolved oxygen within seawater, can increase CO_2 production by 66% relative to the anaerobic conditions that typically pervade in an intact marsh. This potential increase in mineralization results in a loss of organic C within the soil matrix, increasing global warming potential of these marshes. For example, if just 25% of the organic C present within 1 m of the soil profile is mineralized due to submergence and mixing with oxygenated seawater, we can expect approximately 8,472 – 11,866 Gg of C released to the atmosphere annually from this region of coastal LA, based on the mass of C present in these soils.

Additionally, this study highlights the need to collect and study deeper soil cores within dynamic coastal wetland environments. Often, soil cores are collected to shallower depths (i.e. 20 or 30 cm; Gardner and White, 2010; Levine et al., 2017; Marton and Roberts, 2014), owing to the assumption that most microbial activity happens at the surface (DeLaune, 2013). However, many coastal wetland systems have undergone decades of change, including shifts in vegetation communities and deposition patterns, requiring deeper sampling and an understanding of site history to fully determine the implications of submergence on the global C cycle.

CHAPTER FOUR: ASSESSING THE DEGRADABILITY OF DEEP SOIL ORGANIC MATTER IN SUBMERGING COASTAL WETLANDS

Abstract

High rates of relative sea level rise can cause coastal wetland submergence, jeopardizing the stability of soil organic matter (SOM) sequestered within wetlands. Following submergence, SOM can be lost through mineralization, exported into the coastal ocean, or reburied within adjacent subtidal sediments. By combining measures of soil physicochemical properties, microbial community abundance, organic carbon fractionation, and stable isotope signatures, this study characterized subsurface SOM within a coastal wetland to inform its potential fate under altered environmental conditions. Nine soil cores were collected to a depth of 150 cm from a wetland currently experiencing rapid erosion and submergence within Barataria Bay, LA (USA), and were sectioned into 10 cm intervals. Each soil segment was analyzed to determine total carbon (C), nitrogen (N), phosphorus (P), and stable isotope ($\delta^{13}C$ and $\delta^{15}N$) content, as well as extractable ammonium (NH_4^+), nitrate (NO_3^-), and soluble reactive phosphorus (SRP). Extractable NH_4^+ and SRP concentrations increased 7x and 11x, respectively, between 0-10 cm and 130-140 cm. Through quantitative PCR, number of gene copies of bacteria and sulfate reduction genes were found to decrease with depth while there was no change in number of gene copies of archaea. This study also demonstrated only small decreases in labile:refractory C ratios with depth; by combining $\delta^{15}N$ data with labile:refractory C ratios and no observed change in C:N ratios with depth, we inferred the presence of minimally processed organic material within deep soils and high nutrient availability, challenging the applicability of the traditional theory of selective preservation and decreased soil quality with depth. As wetland submergence progresses and soils are exposed to oxygenated seawater, this relatively labile SOM and

bioavailable N and P stored at depth has the potential for rapid mineralization and/or export into the coastal zone.
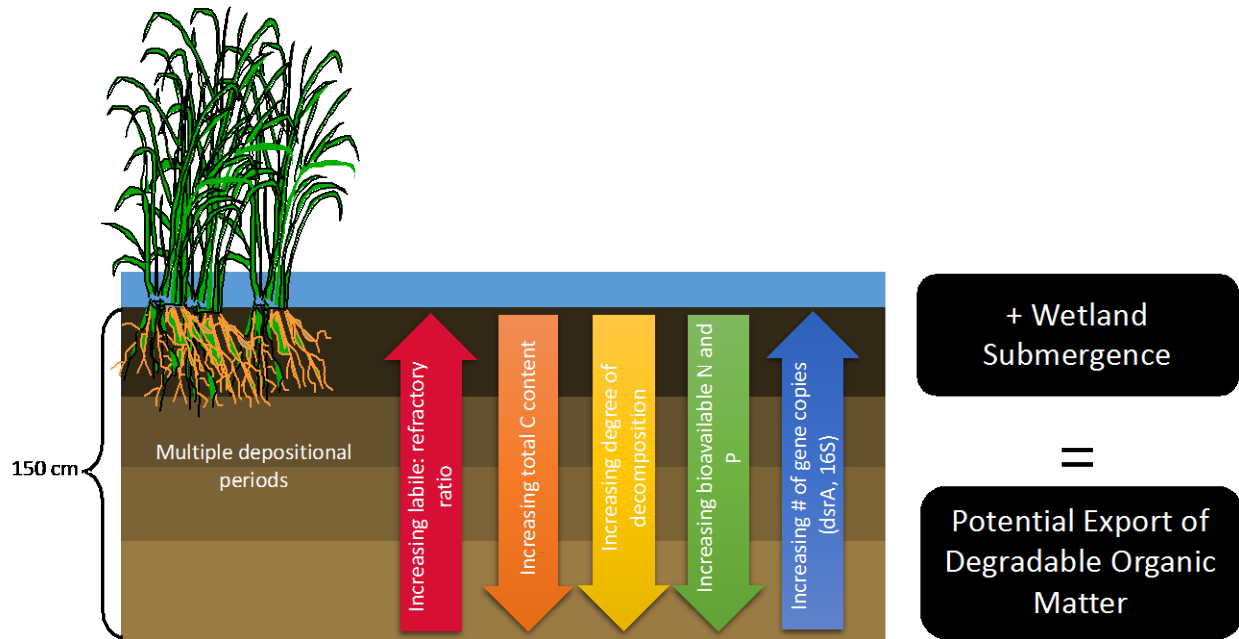
Figure 13: Graphical abstract illustrating major findings from this study.

Introduction

As one of the most productive ecosystem types, salt marsh soils sequester an average of 244.7 g carbon (C) m^{-2} y^{-1}, owing to high rates of primary productivity coupled with tidal flooding imposing anaerobic soil conditions that slow decomposition of organic matter (Amthor and Huston, 1998; Ouyang and Lee, 2014). These soil C stocks are vulnerable to coastal disturbances, such as sea level rise, which is occurring globally at a rate of 3.0 ± 0.4 mm y^{-1} (IPCC, 2013). Coastal wetlands can respond to sea level rise in multiple ways, including vertical accretion, landward transgression, and submergence, with the latter being the most extreme response and resulting in the conversion of the coastal wetland to open water (Kirwan and Megonigal, 2013). An estimated 22% of the areal extent of coastal wetlands are anticipated to be lost by 2100 (Nicholls et al., 1999). The long-term fate of submerged soil organic matter (SOM)

is unknown, though studies have demonstrated that significant portions of previously sequestered SOM can be lost through increased mineralization within an aerobic water column (Steinmuller et al., 2019), export into the coastal ocean (Bianchi et al., 2008), or transported and reburied within adjacent sediments (Macreadie et al., 2013).

In order to assess the fate of SOM stocks under wetland submergence scenarios, it is critical to understand the physical and chemical nature of the stored organic material, which is mediated by input characteristics and decomposition processes. While numerous studies have quantified the stocks of soil C in wetlands (Mitra et al. 2005; Chmura et al. 2003; McLeod et al. 2011 and references therein) the physical and chemical formation and stabilization processes for SOM in wetland soils is less understood. This is in stark contrast to theoretical understanding of SOM preservation in terrestrial soils, which has recently experienced a dramatic increase in research focus (Castellano et al., 2015; Cotrufo et al., 2013; Lehmann and Kleber, 2015; Schmidt et al., 2011). In wetlands, long-term accumulation of SOM in wetlands is attributed to anaerobic conditions, which is often the primary regulator of the balance between inputs (from autochthonous and allochthonous sources) and outputs (decomposition and export) (Reddy and DeLaune, 2008). Beyond redox chemistry, the generally accepted theory of decomposition within wetland soils centers around selective preservation, where inputs of organic matter are classified based on nutrient availability and molecular complexity, with each pool degrading at different rates throughout the decay continuum (Lützow et al., 2006; Melillo et al., 1989; Sollins et al., 1996). Labile components are defined as easily degradable, generally low molecular weight (LMW) compounds, examples of which include carbohydrates and proteins. Recalcitrant (or refractory) components require more energy to degrade and consist of high molecular weight (HMW) compounds such as lignin. As decomposition progresses, the selective preservation

theory states that labile components will be preferentially degraded by heterotrophic microbes while refractory components will be preferentially preserved, resulting in a greater proportion of HMW compounds with increasing soil depth (Sollins et al. 1996, Figure 1). This so called 'carbon quality,' a measure of elemental stoichiometry and/or molecular complexity of organic compounds, is considered a significant regulator of decomposition within soils (Aber et al., 1990; Cadisch and Giller, 1997; Melillo et al., 1989). Concomitant with carbon quality and environmental factors such as redox status, decomposition and eventual SOM storage within wetlands is also regulated by microbial characteristics (i.e., microbial biomass, community structure, production of enzymes, etc.).

Following the decay continuum and selective preservation theory, SOM stored within wetlands is assumed to be increasingly decomposed with depth, with a concomitant increase in the relative abundance of HMW complex compounds resistant to further microbial catabolism and the possible formation of humified substances (i.e., Wang et al., 2011). However, there is limited empirical evidence to support these generally accepted theories, and new research may even contradict them (Kögel-Knabner et al., 1992; Schmidt et al., 2011). For example, in a bottle incubation study that exposed deep wetland soils (100 cm) to oxygen, Steinmuller et al. (2019) reported CO_2 production from the deep soils was roughly 4x greater than CO_2 production within surficial soils, indicating that a) organic material stored at depth can be *more* labile and decomposable than the surface, and b) even at depth, microbial communities remain present and can process organic material rapidly following a change in redox conditions.

The goal of this study was to address the apparent discrepancy between the assumption that SOM quality (defined here as nutrient availability and molecular complexity) decreases with depth, and the observed high rates of potential respiration at depth (Steinmuller et al., 2019).

This was accomplished by evaluating the potential degradability of SOM (to a depth of 150cm) within a submerging coastal wetland through, 1) chemical fractionation of SOM, 2) evaluation of total and bioavailable nutrient pools to support decomposition, 3) stable isotope profiles of SOM, and 4) quantification of microbial community with depth. Together, these four approaches can be leveraged for both assessing the stability of SOM during sea level rise and quantifying potential export of C, N, and P from submerging wetland soils into the coastal ocean. We hypothesized that SOM quality will not decrease with depth and total C content will increase with depth. Additionally, we hypothesize that bacterial abundance (16S) and sulfate reducers will decrease with depth, while Archaea will increase with depth.

Methods
Site Selection and Soil Sampling

The island selected for sampling was located within Barataria Bay, LA, a shallow open water basin located west of the Mississippi River Delta (29°26'36.77'' N, 89°53'59.28'' W). The site experiences diurnal tides, with a salinity of 6-22 ppt (Levine et al., 2017; Rakocinski et al., 1992). The combination of shallow topography, lack of regular sediment inputs, tectonic subsidence, and high wind and wave energy within the bay contributes to an abnormally high erosion rate of 25.9 km^2 y^{-1} (Penland et al., 2000). More specifically, the erosion rate at this site was 141.6 ± 24.4 cm y^{-1} (Sapkota and White, 2019; in review).

In June 2018, soil cores were collected along three transects, roughly 1 m apart, that consisted of three points: the coastal fringe (0 m inland), 1 m inland, and 2 m inland. Soil cores were collected in polycarbonate tubes via the push core method to a depth of 150 cm, and field-extruded into 15 separate 10-cm intervals. Soils were stored in polyethylene bags on ice and immediately transported back to the laboratory, where they were kept at 4 °C until sample analysis was complete.
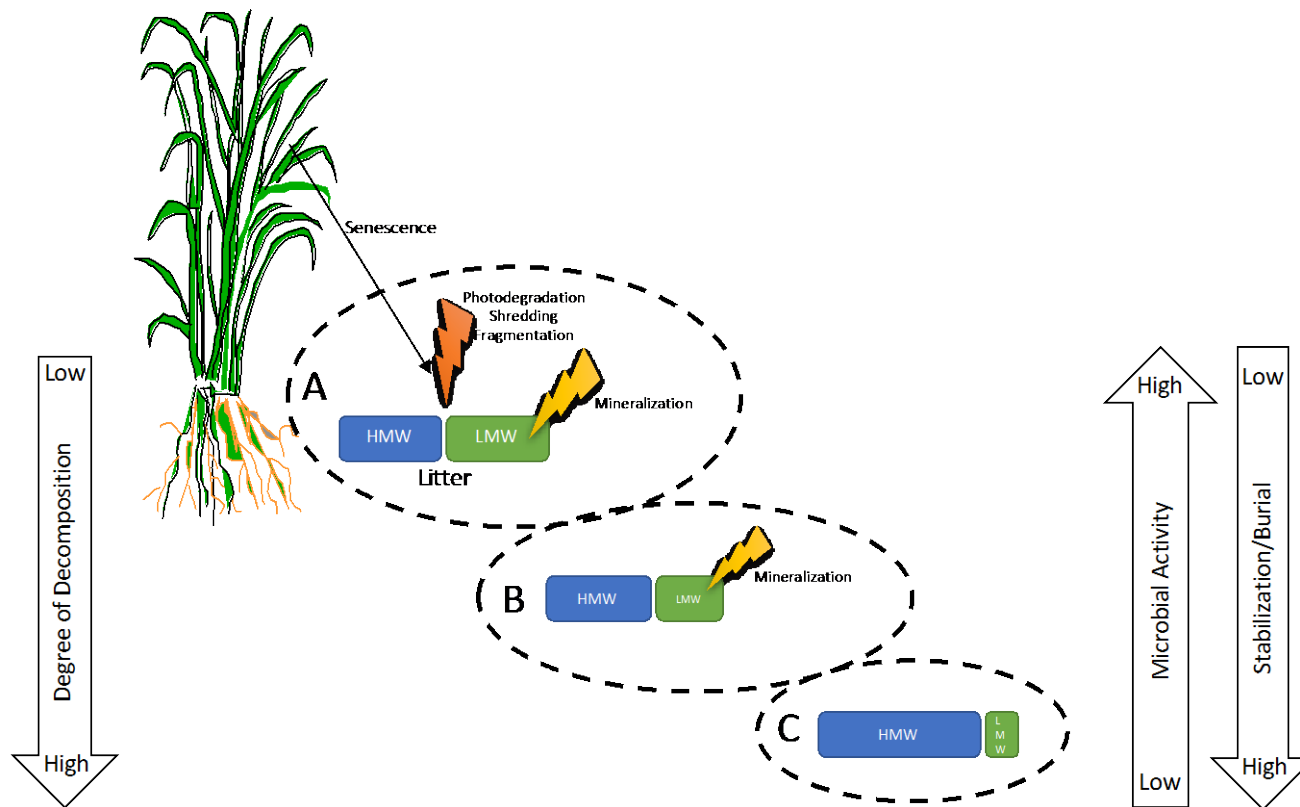
Figure 14: Current paradigm of selective preservation within wetland soils. A) As plants senesce, they deposit litter on the soil surface, which initially undergoes shredding from wetland fauna and microbial attack, targeting the low molecular weight (LMW) organic matter. B) As decomposition continues, LMW compounds continually undergo microbial degradation, reducing the size of the LMW pool. High molecular weight compounds require more energy to breakdown, thus the size of the pool remains generally the same. C) Decreases in microbial activity limit breakdown of the LMW pool resulting in an increase in the HMW pool, and a decrease in the LMW pool. Throughout this decay process, both degree of decomposition and stabilization/burial of organic matter increase, while microbial activity decreases with increasing depth.

Soil Physicochemical Properties

Soil samples were homogenized upon return to the laboratory, and subsamples were dried at 70°C until a constant weight was achieved to determine moisture content and bulk density. Dried samples were then ground on a SPEX Sample Prep 8000M Mixer Mill (Metuchen, NJ, USA). Total C and N content was determined on dried, ground subsamples by use of a Vario Micro Cube CN Analyzer (Elementar Americas Inc., Mount Laurel, NJ, USA). Subsamples of dried, ground material were digested with 50 mL of 1N HCl at 100°C for 30 minutes, then filtered through Whatman #41 filter paper for analysis of total P (Andersen, 1976), which was determined colorimetrically on an AQ2 Automated Discrete Analyzer (Seal Analytical, Mequon, WI; EPA method 365.1 Rev.2

Extractable Nutrients

Subsamples of field-moist soil (2.5 g) were weighed into centrifuge tubes containing 20 mL of 2 M KCl. Samples were placed on a longitudinal shaker in the dark for 1 hour, then centrifuged at 4000 rpm for 10 minutes at 10°C. The supernatant was decanted into 0.45 μL Supor membrane filters and filtered through vacuum filtration, then acidified to a pH of <2 with double-distilled H_2SO_4. Within 21 days, samples were analyzed on an AQ2 Automated Discrete Analyzer (Seal Analytical, Mequon, WI) for nitrate (NO_3^-), ammonium (NH_4^+), and soluble reactive phosphorus (SRP) (EPA methods 231-A Rev. 0, 210-A Rev. 1, and 204-A Rev. 0).

Figure 15: Drone photo of sampling location (A) within the larger context of both coastal Louisiana (B), and the USA (C). Drone photo courtesy of Eddie Weeks and Yadav Sapkota.

Organic Matter Fractionation

To determine fractions of organic matter, dried, ground subsamples were subjected to sequential extraction with H_2SO_4, following Rovira and Vallejo (2002) and Oades et al. (1970), with modifications. The first fraction is referred to hereafter as Labile Pool 1 (LP1) and consists of either plant- or microbially-derived non-cellulosic polysaccharides, including hemicellulose. Labile Pool 1 was extracted by adding 20 mL of 5 N H_2SO_4 into a 50 mL flask containing 0.5 g of soil. The solution was heated for 30 minutes at 105 °C and subsequently allowed to cool. Samples were then filtered through Whatman #41 filters to separate particulates from the solution, and then diluted to a final volume of 50 mL. Labile Pool 2 (LP2), which consists of cellulose, was determined by adding 2 mL of 26 N H_2SO_4 to 0.5g of dried, ground soil. Samples were shaken at 100 rpm for 16 hours, then diluted to a final concentration of 2 N H_2SO_4 with deionized water. Samples were heated for 3 hours at 105°C, then filtered in the same manner as LP1. Determinations of LP1 and LP2 concentrations were conducted by use of a Shimadzu TOC-L (Shimadzu, Kyoto, Japan). The refractory pool was calculated as total soil C minus the sum of the labile pools.

Stable Isotope Analysis ($\delta^{13}C$)

Stable isotope analysis was performed at the Stable Isotope Mass Spectroscopy Laboratory, Department of Geological Sciences, University of Florida. Dried, ground subsamples from only the 1 m inland cores were initially combusted on a Carlo Erba NA1500 CNS elemental analyzer. Following the removal of oxygen and water from the sample gas, the stream was passed through a 0.7 m GC column (120 °C), which separated the N_2 gas from CO_2. Effluent then passed into a ConFlo II system, and into a Thermo Electron Delta V Advantage isotope ratio mass spectrometer, where sample gas was measured in relation to laboratory

reference gases. Carbon isotope results are expressed in relation to Vienna PDB, in standard delta notation.

<div align="center">DNA Extraction, Quantification, and qPCR</div>

Following removal of samples from the field, subsets of field-moist samples from only the 1 m inland cores were frozen at -22 °C and transported back to the laboratory. Samples were allowed to thaw at 4 °C for 24 h before being sieved through a 2 mm mesh sieve to remove particulate plant material. Samples were then centrifuged at 4000 rpm and 25 °C for 1 minute and excess water was decanted. DNA was extracted from 0.25 g subsamples using a DNAeasy PowerSoil Extraction Kit (QIAGEN, Hilden, Germany). DNA quantification was performed by use of a Take3 micro-volume plate analyzed with a BioTek Synergy HTX (BioTek Instruments, Inc., Winooski, VT, USA). Extracted DNA was stored at -22 °C until qPCR analysis was performed.

Primers were selected to amplify specific functional genes: sulfate reduction (dsrA), all bacteria (16S), and all archaea (Arch) within the samples (Table 9). Genomic DNA from *Desulfobacterium autotrophicum* (Strain DSM 3382 (HRM2), ATCC, Manassas, VA, USA) was used to establish standard curves for both amplification of the 16S gene and the dsrA gene, while *Methanococcus voltae* (Strain A3) was used to establish standard curves for amplification of the Arch gene. Each 25uL reaction contained 5uL of DNA, 1.25uL of each 0.1uM primer (forward and reverse), 12.5uL of SYBR green MasterMix, and 12.5uL of PCR-grade water. Each reaction initially proceeded through steps at 50°C and 95°C, then 50 cycles of denaturing at 95°C, annealing (Table 9), and extending at 72°C.

Statistical Analysis

All statistical analysis was performed in R (R Institute for Statistical Computing, Vienna, Austria) using RStudio (RStudio Inc., Boston, MA, USA). The Shapiro-Wilk test was used to verify assumptions of normality, and a logarithmic transformation was performed on all datasets. Levene's test was used to determine homogeneity of variance. A linear mixed-effect model (package 'lmer') was used to test the following predictor variables: depth, distance inland, and the interaction of depth and distance inland on the samples collected from the marsh. Transect was included as a random effect. Distance inland was found to be a non-significant predictor variable for all parameters except for extractable NH_4^+. As such, distance inland was removed as a predictor variable from models except extractable NH_4^+. Isotopic determinations and quantitative PCR analysis was performed exclusively on the three replicate cores taken 1m inland, and thus depth was the only predictor variable tested for those parameters. Following determination of significance within one of the predictor variables, the package 'lsmeans' was used for post-hoc pairwise comparisons using the Tukey method.

Results

Soil Physicochemical Properties and Organic Matter Fractions

Bulk density, moisture content, total C, and total N all significantly differed with depth (Table 10). Bulk density ranged from 0.436 ± 0.036 g cm^{-3} at 30-40 cm to 0.177 ± 0.013 g cm^{-3} at 120-130 cm (Figure 16). In contrast, moisture content was lowest at 30-40 cm, averaging 60.3 ± 2.86 %, and greatest at 120-130 cm, averaging 81.2 ± 0.641 %.

Table 9: Forward and reverse primer sequences and names for each functional gene selected, as well as annealing temperatures used in qPCR analysis.

Gene	Forward Primer	Sequence (5'-3')	Reverse Primer	Sequence (5'-3')	Annealing Temperature (°C)
dsrA	dsrA_290F	CGGCGTTGCGCATTTYCAYACVVT	dsrA_660R	GCCGGACGATGCAGHTCRTCCTGRWA	60
16S	Eub338	ACTCCTACGGGAGGCAGCAG	Eub518	ATTACCGCGGCTGCTGG	55.5
Arch	Arch967F	AATTGGCGGGGGAGCAC	Arch-1060R	GGCCATGCACCWCCTCTC	59

Table 10: Significance values (p-values) derived from linear model for each parameter ($\alpha = 0.004$). 'NS' indicates a non-significant p-value, while 'NA' indicates the analysis was not performed.

Parameter	Depth
Bulk Density	<0.0001
Moisture Content	<0.0001
Organic Matter	<0.0001
Total C	<0.0001
Total N	<0.0001
Extractable NO_3^-	<0.0001
Extractable SRP	<0.0001
Extractable NH_4^+	<0.0001
Labile Pool 1	<0.0001
Labile Pool 2	<0.0001
Refractory Pool	<0.0001
$\delta^{13}C$	<0.0001
$\delta^{15}N$	<0.0001
16S	<0.0001
dsrA	<0.0001
Arch	NS

Total soil C was lowest at 50-60 cm, averaging 72.6 ± 8.18 g kg^{-1}, and highest at 130-140 cm, averaging 318 ± 6.66 g kg^{-1} (Figure 16). Total N concentrations exhibited a similar trend, ranging from 3.80 ± 0.438 g kg^{-1} at 50-60 cm to 18.2 ± 0.417 g kg^{-1} at 130-140 cm (Figure 16). Interestingly, the ratio of C:N was not significantly predicted by depth. Organic matter (OM) content was significantly predicted by depth (Table 10) and ranged from 18.0 ± 3.32 % at 40-50 cm to 63.7 ± 1.13 % at 120-130 cm. Bulk density was negatively correlated to all other physicochemical properties, all extractable nutrients, and organic matter fractions (Table 11). Moisture content, total C, and total N were all positively correlated to all physicochemical properties, extractable nutrients, and organic matter fractions (Table 11). Organic matter content was negatively correlated to bulk density and positively correlated to all other physicochemical parameters (Table 11).

Labile pool 1 (LP1) significantly differed with depth only (Table 10), ranging from 11.2 ± 2.15 mg g^{-1} at 40-50 cm to 35.1 ± 2.39 mg g^{-1} at 120-130 cm (Figure 17). Depth was a significant predictor variable for labile pool 2 (LP2) as well, which ranged from 6.45 ± 1.20 mg g^{-1} at 30-40 cm to 37.4 ± 6.98 mg g^{-1} at 130-140 cm (Figure 17). The refractory C pool was also significantly predicted by depth (Table 10), and ranged from 48.3 ± 6.57 mg g^{-1} at 30-40 cm to 247 ± 10.5 mg g^{-1} at 120-130 cm (Figure 17). When combined, the ratios of LP1+LP2: refractory (henceforth referred to as labile: refractory ratio) was significantly different with depth ($p < 0.001$; Figure 17). Labile: refractory ratios remained relatively consistent between 0-60 cm, averaging 0.363 ± 0.018, then decreased to an average of 0.256 ± 0.009 between 60 and 150 cm (Figure 17). All three organic matter pools were significantly positively correlated to each other, as well as total N, total C, moisture content, and all extractable nutrients (Table 10). All pools were negatively correlated to bulk density (Table 10).

Table 11: Correlation matrix for all parameters with a distance treatment (n = 136, α = 0.001, critical value = 0.279). Values in bold are positively correlated, while values in italics are negatively correlated.

	Bulk Density	Moisture Content	Organic Matter	Total N	Total C	Extractable NO_3^-	Extractable SRP	Extractable NH_4^+	LP1	LP2
Moisture Content	*-0.962*									
Organic Matter	*-0.812*	**0.809**								
Total N	*-0.719*	**0.722**	**0.933**							
Total C	*-0.768*	**0.772**	**0.971**	**0.959**						
Extractable NO_3^-	*-0.640*	**0.673**	**0.601**	**0.505**	**0.545**					
Extractable SRP	*-0.671*	**0.679**	**0.769**	**0.740**	**0.752**	**0.687**				
Extractable NH_4^+	*-0.604*	**0.631**	**0.692**	**0.656**	**0.667**	**0.633**	**0.835**			
LP1	*-0.627*	**0.625**	**0.766**	**0.710**	**0.756**	**0.367**	**0.432**	**0.405**		
LP2	*-0.524*	**0.521**	**0.597**	**0.661**	**0.638**	**0.404**	**0.568**	**0.458**	**0.353**	
Refractory OM	*-0.749*	**0.754**	**0.961**	**0.944**	**0.991**	**0.537**	**0.750**	**0.668**	**0.709**	**0.554**
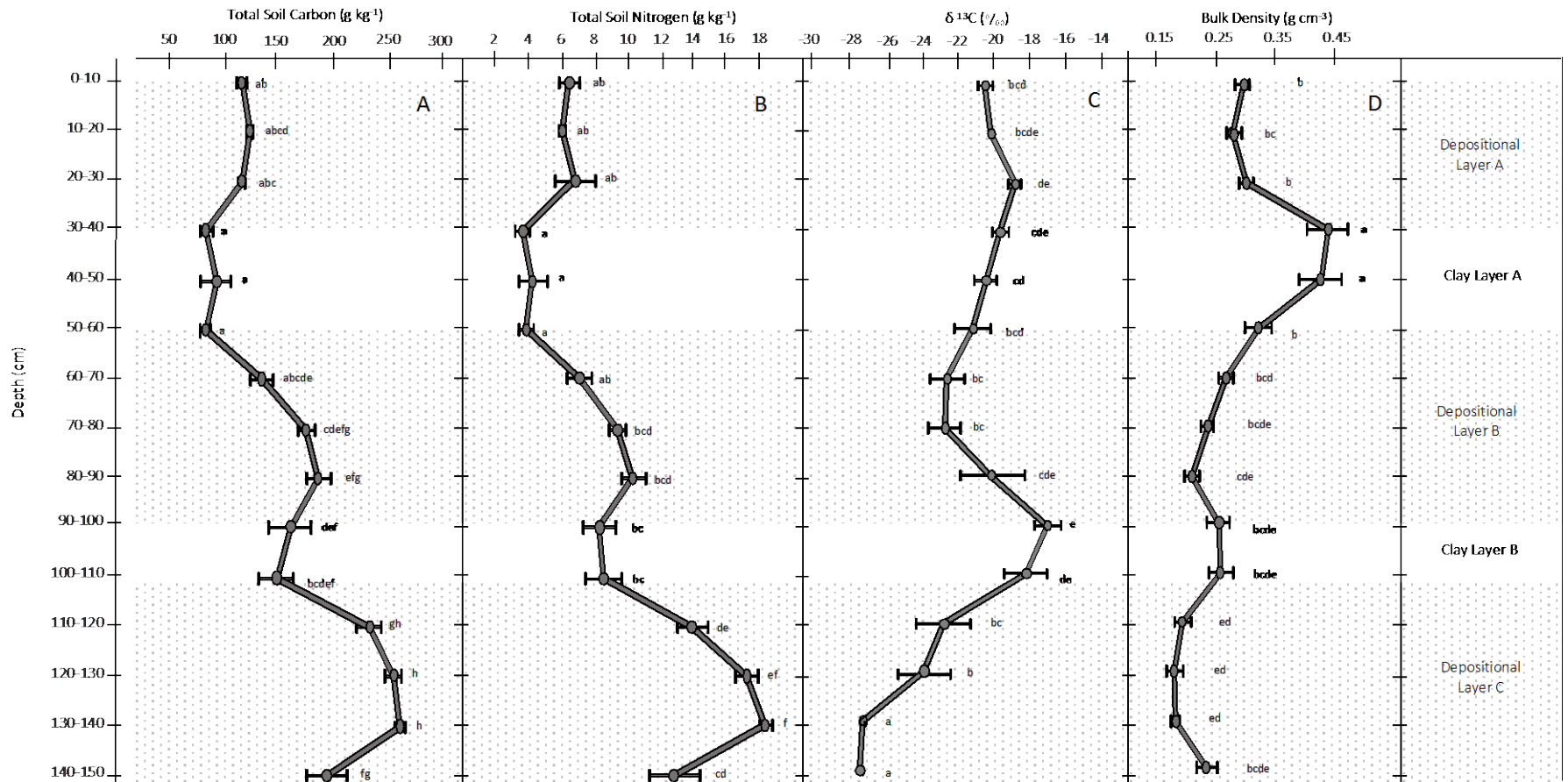
Figure 16: Total soil carbon content (A), total soil nitrogen content (B), soil δ ^{13}C, and bulk density (D) as well as multiple depositional periods.

Values are mean ± standard error, n=9. Lowercase letters denote significance (α = 0.05).
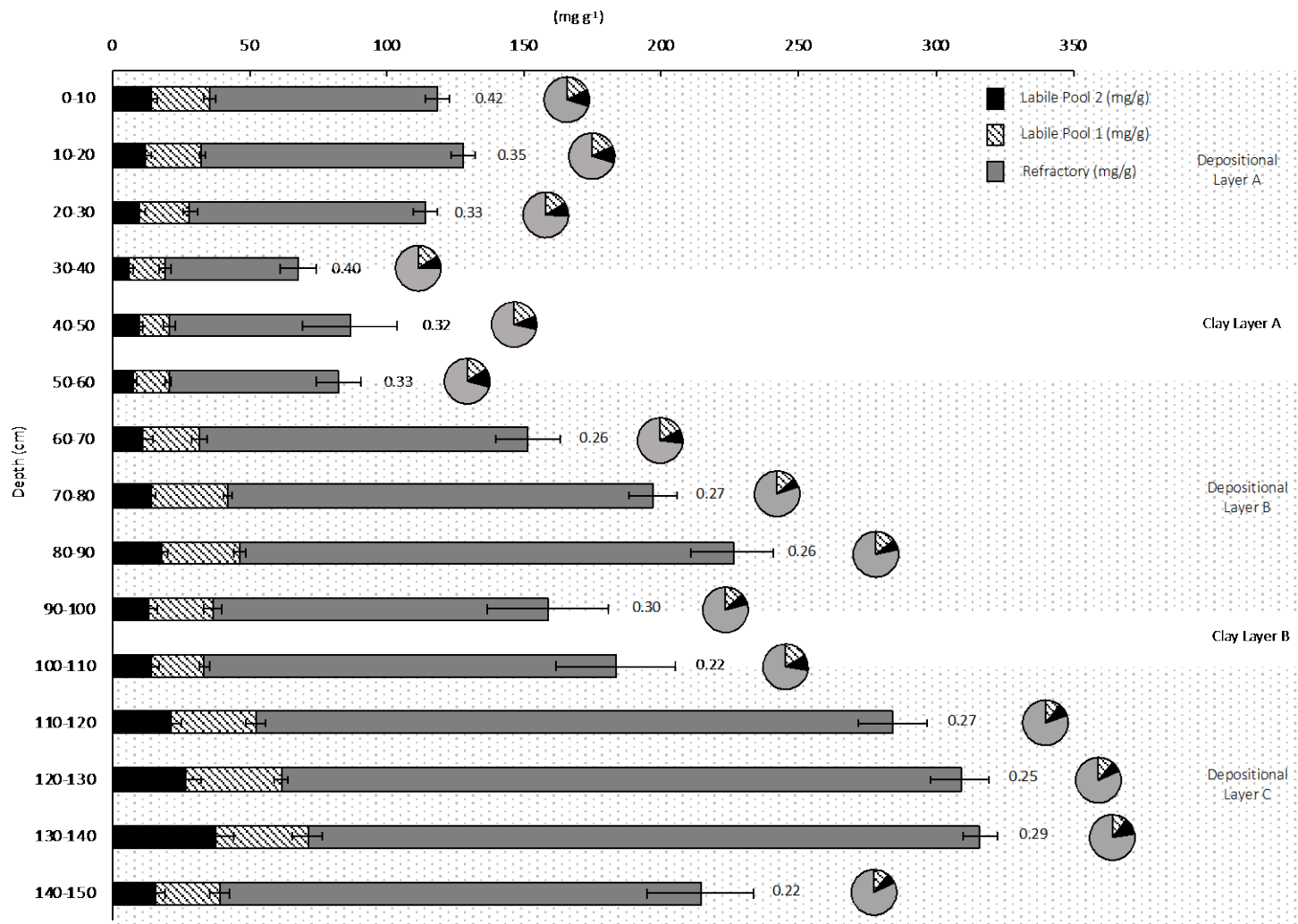
Figure 17: Fractionation of organic C into two labile pools and a refractory pool overlaid on clay and depositional layers. Values are mean ± standard error. Numbers adjacent to bars indicate labile: refractory ratio for that soil depth. Pie charts represent the percentage of total C that each pool represents for the associated depth.

Extractable Nutrients

Extractable NO_3^- concentrations increased with depth (Table 10), ranging from 1.44 ± 0.130 g kg^{-1} at 30-40 cm to 3.47 ± 0.527 g kg^{-1} at 120-130 cm (Figure 18). Both extractable SRP and NH_4^+ concentrations generally increased with depth (Table 10, Figure 18), though concentrations decreased precipitously between 130-140 cm and 140-150 cm. Extractable SRP concentrations ranged from 0.908 ± 0.126 g kg^{-1} at 30-40 cm to 12.0 ± 0.973 g kg^{-1} at 130-140 cm (Figure 18). The lowest extractable NH_4^+ concentrations were at 20-30 cm, averaging 9.64 ± 4.27 g kg^{-1}, while the greatest concentrations were at 130-140cm, averaging 206 ± 33.3 g kg^{-1} (Figure 18). All extractable nutrients were positively correlated to each other and total nutrients (Table 11).

$\delta^{13}C$ and $\delta^{15}N$ Values

Both $\delta^{13}C$ and $\delta^{15}N$ values significantly different with depth (Table 10). $\delta^{13}C$ was most depleted at 130-140 cm, averaging -27.3 ± 0.131, and most enriched at 90-100 cm, where values averaged -16.9 ± 0.729 (Figure 16). Generally, $\delta^{15}N$ values decreased with depth, ranging from 1.90 ± 0.110 at the surface to -0.65 ± 0.124 at 110-120 cm (Figure 19). $\delta^{13}C$ was negatively correlated to total C and N content, as well as extractable SRP, extractable NH_4^+, and the refractory OM component (Table 12). $\delta^{15}N$ positively correlated to bulk density, and was negatively correlated to moisture content, total C and N, all extractable nutrients, and the refractory OM component (Table 12).

Quantitative PCR

Gene abundance of 16S and dsrA both significantly different with depth (Table 10, Figure 20). Gene abundance of 16S was greatest at 0-10 cm, averaging $5.92 \times 10^9 \pm 6.98 \times 10^8$ gene copies, while dsrA gene abundance was greatest at 10-20 cm, and averaged $9.58 \times 10^9 \pm 1.39 \times 10^9$. The lowest abundance of both genes was recorded at 50-60 cm, where 16S averaged

1.59 x 10^9 ± 8.02 x 10^8 gene copies, while dsrA averaged 2.95 x 10^9 ± 7.66 x 10^8 gene copies.

Gene abundance of the Archaea gene (Arch) was not significantly predicted by depth (Table 10, Figure 20). Both 16S and dsrA gene abundance were positively correlated to each other (Table 12).

Discussion
Site History

Previous studies within Barataria Bay, LA have documented non-linear changes in soil C content with depth (Dodla et al., 2012; Steinmuller et al., 2019), as was observed here. Total C content increased dramatically, though not linearly, from the surface to 150 cm (Figure 3). Combining C content with $\delta^{13}C$ values, we can infer the presence of multiple habitat types or depositional periods over the chronological timescale the soil core represents. The majority of brackish marsh vegetation are C4 plants, which have more depleted $\delta^{13}C$ values compared to the C3 plants that inhabit freshwater marshes (Smith and Epstein, 1971). The C3 plant signature of less depleted $\delta^{13}C$ values is evident within the first 30 cm of the soil (Figure 1, Habitat Layer A), under which there is a distinct clay layer (Clay Layer A), likely a relic of hydrologic change in the area (Delaune, 1986). Under the clay layer, the $\delta^{13}C$ values indicate a more depleted environment (-21.7), likely a freshwater marsh (Figure 1, Habitat Layer B). Delaune (1986) identified a similar trend in Barataria Bay, where isotopic signatures of a freshwater marsh underlaid those of a brackish marsh, separated by a clay later. Deeper in the soil profile, between 90-110 cm, the soil again shifted to more clay dominated (Clay Layer B), possibly indicating another event, under which $\delta^{13}C$ values again shifted to more depleted (Habitat Layer C). Both total soil C and N content are different within each of these layers, and are greatest within Habitat Layer C. The unique history and habitat switching at this site allows for the storage of considerably more C than would be assumed if only surface (e.g., 0-30 cm) cores were collected,

as is common in wetland studies (Reddy et al., 2013). This study indicates the importance of

collecting deep soil cores (1+ m) in establishing coastal wetland C budgets, particularly in this

systems where ~1-2 m of peat could be lost to the bay during erosion (DeLaune and White,

2012).

<center>Carbon Quality and Degree of Decomposition</center>

Though the quantity of organic C sequestered within this site is greatest at deeper depths,

the quality of that organic matter is also critical to consider when evaluating potential

degradability. By parsing-out relative contributions of labile and recalcitrant organic matter

within the soil at multiple depths, we can infer the relative mineralization potential of these C

stocks via microbial respiration (Dodla et al. 2012). Use of the selective preservation model

would suggest that at deeper depths, where decomposition processes have been greatest, SOM

should consist of generally refractory C that is resistant to decomposition(Sollins et al., 1996).

Within this study, the ratio of labile: refractory C did decrease with depth (0.42 at 0-10 cm to

0.22 at 140-150 cm; Figure 4), implying decomposition has taken place, though labile fractions

still comprise a range of 17 – 30% of the total C pool between 100 and 150 cm below the soil

surface. Placing this number in context is difficult; to our knowledge, this analysis method has

not previously been performed on wetland soils, and thus it is challenging to determine whether

this number represents either extensive or minor decomposition of labile components. Using a

different method, Dodla et al., (2012) assessed acid-hydrolyzable C content (assumed to be

somewhat similar to our labile fractions) to be 17% of total organic C at depth (150-175 cm) and

23% at the surface (0-50 cm) within brackish marsh soils in Barataria Bay (though non-linear

with depth). This is slightly lower than the 24 - 32% of labile soil organic C reported within

forested wetlands (0-20 cm) (Silveira et al., 2008). In a study comparing the acid hydrolyzable C

<center>80</center>

content within three upland soils, Xu et al., (1997) documented a range of 29 - 34% hydrolyzable soil organic C fractions in surface soils (0-15 cm), which would likely be indicative of relatively labile, undecomposed material.

The degree of decomposition of the SOM at depth can also be ascertained by examining $\delta^{15}N$ isotope values, which can provide insight by indicating whether these soils have undergone substantial fractionation, and therefore decomposition. Within our study, $\delta^{15}N$ decreased with depth (Figure 2). Within the continuum of decomposition, fractionation of N isotopes occurs as soil microbial biomass processes organic material (Craine et al., 2015). Initially during the process of decomposition, $\delta^{15}N$ within the soil becomes more depleted (Melillo et al., 1989) as a result of net immobilization of N and microbial anabolism. However, as mineralization progresses, microbial consortia no longer require significant N constituents for anabolism, and mineralization processes begin to prevail over immobilization, with $\delta^{15}N$ values becoming more enriched over the long term. As a result, soil $\delta^{15}N$ values have been shown to become more enriched with depth within upland systems (Hobbie and Ouimette, 2009). In wetlands, where soils are generally water-logged and decomposition proceeds much slower, our $\delta^{15}N$ profile may suggest, a) SOM only advances through the initial stage of decomposition before being inhibited by low redox conditions (i.e., a lack of available terminal electron acceptors), or b) habitat switching/major disturbances within this system resulted in multiple depositional periods and rapid burial of organic soils. Overall, the $\delta^{15}N$ profile, taken in concert with the trends observed for labile: refractory ratios and the lack of changes in elemental C:N with depth, suggest that only limited SOM decomposition has occurred at depth, though additional studies of deep wetland soil profiles are needed to corroborate this idea. The potential implication of the

existence of relatively labile C deep within the soil profile is an increased likelihood of rapid

mineralization if the abiotic conditions are altered, such as due to coastal erosion.

<center>Microbial Gene Abundance at Depth</center>

Microbial abundance and function are regulated by a variety of both biological and

physicochemical factors within wetland systems.   The prevailing anaerobic conditions within

wetlands regulate which microbial communities are functioning, a result of the availability of

terminal electron acceptors (Reddy and DeLaune, 2008). Within surface soils in brackish and

saltwater wetlands, sulfate reduction is the dominant respiration pathway for microbial consortia

and is replaced by methanogenesis in deeper soils where either sulfate concentrations have been

depleted, or do not penetrate (DeLaune et al., 1983). While this study did not quantify gene

copies of mcrA, the gene for methanogenesis, abundance of dsrA, the gene for sulfate reduction,

was highest at surface depths, indicating that the microbial communities at the surface are likely

respiring via sulfate reduction. The number of copies of the 16S gene, an indicator of abundance

of all bacteria, was lower than the number of gene copies of dsrA between 0-40 cm, likely a

product of decreased efficiency of primers for the 16S gene, relatively to primers amplifying

dsrA. Interestingly, the abundance of the Arch gene was greater than the Bac gene deeper than

20 cm, which is likely an indication of methanogenesis, a process controlled by *Archaea* rather

than *Bacteria* being the dominant microbial respiration pathway at depth (Reddy and DeLaune,

2008).

Carbon quality and quantity have been documented to strongly regulate microbial

abundance and function within wetland systems (Reddy and DeLaune, 2008). However, within

this study, neither C density, total C content, nor C quality correlated well with abundance of any

microbial gene quantified (Table 4). This indicates that there is potentially another regulator of

<center>82</center>

microbial abundance within this system, such as redox conditions or environmental factors, or that the microbial community composition itself is shifting with C indices, but not overall abundance of the genes we analyzed. Further research is required to determine the importance of organic matter quality and quantity as regulators of microbial functional abundance within wetland systems.

Similarly, determining whether those microbial communities present at depth are active and alive is critical in further determining the fate of sequestered organic material at depth. Based on the data collected here, we can determine that microbial communities are present in significant proportions at depth but cannot determine whether those communities are metabolically dormant. However, the presence of these microbial communities at depth, coupled with the high potential degradability of these C stocks demonstrated in Steinmuller et al. (2019), indicates these microbial communities can become active when conditions change, such as soil disarticulation and oxygenation following submergence into coastal waters.

Fate of Stored Carbon, Nitrogen, and Phosphorus

Both extractable NH_4^+ and SRP increased an order of magnitude below the root zone (~30 cm) within these soils (Figure 5). Within the active root zone, these bioavailable nutrients are assimilated by plants to sustain growth and primary productivity (Brannon, 1973). Below the root zone, availability of these nutrients is mediated by microbiota (i.e. mineralization versus immobilization) or physicochemical properties (i.e. binding to the cation exchange complex). The 11x and 7x increase in SRP and NH_4^+ concentrations between 0-10 cm and 130-140 cm, coupled with the significant C stocks within this wetland, represent bioavailable nutrients and relatively labile C that is vulnerable to export into the coastal zone through physical and chemical processes associated with both sea level rise and erosion. Bioavailable N and P

exported from coastal marshes can contribute the formation of a hypoxia zone that develops annually within the northern Gulf of Mexico (Bianchi et al., 2008; Dagg et al., 2007). Similarly, export of C from coastal marshes is estimated to account for 3-34 % of the organic C within the inner Louisiana shelf (Bianchi et al., 2011) and could increase with wetland submergence. In addition to export, these stores of minimally decomposed organic material and high concentrations of bioavailable nutrients, when combined with oxygenated seawater and/or available sulfate, represent optimal conditions for mineralization and loss of C into the atmosphere as a climate change feedback. Specifically, Steinmuller et al. (2019) documented a 66 % increase in mineralization following exposure of soils from this site to aerobic seawater.

Understanding SOM Stabilization in Wetlands

Recently, multiple conceptual models have emerged within the upland literature to explain SOM formation and stabilization, most of which indicate SOM persistence is more closely linked to environmental factors, the degree of microbial processing, and protection via association with minerals and aggregation, rather than the inherent molecular properties of the SOM that are highlighted by the selective preservation theory (Castellano et al., 2015; Cotrufo et al., 2013; Lehmann and Kleber, 2015; Schmidt et al., 2011). Although application of these conceptual models has yet to be tested in wetlands, evidence from the current study suggests selective preservation may not be the dominant regulator of SOM formation in coastal wetlands. Rather, our results indicate the percent of refractory material only increased by 7 % over the entire 150 cm depth interval, while labile material decreased roughly 10 %. This, taken together with the lack of change in C:N with depth and a depletion of $\delta^{15}N$ values, suggests this SOM remains relatively degradable (i.e., has high C quality) to a depth of 150 cm. While we cannot yet theorize which conceptual models most accurately depict SOM stabilization within peat-

forming wetlands, our data suggest it is more complex than selective preservation and may be linked to microbial access and efficiency (Lehman and Kleber 2015; Cotrufo et al., 2013).

Conclusion

Currently, much of the coastal wetland soils research focuses on C quantity, such as documenting blue C pools, with less attention given to the properties of the SOM itself (e.g., molecular complexity, nutrient availability, microbial community). Since few studies on SOM structure and stabilization have been performed in wetlands, it is often assumed wetland soils follow the traditional concepts for SOM decomposition and preservation developed in terrestrial soils, such as the decay continuum and the theory of selective preservation (Melillo et al. 2002; Reddy and DeLaune, 2008). Under these conceptual models, soil quality is anticipated to decrease significantly with depth in wetlands, making only the more surficial soils easily degradable and at risk of rapid mineralization if conditions were altered, such as a shift in redox status. Understanding SOM quality, how it changes with depth, and how it influences the biogeochemical response of soils to shifting environmental conditions is particularly important in Barataria Bay, LA (USA), where coastal wetlands are rapidly submerging into oxygenated coastal waters due to the combined effects of high rates of relative sea level rise and edge erosion.

This study assessed key SOM properties that commonly regulate the rate of decomposition, and thus the properties of buried SOM: molecular complexity (through acid hydrolysis), C and nutrient availability (total and extractable pools), and the abundance of key microbial taxa and functional genes. All parameters were assessed based on depth (down to 150 cm), along with soil $\delta^{13}C$ and $\delta^{15}N$ values, to better understand the composition and potential degradability of the sizable C reservoir stored within these submerging wetland soils. Soil

stratigraphy inferred from changes in physicochemical properties with depth revealed a highly dynamic environment with multiple depositional phases and shifts between vegetation communities (from C3-dominated (more common of freshwater marsh species) to C4-dominanted communities (more indicative of brackish marsh species)). These dynamics, along with persistent anaerobic conditions, promoted the preservation and burial of large stores of SOM that appear to have only undergone minimal processing and decomposition, based on the existence of only small changes in the ratio of labile:recalcitrant material with depth, no change in soil C:N, and a profile of diminishing $\delta^{15}N$ values with depth. In addition to these indices suggesting the presence of high quality SOM at depth, our data also indicates total C content and extractable nutrient (NH_4^+ and SRP) availability peaks at depth (between ~110-140 cm) without any significant declines in the abundance of bacteria or archaea below the root zone. Taken together, these results demonstrate a high potential for rapid mineralization of this SOM when redox constraints are released during mixing with oxygenated coastal waters, and the release of C and nutrients into coastal waters following wetland erosion and submergence. This work also highlights the need for additional analysis on wetland SOM properties with depth and development of a conceptual framework for SOM formation and preservation in wetland soils that may be unique from those developed for terrestrial soils.

.

Table 12: Correlation matrix for parameters that did not include a distance treatment (n=46, α = 0.001, critical value = 0.469). Values in bold are positively correlated, while values in italics are negatively correlated. Non-significant r values are denoted with a dash. Ext. refers to 'extractable', MC refers to Moisture Content.

	Bulk Density	MC	Organic Matter	Total N	Total C	Ext. NO$_3^-$	Ext. SRP	Ext. NH$_4^+$	LP1	LP2	Refractory	16S	dsrA	Arch	δ15N
MC	*-0.957*														
Organic Matter	*-0.858*	**0.861**													
Total N	*-0.748*	**0.756**	**0.933**												
Total C	*-0.789*	**0.791**	**0.946**	**0.979**											
Ext. NO$_3^-$	*-0.753*	**0.767**	**0.729**	**0.633**	**0.669**										
Ext. SRP	*-0.688*	**0.649**	**0.817**	**0.845**	**0.815**	**0.581**									
Ext. NH$_4^+$	*-0.592*	**0.612**	**0.708**	**0.696**	**0.659**	**0.611**	**0.700**								
LP1	*-0.623*	**0.663**	**0.709**	**0.623**	**0.646**	-	**0.475**	**0.477**							
LP2	*-0.475*	-	**0.561**	**0.649**	**0.616**	-	**0.621**	-	-						
Refractory	*-0.767*	**0.778**	**0.927**	**0.960**	**0.989**	**0.668**	**0.789**	**0.651**	**0.614**	**0.521**					
16S	-	-	-	-	-	-	-	-	-	-	-				
dsrA	-	-	-	-	-	-	-	-	-	-	-	**0.622**			
Arch	-	-	-	-	-	-	-	-	-	-	-	-	-		
δ15N	**0.663**	*-0.651*	*-0.762*	*-0.710*	*-0.719*	*-0.601*	*-0.736*	*-0.541*	-	-	*-0.714*	-	-	-	
δ13C	-	-	**0.508**	*-0.654*	*-0.560*	-	*-0.510*	*-0.534*	-	-	*-0.554*	-	-	-	-
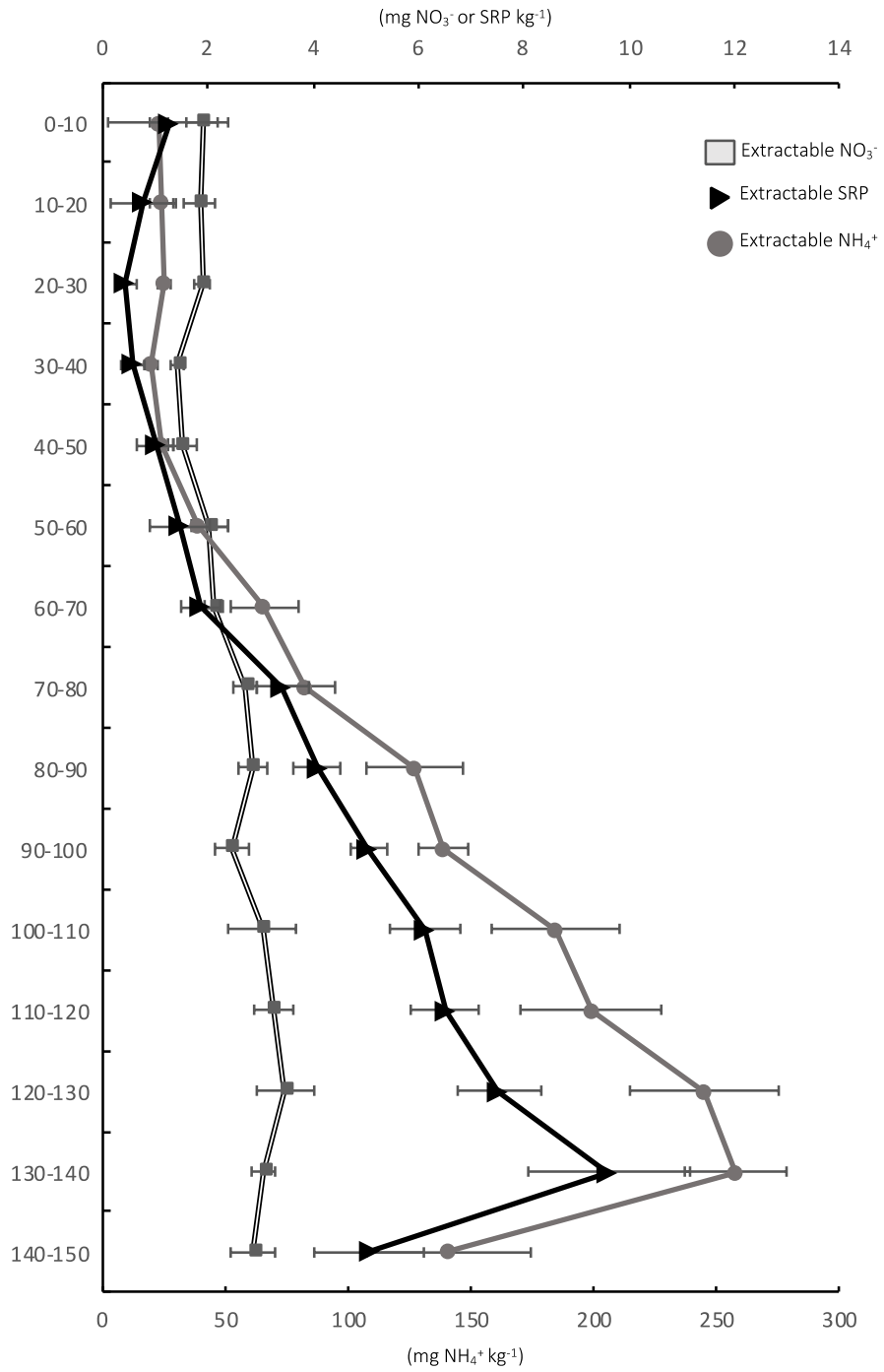
Figure 18: Extractable nutrient concentrations at each soil depth. Values are mean ± standard error.
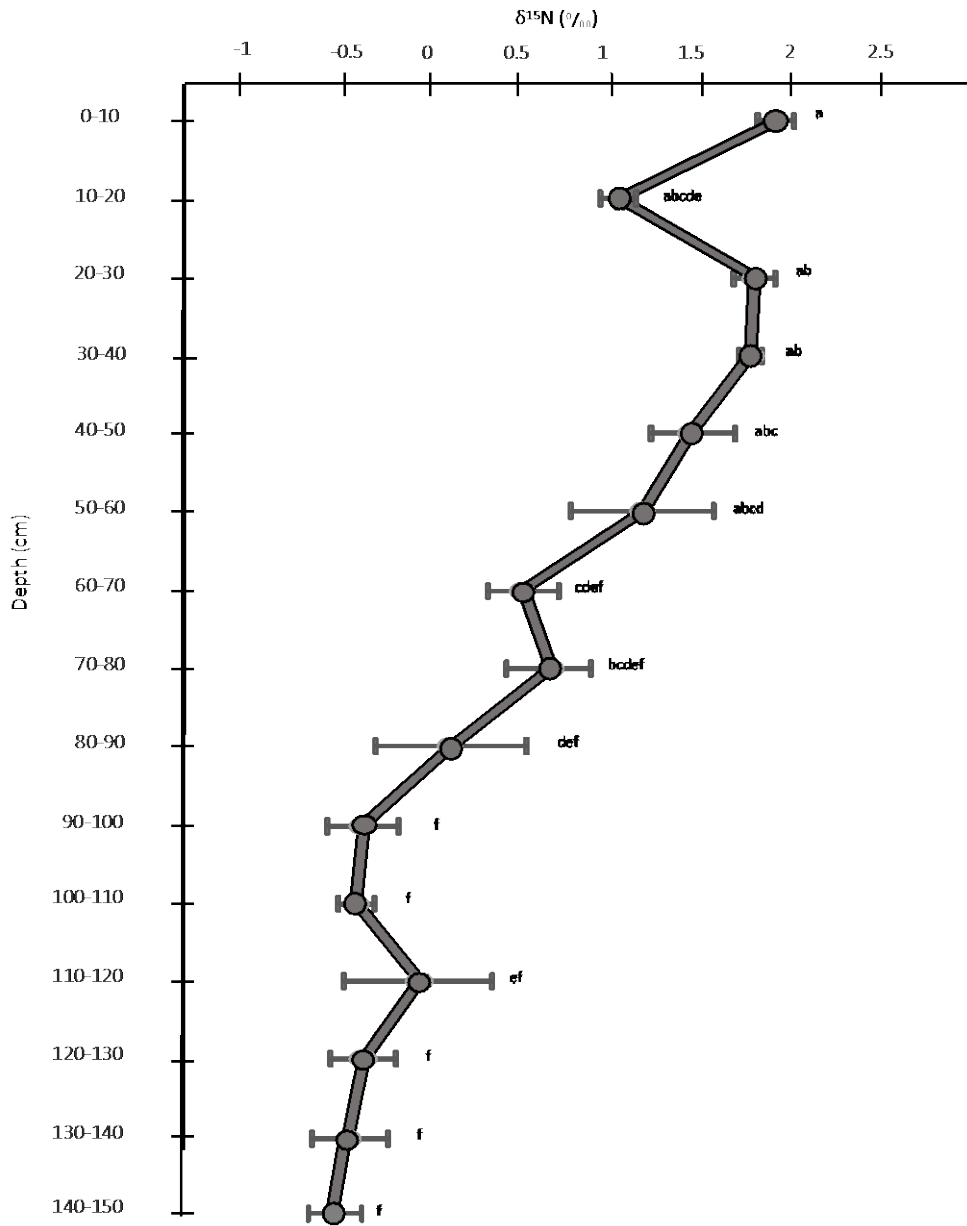
Figure 19: Values of $\delta^{15}N$ within each soil depth. Plotted values are mean ± standard error. Letters indicate significance ($\alpha = 0.05$).
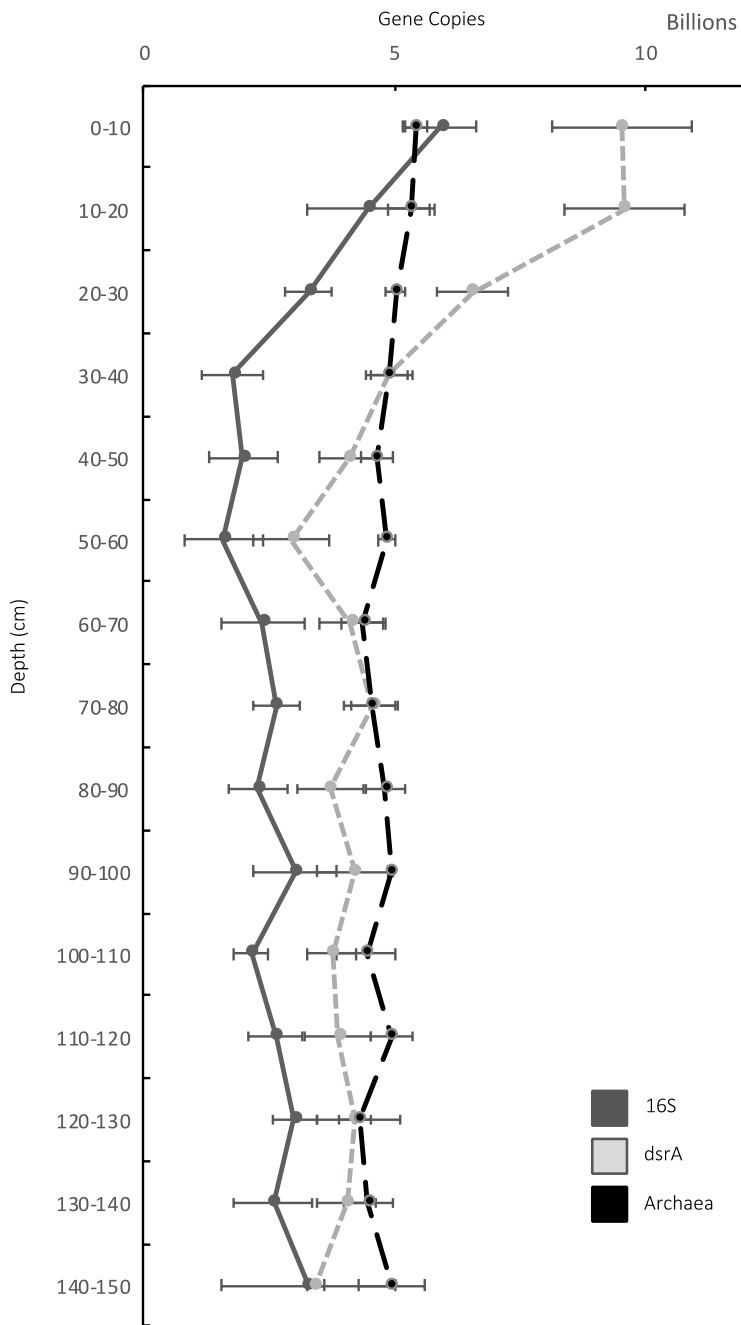
Figure 20: Number of gene copies for each functional gene (dsrA, 16S, Arch) in billions for each soil

depth. Values are mean ± standard error

CHAPTER FIVE: TIPPING POINTS IN THE MANGROVE MARCH: CHARACTERIZATION OF BIOGEOCHEMICAL CYCLING ALONG THE MANGROVE-SALTMARSH ECOTONE

Abstract

Coastal wetland vegetation communities can respond to sea level rise via the encroachment of more salt- and inundation tolerant species into existing vegetation communities. Black mangroves (*Avicennia germinans L.*) are encroaching on saltgrass (*Distichlis spicata L.*) within the Merritt Island National Wildlife Refuge in east-central Florida (USA). Nine (9) soil cores collected along three transects captured the transitions of both perceived abiotic drivers (salinity and inundation) and vegetation communities during both high and low-water seasons to investigate patterns in soil biogeochemical cycling of carbon (C), nitrogen (N), and phosphorus (P). Results showed no change in soil carbon dioxide production along the ecotone during either season, though changes in enzyme activity and mineralization rates of N and P could indicate changes in C quality and nutrient availability impacting C degradation along the ecotone. All parameters, excluding microbial biomass carbon, showed higher rates of activity or availability during the low-water season. Long-term soil nutrient pools (total C, N, P) were greatest in the salt-grass soils, and similar between the mangrove and transition zone soils, indicating a 'tipping point' in biogeochemical function where the transition zone is functionally equivalent to the encroaching mangrove zone. Indicators of current biogeochemical cycling (i.e. enzyme activity, potentially mineralizable N rates, and extractable ammonium concentrations) showed alterations in activity across the ecotone, with the transition zone often functioning with lower activity than within end members. These indicators of current biogeochemical cycling change in advance of

full vegetation shifts. Increases in salinity and inundation were linked to mangrove encroachment.

Introduction

Globally, coastal wetlands can respond to relative rates of sea level rise in one of three ways: vertical accretion to 'keep pace' with sea level, landward transgression, or wetland submergence (Kirwan and Megonigal 2013). Landward transgression occurs when a minimally disturbed coastal wetland experiences a gradual rate of relative sea level rise that exceeds the rate of accretion. Changing abiotic factors disrupt the classic zonation of vegetation within salt marsh ecosystems, pressuring vegetation to slowly migrate upslope to continually occupy their optimal ecological niche (Bertness 1991; Donnelly and Bertness 2001; Morris and others 2002). Also known as 'coastal squeeze', landward transgression is occurring around the globe, resulting in ecosystem conversion when wetlands begin to converge upon immovable, developed upland systems (Pontee 2013; Torio and Chmura 2013).

In addition to vegetation communities changing position within the coastal plain, the altered physicochemical environment as a result of sea level rise can catalyze the encroachment of more salt- and flood-tolerant species along the seaward edge of coastal wetlands (i.e. Donnelly and Bertness, 2001; Rogers and others, 2006). While global poleward expansion of mangroves is attributed to latitudinal expansion from decreased frequency of extreme freeze events (Cavanaugh and others 2014), regional landward transgression is occurring where mangroves are able to opportunistically invade marshes by outcompeting the stressed native vegetation (Raabe and others 2012; Kelleway and others 2016).   Within south and central Florida (USA), mangroves are expanding along the coastal fringe and altering coastal wetland function and structure (Saintilan and others 2014), as they are able to tolerate high salinities and wide

92

fluctuations in water levels. For example, the saltmarsh to mangrove conversion rate within Tampa Bay (FL) wetlands is 72% over 125 years (Raabe and others 2012). Though mangroves are able to stabilize shorelines, provide buffer from storm surge, trap tidal debris and sediments, and provide shade and habitat, the full extent of ecosystem consequences of mangrove encroachment on native saltmarshes is relatively unexplored (Field and others 1998; Kelleway and others 2017).

Perhaps the most well-documented ecological consequence occurring with mangrove encroachment into saltmarshes concerns ecosystem C stocks. Mangroves are structurally and physiologically distinct from saltmarsh grasses, which contributes to differences in potential C storage within biomass (Duarte and others 2013). Multiple studies have reported greater potentials for C storage within both the aboveground and belowground tissues of mangroves relative to saltmarsh grasses (Duarte and others 2013; Doughty and others 2016; Kelleway and others 2016). However, in addition to aboveground- and belowground C storage within plant tissues, there have been documented differences in the mangrove and saltmarsh C deposition and burial (Lunstrum and Chen 2014; Doughty and others 2016). While C accumulation is a critical factor in understanding C dynamics between the two vegetation types, the residence time and quality (i.e. chemical structure) of C could affect long-term C storage. Mangroves generally contain more recalcitrant compounds that require more energy to decompose than their saltmarsh grass counterparts (Bianchi and others 2013; Middleton and Mckee 2014). To date, very few studies have focused on differences in soil respiration between the two vegetation types, which factors heavily into source-sink dynamics of C within coastal wetlands experiencing mangrove encroachment (Simpson and others 2018).

The breakdown of organic matter also alters nutrient availability within coastal wetland soils. Thus, changes in soil respiration, soil quality, and vegetation type could alter the cycling of other biologically-important macronutrients (nitrogen, phosphorus, and sulfur). While many studies have focused on nutrient limitation (i.e. total soil nutrients) within saltmarsh and mangroves soils separately (Feller 1995; Feller and others 1999, 2013; Feller, I.C., Whigham, D.F., Mckee, K.L., Lovelock 2003; Simpson and others 2013), no study has yet explored changes to biogeochemical cycling of nutrients as a result from encroachment. To understand mangrove encroachment and ecosystem conversion as a whole, it is critical to examine the biogeochemical changes occurring within soils underlying these two vegetation types. The goal of this study is to fill this knowledge gap and evaluate microbially-mediated biogeochemical cycling of C, nitrogen (N), and phosphorus (P) (i.e. decomposition and nutrient availability) along a transect of mangrove encroachment into saltmarsh during both the high and low-water seasons in central Florida (USA). Additionally, we sought to determine the timescale upon which biogeochemical cycling is affected during mangrove encroachment by comparing biogeochemical functions in the transition zone to that of the two end member community types. Furthermore, we anticipated the impacts of encroachment may differ by season, such that the low-water season would increase decomposition and nutrient availability, while high-water season would dampen the magnitude of these measurements (Foster and others 2017). To study the biogeochemical effects of mangrove encroachment, we constructed multiple competing hypotheses: a) the null hypothesis, where vegetation community had no effect (Figure 21, panel A); b) a linear trend in decomposition and nutrient availability from one vegetation community to another, across the transition zone (Figure 21, panels B and E); c) greatest decomposition and nutrient availability within the end member communities (Figure 21, panel C); d) greatest

decomposition and nutrient availability within the transition zone (Figure 21, panel D), and e) a tipping point in decomposition and nutrient availability, where the transition zone is functionally the same as one end member vegetation community (Figure 21, panels F and G). In addition to the effects of vegetation community on biogeochemical processes, we further hypothesized that a gradient of salinity and inundation would be present within the selected site; increases in both of these abiotic factors have been theorized to encourage mangrove encroachment into salt marshes (i.e. Krauss and others 2011), but there remains a lack of empirical evidence linking the abiotic forcings to biotic gradients.

Methods
Site Description

A site was selected to span the ecotone of encroachment of black mangrove (*Avicennia germinans*) on endemic saltgrass (*Distichlis spicata L.*) within the Merritt Island National Wildlife Refuge, Cape Canaveral, FL (Figure 22) Specifically, the site was located within the cell designated as T9-North by the Brevard County Mosquito Control (28°42'49.71"N, 80°44'32.99"W). Soils at the site are fine, smectitic, nonacid hyperthermic typic hydraquent soils (Turnbull muck and Riomar clay loam), and the mangroves were defined as dwarf or fringe mangroves, exhibiting shorter tree heights when compared to mangroves within more subtropical zones (Doughty and others 2016). Within a proximal site, Simpson and others (2017) recorded canopy heights as 0.84 ± 0.1 m.
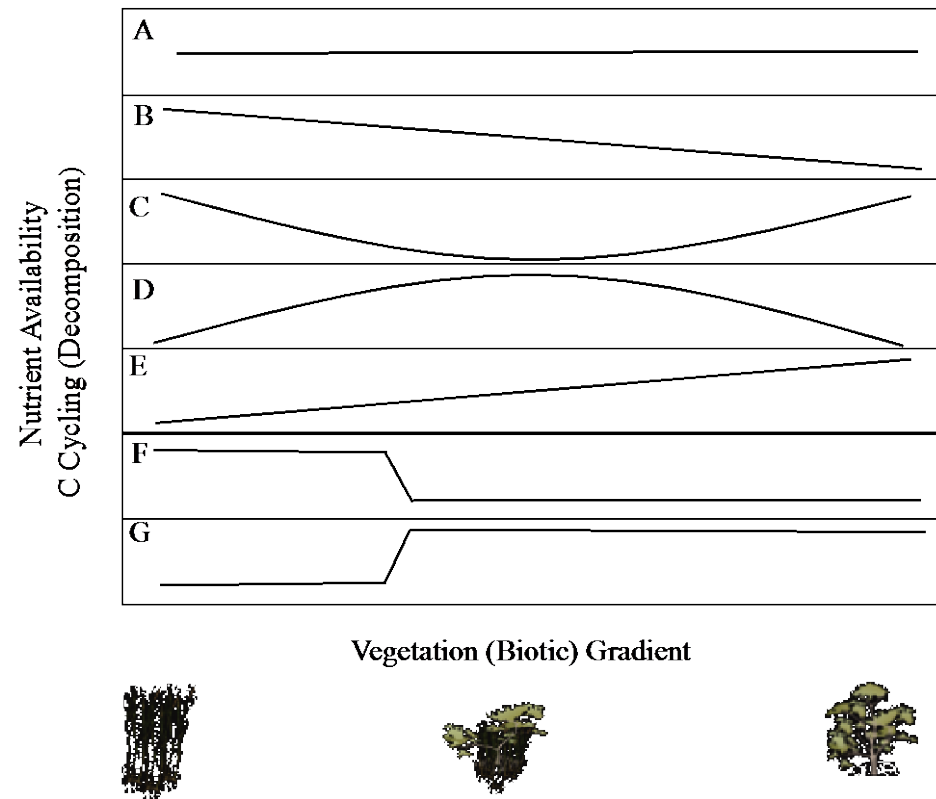
Figure 21: Conceptual diagram outlining hypotheses where a) is the null hypothesis (no change), b) represents higher decomposition and nutrient availability in the first vegetation community type, c) represents higher decomposition and nutrient availability within the end members, d) represents higher decomposition and nutrient availability within the transition zone, e) represents higher decomposition and nutrient availability within the second vegetation community type, f) similar to b) but with a non-linear change, and g) similar to e) but with a non-linear change (tipping point).
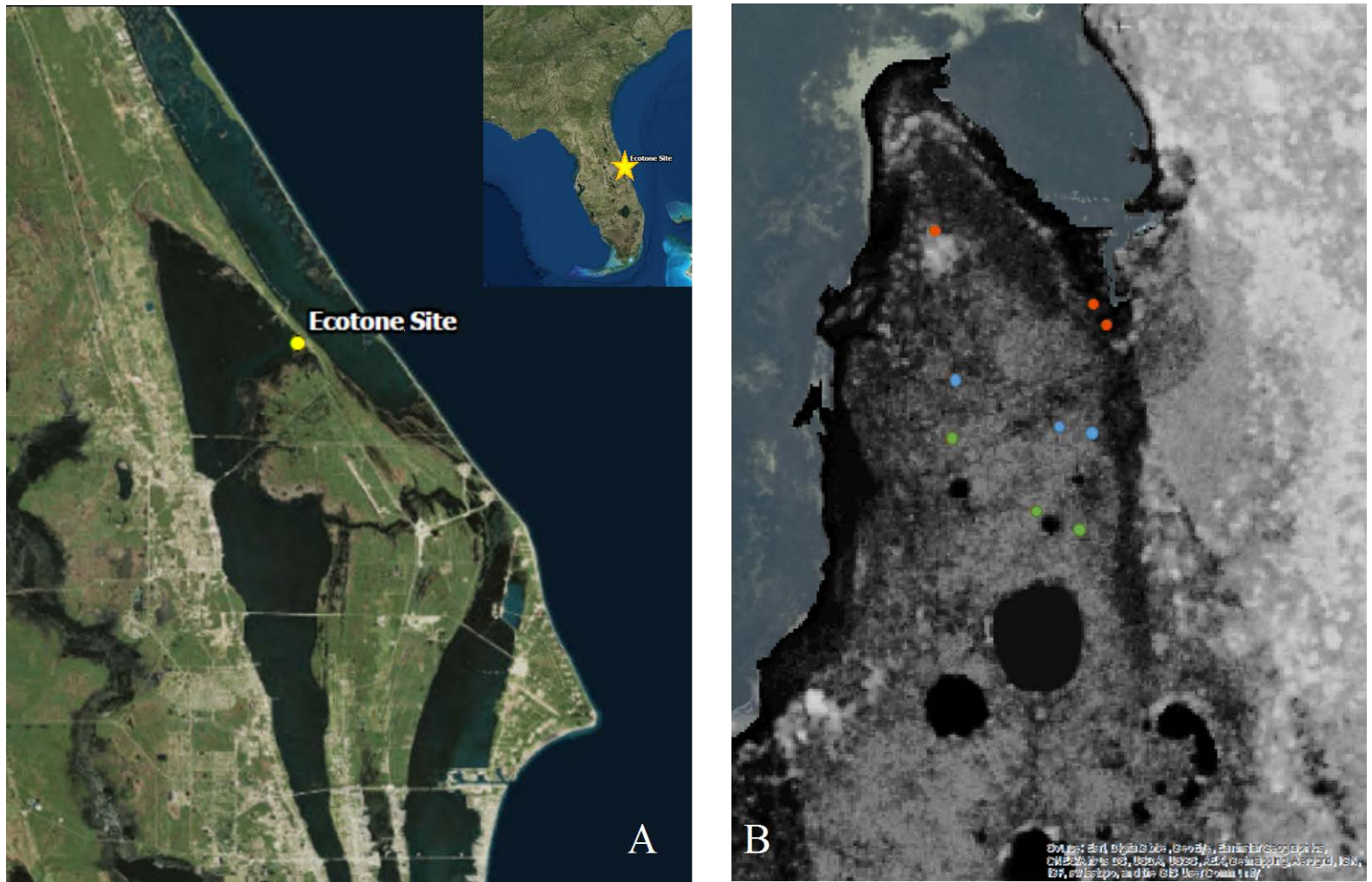
Figure 22: Map of the site, located within the Merritt Island National Wildlife Refuge (cell T9). A) Shows the site in the larger context of Eastern Florida, B) Digital elevation model depicting elevation at the site from LiDar data (darker colors correspond to lower elevations) overlaid on aerial photography. Orange corresponds to mangrove points, blue indicates transition zone points, and green indicates saltgrass points.

Three transects consisting of 3 plots ($4m^2$) were established to span the ecotone, with end members in both the mangrove and saltgrass and one plot within the transition zone, where both mangroves and saltgrass are present. The site experienced peak precipitation between June to September; combined with seasonal variation of water levels within the adjacent estuary (Indian River Lagoon, IRL), the high-water season occurred during August – November (Figure 23), while low-water season occurring during February – April (Brockmeyer and others 2005).

Soil Sampling

Soil sampling was conducted within two separate seasons that will be henceforth referred to as high-water (August 2017) and low-water (February 2018). Sampling consisted of obtaining 3 cores per plot (for a total of 27 cores per site per season) down to 30 cm via the push-core method. Cores were field-extruded into three 10 cm intervals: 0-10, 10-20, and 20-30 cm. Samples were immediately transferred into gallon-sized polyethylene bags and transported back to the laboratory where they were stored at 4 °C until sample analysis was completed.

Salinity and Elevation Data

Ambient salinity was determined at each plot along the middle transect during both the high and low-water sampling by use of a handheld optical refractometer (ThermoFisher Scientific, Waltham, MA). Elevation was determined by use of a Trimble Geo 7x (Trimble Inc., Sunnyvale, California, USA) coupled with LiDar data (NAVD88).

Soil Physicochemical Parameters

Soil moisture content was determined by drying a subsample of soil within a gravimetric oven for 3 days at 70°C, when a constant weight was achieved. Bulk density was calculated based on soil wet weight and volume for all samplings at all sites except for high-water within the mangrove site. Following drying, soils were ground using a SPEX Sample Prep 8000M

98

Mixer Mill (Metuchen, NJ). The loss-on-ignition method was used to determine percent organic matter within the dried, ground subsamples. Following determination of percent organic matter via ashing at 550 °C in a muffle furnace for a total of 3 hours, soils were digested with 50 mL of 1M HCl at 100°C for 30 minutes, then filtered through Whatman #41 filters for total P analysis (Andersen, 1976 with modifications). Total P content was measured colorimetrically on an AQ2 Automated Discrete Analyzer (Seal Analytical, Mequon, WI) via EPA method 365.1 (Rev.2). Total C and total N were determined on dried, ground subsamples on a Vario Micro Cube CHNS Analyzer (Elementar Americas Inc., Mount Laurel, NJ). Soil pH was determined by creating a 1:5 slurry of soil to distilled, deionized water, and measurement using an Accumet benchtop pH probe (AccumetXL200, ThermoFisher Scientific, Waltham, MA, USA).

<div align="center">Extractable Nutrients and Microbial Biomass</div>

Extractable nutrient analyses (nitrate (NO_3^-), ammonium (NH_4^+), soluble reactive phosphorus (SRP)) were conducted immediately upon return to the laboratory. Approximately 2.5 g of field-moist soils were weighed into 40 mL centrifuge tubes containing 25 mL of 2M KCl. Samples were shaken at 125 rpm for 1 hour, then centrifuged at 5000 rpm for 10 minutes at 10°C. Samples were filtered through Supor 0.45 µm filters and acidified with double distilled (DD) H_2SO_4 to a pH of <2 for preservation. Samples were then analyzed colorimetrically on an AQ2 Automated Discrete Analyzer (Seal Analytical, Mequon, WI) within 28 days, according to EPA methods 231-A (Rev. 0), 210-A (Rev. 1), and 204-A (Rev. 0).

Similarly, replicate samples of 2.5 g field-moist soil were weighed into 40 mL centrifuge tubes, and fumigated with chloroform for 24 h in a glass desiccator (Vance and others 1987). Following the fumigation, samples were extracted as outlined above. Both initial and fumigated samples were analyzed for dissolved organic carbon on a Shimadzu TOC-L Analyzer (Shimadzu

Instruments, Kyoto, Japan). Microbial biomass C was calculated as the difference in dissolved

organic carbon (DOC) between the fumigated samples and non-fumigated samples.

Greenhouse Gas Production

Samples were immediately homogenized upon return to the laboratory, and 7-10 g of soil

from each sample was weighed into a 120 mL glass serum bottle. Bottles were capped with

rubber septa, crimped with aluminum crimps, evacuated to -75 mmHg, then purged with 99 %

O_2-free N_2 gas for three minutes. Bottles were then injected with artificial seawater matching the

ambient salinity at the time of sampling to create a 1:2 slurry of soil to artificial seawater.

Bottles were placed on an orbital shaker in the dark at 100 rpm and 25 °C. Samples of the

headspace were taken at 24, 72, 120, 168, and 240 hours and injected into a GC-2014 gas

chromatograph (Shimadzu Instruments, Kyoto, Japan). Respiration rates were calculated as the

change in CO_2 and methane production over time using Henry's law to determine the amount of

CO_2 and CH_4 dissolved in either the liquid phase or within the headspace. Methane peak areas

were consistently low (often below detection) and thus will not be discussed.

Potentially Mineralizable Nitrogen and Phosphorus

Following the 10-day bottle incubation outlined above, 25 mL of 2 M KCl was added to

the bottles, which were then shaken for 1 h at 125 rpm and 25°C. Bottles were deconstructed,

transferred to centrifuge tubes, and centrifuged for 10 minutes at 10°C. The supernatant was

decanted and filtered using Supor 0.45 μm filters, then acidified with DD H_2SO_4 to a pH of <2

for preservation. Samples were analyzed on an AQ2 Automated Discrete Analyzer (Seal

Analytical, Mequon, WI) within 28 days. Rate of mineralization of N or P were calculated as the

NH_4^+ (or SRP) concentration at day 10 minus the initial extractable NH_4^+ (or SRP)

concentration, divided by 10 days.

Extracellular Enzyme Activity

Fluorometric assays were performed to determine activity of N-acetyl-β-D-glucosidase (NAG), alkaline phosphatase (AP), β-glucosidase (BG), xylosidase (XY), and cellobiosidase (CB) and aryl sulfatase (AS). Thirty-nine (39) mL of distilled, deionized water was added to approximately 0.5 g of field-moist soil and shaken for 1 h at 25°C and 125 rpm. Both samples and fluorescently labeled MUF-specific substrates for each enzyme were pipetted into clear 96 well plates then measured on a BioTek synergy HTX (BioTek Instruments, Inc., Winooski, VT, USA) at excitation/emission wavelengths 360/460 nm. Samples were measured again 24 hours later to determine a rate of enzyme activity.

Porewater Nutrients

During each sampling, porewater equilibrators (peepers) were deployed at each plot to determine porewater nutrient (NH_4^+, NO_3^-, SRP, DOC) concentrations and specific conductivity with depth. Prior to deployment, peepers were filled with N_2-purged nanopure water, then assembled and transported within an anaerobic environment. Peepers were left to equilibrate within the soil for 10 days. Immediately after removal from the soil, sample wells were extracted using a syringe and consolidated into 7 separate 5 cm increments down to 35 cm. Samples were filtered using 0.45 μm syringe filters and acidified with DD H_2SO_4 to a pH of <2. Samples were placed on ice for transportation back to the laboratory. Ammonium, NO_3^-, and SRP concentrations was determined colorimetrically on an AQ2 Automated Discrete Analyzer (Seal Analytical, Mequon, WI) within 28 days. Porewater NO_3^- concentrations were consistently below detection limits, and thus will not be discussed. Dissolved organic carbon concentrations were analyzed via a Shimadzu TOC-L Analyzer (Shimadzu Instruments, Kyoto, Japan). Specific conductivity was determined by use of an Accumet bench top conductivity probe (Accumet XL200, ThermoFisher Scientific, Waltham, MA).

Statistical Analysis

Data were separated by season for statistical analyses because parameters tended to vary significantly between high and low water seasons; our interest was in understanding the effects of vegetation community on biogeochemistry under these two distinct abiotic conditions. Data analysis was performed in R (R Foundation for Statistical Computing, Vienna, Austria) via RStudio (RStudio Inc., Boston, MA, USA). Before determining significance, each parameter was analyzed for assumptions of normality using the Shapiro-Wilk test, and homogeneity of variance using Levine's test. A log transform was applied to all data sets to meet these assumptions. Data were analyzed with a linear mixed model (package 'lme4'), accounting for soil depth and vegetation community as fixed effects, while the random effects included replicate core nested in transect. The interaction between depth and vegetation community was consistently non-significant, and was thus removed from the model during the process of model simplification and validation using AIC scores. Due to the number of iterations of the model performed, a Bonferroni correction was applied to the alpha value of 0.1, lowering the p-value to reject the null hypothesis to 0.005. Least-square means post-hoc tests were used to determine differences among vegetation types and depth intervals.

Results

Conductivity and Elevation

The mangrove plots had the lowest elevation, averaging -9.15 ± 0.23 cm (NAVD88). Elevation within the transition zone plots averaged 0.069 ± 2.58 cm, and the saltgrass plots averaged 5.99 ± 2.16 cm. Elevation was used as a proxy for water level throughout the experiment with lower elevations corresponding to higher water level. During high-water, salinity (as determined by refractometer) at the mangrove plots was highest, approximately 35 ppt, followed by the transition plots and saltgrass plots, which were approximately 25 and 15 ppt,

respectively (Figure 23). Low-water prevented measurement of ambient salinity, and the high-water salinity measurements were used for bottle incubations (Figure 23).

Soil Physiochemical Properties

Both vegetation community and soil depth were significant predictors of soil moisture content and pH during both high and low-water seasons (Table 13). During both seasons, the trend was the same: the saltgrass plots had significantly higher soil moisture than the transition and mangrove plots (which did not differ from one another), while pH was higher in the mangrove plots and did not differ between the transition and saltgrass (Table 14). The highest soil moisture was observed in the saltgrass plots during high water (mean ± standard error; 72 ± 1.1%) and the lowest in the mangrove plots during low-water (54 ± 3.6 %; Table 15). Soil moisture content decreased with depth, while pH increased with depth (Table 15). In general, soil moisture content showed a strong positive correlation with nearly all other biogeochemical parameters of interest, while pH demonstrated a negative correlation with several key parameters (e.g., extractable NO_3^-, extractable SRP, PMN rates, CO_2 production, and all enzyme activity), particularly during low-water season (Supplementary Tables 1 and 2)

Total soil nutrient pools (C, N, P, and organic matter content) remained consistent between high and low-water samplings and were affected by vegetation community and soil depth (Table 13). The saltgrass plots had the highest concentrations of every nutrient (Table 15), while the transition and the mangrove plots did not differ from one another (Table 14).
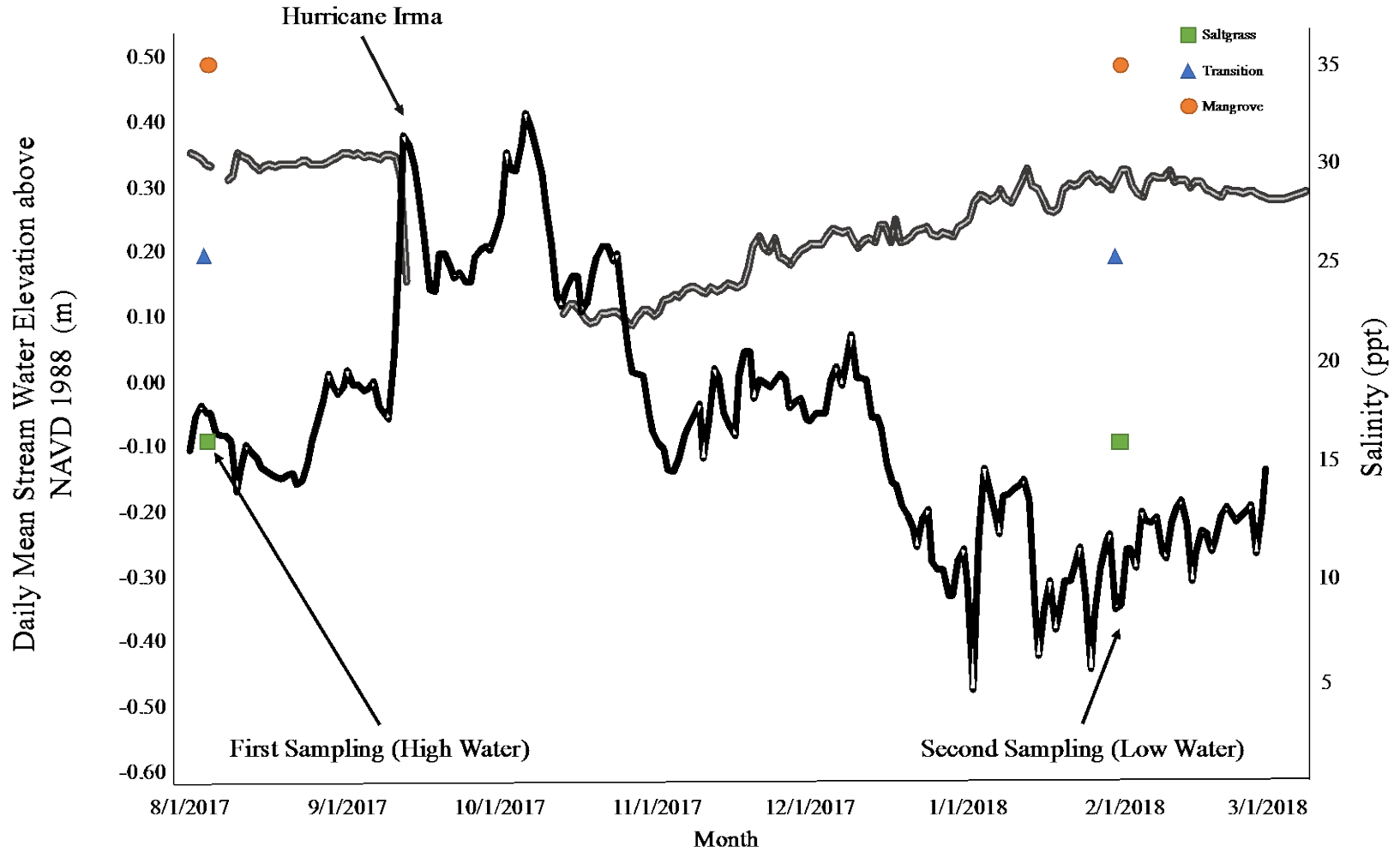
Figure 23: Daily mean stream water elevation (black line) above NAVD 1988 (m) at Haulover Canal, Mims, FL (<1.1 km from site, data from USGS station 02248380), and ambient salinity (gray line) of the Indian River Lagoon at Max Brewer Memorial Parkway Fishing Pier (SJRWMD 33954622-CM, 10 km from site) from 8/01/2017 to 3/01/2017. Symbols indicate ambient salinity at each plot during sampling.

Table 13: p-values for each tested parameter using the linear model (where fixed effects included community type and depth, and random effects included transect and replicate). The applied Bonferroni correction lowered the α value to 0.005. Underlined values are significant. (n=81 for each season).

	Woody - Herbaceous Transition			
	High-water		**Low-water**	
	Community	*Depth*	*Community*	*Depth*
Moisture Content	0.0001	0.0001	0.0007	0.0003
Total C	<0.0001	<0.0001	<0.0001	<0.0001
Total N	<0.0001	<0.0001	<0.0001	<0.0001
Total P	0.0001	<0.0001	0.0040	<0.0001
Organic Matter	<0.0001	<0.0001	<0.0001	<0.0001
pH	<0.0001	0.0002	<0.0001	<0.0001
Ext. Nitrate	0.1185	0.1583	<0.0001	<0.0001
Ext. Ammonium	0.0370	0.6668	0.0001	0.0753
Ext. SRP	0.0020	0.0005	0.0121	<0.0001
Microbial Biomass C	0.0072	0.8358	0.0001	<0.0001
NAG	0.0406	0.0001	0.0140	<0.0001
AP	0.0022	0.0002	<0.0001	<0.0001
BG	0.0008	<0.0001	0.0559	<0.0001
CB	0.0041	0.0002	0.0299	<0.0001
XY	0.0003	0.0001	<0.0001	<0.0001
AS	0.0030	0.0010	0.0001	<0.0001
CO_2 Production	0.1874	0.0002	0.0756	<0.0001
PMN	0.0088	0.0119	0.0012	<0.0001
PMP	0.1123	0.0009	0.0091	<0.0001

Table 14: Similarity matrix derived from post-hoc least squares mean tests where the community effect was significant in the linear model. Green boxes indicate no significant difference, while yellow boxes indicate that a significant difference between vegetation communities. Dashes indicate no significance within linear model.

	High-Water			Low-Water		
	Mangrove	Transition	Saltgrass	Mangrove	Transition	Saltgrass
Moisture Content	green	green	yellow	green	green	yellow
Total C	green	green	yellow	green	green	yellow
Total N	green	green	yellow	green	green	yellow
Total P	green	green	yellow	green	yellow	green
Organic Matter	green	green	yellow	green	green	yellow
pH	yellow	green	green	yellow	green	green
Ext. Nitrate	-	-	-	yellow	green	green
Ext. Ammonium	-	-	-	yellow	green	green
Ext. SRP	-	-	-	-	-	-
Microbial Biomass C	-	-	-	green	green	yellow
NAG	-	-	-	-	-	-
AP	green	green	(white)	green	green	yellow
BG	green	yellow	green	-	-	-
CB	green	yellow	green	-	-	-
XY	green	green	yellow	green	green	yellow
AS	green	yellow	green	green	green	yellow
CO_2 Production	-	-	-	-	-	-
PMN Rate	-	-	-	green	green	yellow
PMP Rate	-	-	-	-	-	-

Table 15: Soil physiochemical properties by season, community, and depth. StErr stands for standard error (n=9).

Season	Community	Depth (cm)	pH Mean	pH StErr	Moisture Content (%) Mean	Moisture Content (%) StErr	Organic Matter (%) Mean	Organic Matter (%) StErr	Total C g kg⁻¹ Mean	Total C g kg⁻¹ StErr	Total N g kg⁻¹ Mean	Total N g kg⁻¹ StErr	Total P mg g⁻¹ Mean	Total P mg g⁻¹ StErr
High-Water	Saltgrass	0-10	5.45	0.10	76.08	0.64	64.90	1.61	312.39	7.51	20.34	0.49	502.69	21.66
		10-20	5.64	0.06	73.06	2.09	48.54	5.31	220.63	20.73	13.84	1.32	354.69	11.40
		20-30	6.19	0.06	69.00	2.30	43.32	4.14	208.61	20.31	12.89	1.24	297.80	10.35
	Transition	0-10	5.53	0.10	70.10	2.21	46.09	6.10	137.13	10.34	8.74	0.67	396.01	50.70
		10-20	5.90	0.08	61.65	5.94	30.81	6.87	118.39	25.64	7.61	1.65	241.80	40.40
		20-30	6.45	0.11	56.38	6.84	21.63	5.17	62.20	22.36	3.96	1.49	192.13	33.89
	Mangrove	0-10	6.67	0.22	65.09	1.94	27.51	2.61	220.92	29.83	14.11	1.93	310.26	50.34
		10-20	6.60	0.26	57.34	4.00	26.47	5.60	158.50	37.42	9.57	2.21	265.30	58.02
		20-30	6.71	0.23	46.52	6.21	16.82	5.12	103.79	25.13	6.57	1.74	188.69	44.34
Low-Water	Saltgrass	0-10	6.11	0.08	75.71	0.81	67.37	1.12	313.14	8.72	18.90	2.38	547.02	44.52
		10-20	6.48	0.07	71.66	1.99	46.88	5.74	210.55	26.87	13.75	1.77	321.24	41.06
		20-30	6.65	0.09	63.35	7.86	44.37	6.22	211.61	35.36	13.00	1.94	266.34	27.44
	Transition	0-10	6.00	0.12	68.70	3.76	47.30	8.08	166.03	16.21	10.90	0.85	401.00	71.17
		10-20	6.46	0.16	60.61	3.50	25.91	4.90	108.36	31.77	7.15	2.08	222.60	40.09
		20-30	6.77	0.11	49.94	7.20	16.86	5.11	74.64	27.07	4.98	1.88	142.44	31.97
	Mangrove	0-10	6.53	0.23	62.39	6.71	37.16	3.26	224.21	34.63	15.14	2.27	439.65	43.68
		10-20	6.78	0.20	56.23	4.68	23.86	5.99	109.33	20.81	7.38	1.44	259.30	53.27
		20-30	7.00	0.16	44.64	6.40	16.21	5.28	78.31	23.95	5.29	1.67	190.34	44.72

All concentrations decreased with increasing soil depth and showed strong positive correlations to all other biogeochemical parameters except extractable NH_4^+ (Table 15; Supplemental Tables 1 and 2)

Extractable Nutrients and Potentially Mineralizable Nutrients

Neither depth nor vegetation community significantly predicted extractable NO_3^- or NH_4^+ concentrations during high-water (Table 13, Figure 24). High-water extractable SRP differed between the saltgrass plots, averaging 2.11 ± 0.295 mg kg^{-1}, and transition plots, 1.01 ± 0.203 mg kg^{-1} (Tables 13 and 14). Extractable SRP during high-water was significantly correlated to PMN and PMP rates, CO_2 production, and all enzyme activity (Supplementary Tables 1 and 2). High-water extractable NO_3^- was correlated to PMP rates, NAG activity, phosphatase activity, xylosidase activity, and sulfatase activity. In contrast, high-water extractable ammonium concentrations were correlated to extractable SRP concentrations, NAG activity, and sulfatase activity.

During low-water, extractable NO_3^- and NH_4^+ were significantly different between vegetation communities, while extractable NO_3^- and SRP were significantly different between depths (Table 13). The highest extractable NO_3^- concentrations during low-water were within the saltgrass plots, averaging 2.02 ± 0.211 mg kg^{-1}; lowest concentrations were within the mangroves, averaging 1.36 ± 0.128 mg kg^{-1}, but the transition and mangrove plots did not differ from one another (Table 14). Low-water extractable NO_3^- concentrations were roughly 3.5x higher than concentrations during high-water. Extractable NO_3^- concentrations were positively correlated to extractable NH_4^+ concentrations, extractable SRP concentrations, PMP and PMN rates, MBC, CO_2 production, and all enzyme activity (Supplementary Tables 1 and 2). Extractable NH_4^+ concentrations during low-water ranged from 18.1 ± 4.43 mg kg^{-1} to $5.43 \pm$

0.764 mg kg^{-1} within the mangrove and transition plots, respectively (Figure 24). Concentrations within the saltgrass plots and transition plots did not differ during low-water (Table 14). Low-water extractable NH_4^+ was significantly correlated to PMP rates, MBC, and cellobiosidase activity (Supplementary Tables 1 and 2), and concentrations were roughly 2.5x higher than concentrations during high-water. Low-water concentrations of extractable SRP were significantly correlated to PMN and PMP rates, MBC, CO_2 production, and all enzyme activity (Supplementary Tables 1 and 2).

During high-water, PMN rates were not significantly predicted by either community or depth (Table 13). During low-water, both depth and vegetation significantly affected PMN rates (Table 13, Figure 24, which were roughly 2x greater than during the high-water season. While the low-water transition plots were not different from the low-water mangrove plots, all other comparisons were significant (Table 14). The low-water saltgrass plots contained the highest PMN rates, averaging 13.4 ± 2.21 mg NH_4^+ kg^{-1} d^{-1}, while the mangrove and transition plots averaged 8.77 ± 2.02 mg NH_4^+ kg^{-1} d^{-1}. High-water PMN rates were significantly correlated to PMP rates, CO_2 production, and all enzyme activity (Supplementary Tables 1 and 2). Similarly, low-water PMN rates were significantly correlated to PMP rates, MBC, CO_2 production, and all enzyme activity (Supplementary Tables 1 and 2).

Both high-water and low-water PMP rates were significantly influenced by depth (Table 13). High-water PMP rates were correlated to CO_2 production and all enzyme activity, while low-water PMP rates were correlated to MBC, CO_2 production, and all enzyme activity (Supplementary Tables 1 and 2).

Microbial Biomass C and CO_2 Production

Microbial biomass C content was roughly 1.5x higher during high-water than during low-water. Neither community type nor depth significantly predicted MBC content within the high-water season, both significantly predicted MBC content during low-water (Table 13, Figure 25). Microbial biomass C in the saltgrass plots at low-water averaged 2303 ± 312 mg kg^{-1}, which was significantly greater than both the transition and mangrove plots, which were not different from each other. The transition plots at low-water contained an average MBC content of 1006 ± 133 mg kg^{-1}. Low-water MBC was significantly correlated to PMN and PMP rates, CO_2 production, and all enzyme activity (Supplementary Tables 1 and 2).

CO_2 production significantly differed with depth during both seasons, but not with vegetation community (Table 13, Figure 25). High-water CO_2 production rates were correlated to extractable SRP, PMN rates, PMP rates, and all enzyme activity. Carbon dioxide production was 30% higher during low-water than during high-water. Carbon dioxide production was positively correlated to all enzyme activity during low-water (Supplementary Tables 1 and 2).

Extracellular Enzyme Activity

Both BG and CB activity were significantly different between both vegetation community and depth during high-water, and only with depth during low-water (Table 13, Figure 26). Activity of both BG and CB during low-water was approximately 2.8x higher than activity during high-water. Activity of BG at high-water averaged 1.71 ± 0.251 nmol MUF g^{-1} h^{-1} at the mangrove plots, which was not significantly different from activity at the saltgrass plots. The transition plots had the lowest activity at high-water, averaging 1.02 ± 0.161 nmol MUF g^{-1} h^{-1}.
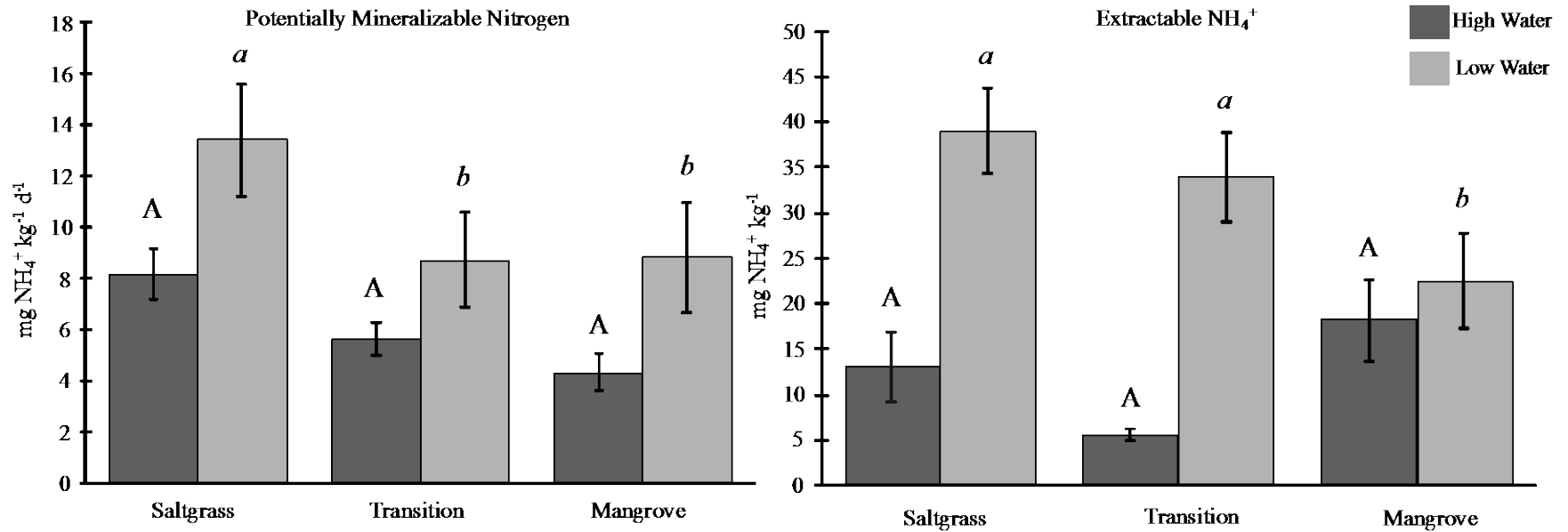
Figure 24: Potentially mineralizable N rates and extractable ammonium at high water and low water along transects of saltgrass, transition, and mangroves. Values are mean ± standard error (n=9). Dark bars represent high water levels while light bars represent low water levels. Capital letters denote significance ($p < 0.05$) between high water means while lowercase, italicized letters denote significance ($p < 0.05$) between low water means when the main effect was significant ($p < 0.005$).
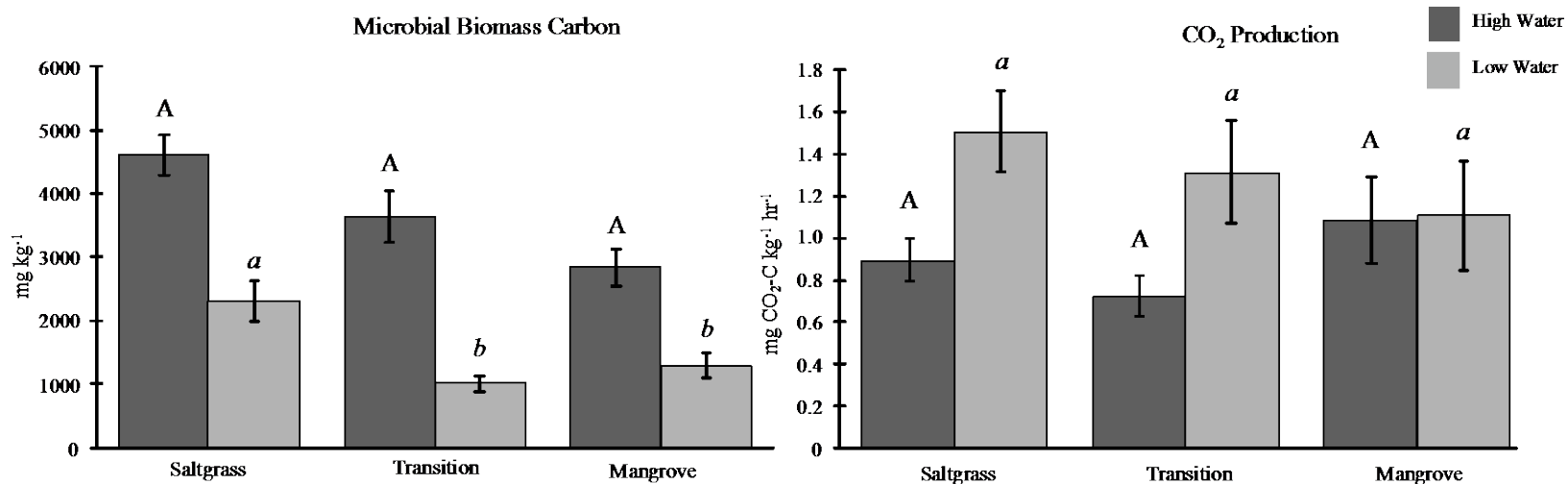
Figure 25: Microbial biomass C and rates of CO_2 production at high water and low water along transects of saltgrass, transition, and mangroves. Values are mean ± standard error (n=9). Dark bars represent high water levels while light bars represent low water levels. Capital letters denote significance ($p < 0.05$) between high water means while lowercase, italicized letters denote significance ($p < 0.05$) between low water means when the main effect was significant ($p < 0.005$).

Similarly, high-water CB activity ranged from 0.524 ± 0.043 nmol MUF g^{-1} h^{-1} within the saltgrass plots to 0.359 ± 0.029 nmol MUF g^{-1} h^{-1} within the transition plots, though there was no significant difference between activity within the saltgrass and mangrove plots.

Activity of XY was nearly 3x higher during low-water than high-water and was significantly different with depth and vegetation community during both seasons (Table 13, Figure 26). Greatest XY activity during high-water was within the saltgrass plots, averaging 0.520 ± 0.030 nmol MUF g^{-1} h^{-1}, while the lowest activity was within the mangrove and transition plots, which were not significantly different from each other (Table 14). During low-water, XY activity was also highest within the saltgrass plots, followed by the transition plots, and lowest within the mangroves.

Both vegetation community and depth significantly predicted AP activity during both high and low-water (Table 13, Figure 27), though activity was nearly 3x higher during the low-water sampling. High-water AP activities averaged 4.52 ± 0.303 nmol MUF g^{-1} h^{-1} within the saltgrass plots, 2.55 ± 0.291 nmol MUF g^{-1} h^{-1} within the transition plots, and 3.05 ± 0.535 nmol MUF g^{-1} h^{-1} within the mangrove plots, though there was no significant difference in activity between the transition and mangrove plots (Table 14).

Activity of AS was roughly 2x higher during low-water than high-water, averaging 0.483 ± 0.037 nmol MUF g^{-1} h^{-1} during high-water and 0.935 ± 0.100 nmol MUF g^{-1} h^{-1} during low-water. Both vegetation community and depth were significant predictors of AS activity in both low-water and high-water (Table 13, Figure 27). High-water AS activity ranged from 0.572 ± 0.027 nmol MUF g^{-1} h^{-1} within the saltgrass plots to 0.396 ± 0.031 nmol MUF g^{-1} h^{-1} in the transition plots. Low-water activity was also highest in the saltgrass plots and lowest in the mangrove plots.
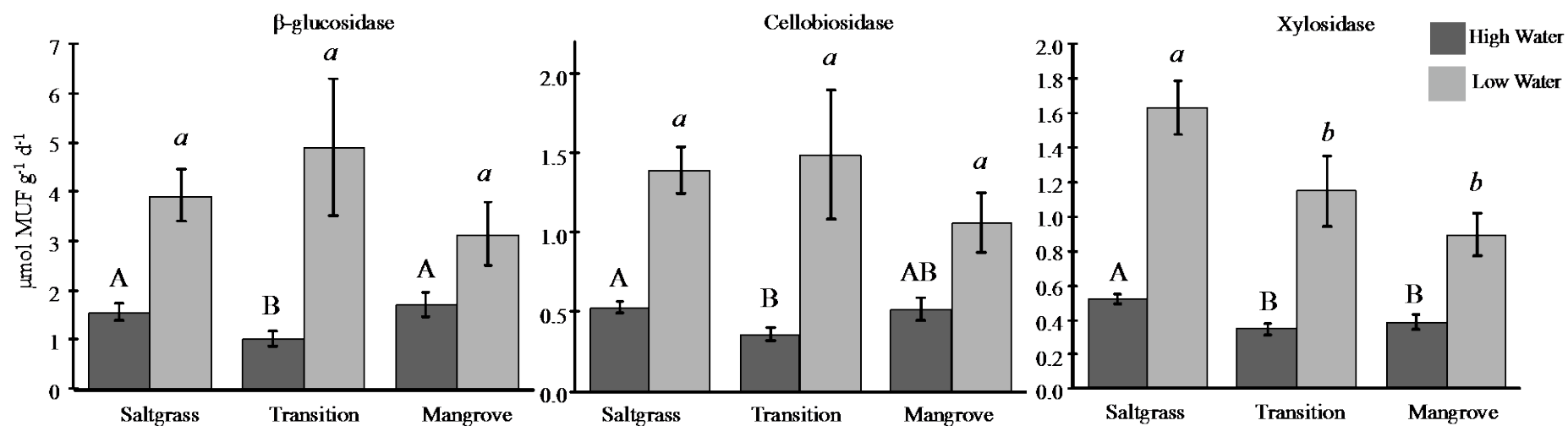
Figure 26: Enzyme activity of C enzymes (BG, CB, XY) at high water and low water along transects of saltgrass, transition, and mangroves.

Values are mean ± standard error (n=9). Dark bars represent high water levels while light bars represent low water levels. Capital letters denote

significance ($p < 0.05$) between high water means while lowercase, italicized letters denote significance ($p < 0.05$) between low water means when

the main effect was significant ($p <0.005$).
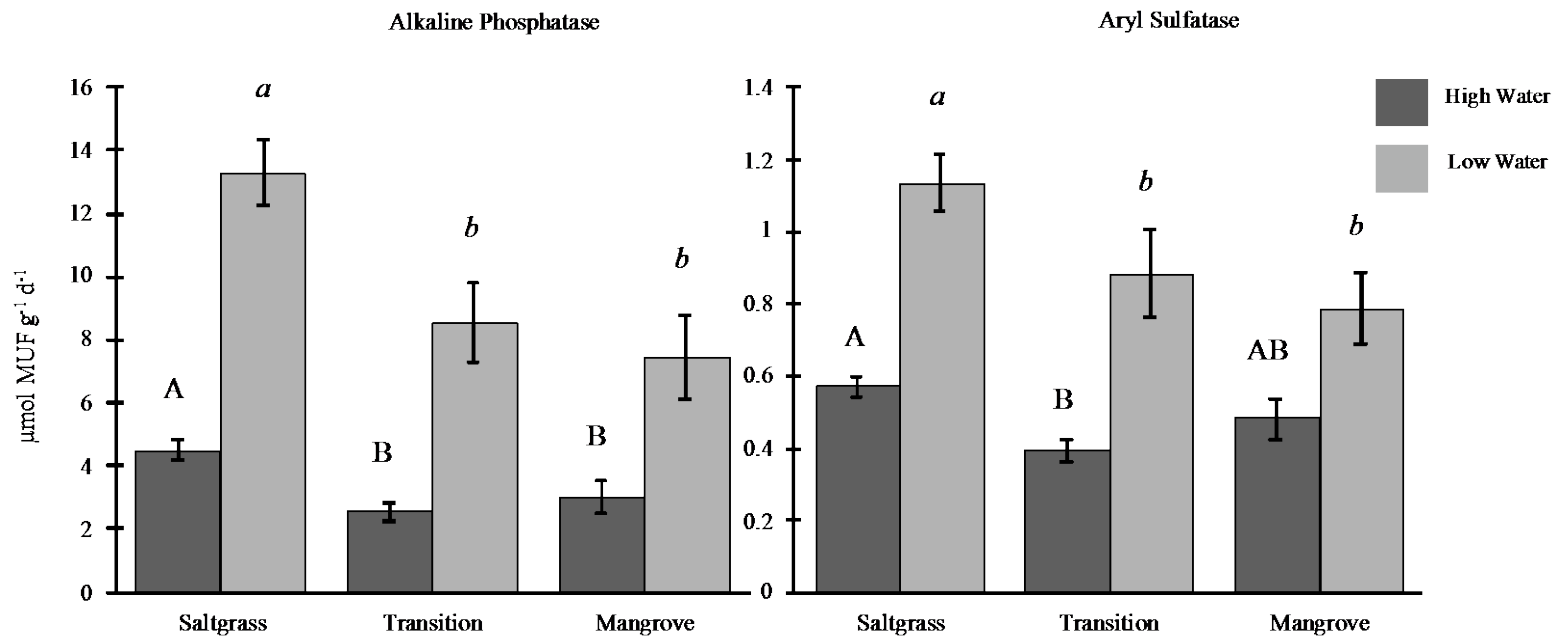
Figure 27: Enzyme activity of extracellular enzymes (AP and AS) at high water and low water along transects of saltgrass, transition, and mangroves. Values are mean ± standard error (n=9). Dark bars represent high water levels while light bars represent low water levels. Capital letters denote significance ($p < 0.05$) between high water means while lowercase, italicized letters denote significance ($p < 0.05$) between low water means when the main effect was significant ($p < 0.005$).

Depth predicted NAG activity during both low and high-water (Table 13); community type had no effect during either season. N-acetyl-β-D-glucosidase activity was roughly 2.75x higher during the low-water season. All enzyme activity was significantly correlated to each other during both high and low-water (Supplementary Tables 1 and 2).

Porewater Nutrients

During high-water, porewater NH_4 was higher within the mangrove plots (7.15 ± 0.335 mg NH_4 L^{-1}) and lowest within the saltgrass and transition plots (2.80 ± 0.776 mg NH_4 L^{-1}), which were not significantly different from each other (Table 13). Vegetation community similarly affected porewater NH_4 concentrations during the low-water season, though all concentrations were higher (13.7 ± 0.513, 7.63 ± 1.12, and 9.77 ± 1.24 mg NH_4 L^{-1}, for the mangrove, transition, and saltgrass, respectively). Depth did not significantly affect porewater NH_4 values during either high or low-water.

Vegetation community significantly affected porewater SRP concentrations during both seasons (Table 13), though concentrations were slightly higher during low-water. High-water porewater SRP concentrations were greatest in the mangrove plots, averaging 0.460 ± 0.053 mg L^{-1}. The transition zone and saltgrass plot concentrations were not different from each other. During low-water, porewater SRP concentrations averaged 0.507 ± 0.068 mg L^{-1}, 0.185 ± 0.061 mg L^{-1}, and 0.402 ± 0.109 mg L^{-1}, within the mangrove, transition, and saltgrass plots, respectively. Similarly to porewater ammonium, porewater SRP concentrations did not differ with depth during high-water, but were significant during low-water (Table 13). Porewater SRP concentrations were relatively stable from the surface to 30 cm, then increased between 30 cm and 35 cm.

Porewater dissolved organic C (DOC) differed between vegetation community types during high-water and low-water (Table 13). Concentrations of porewater DOC during high-water were greatest in the mangrove plots, averaging 11.7 ± 0.670 mg L^{-1}, and lowest in the transition zone, where concentrations averaged 6.87 ± 1.00 mg L^{-1}. The saltgrass plots and transition zone plots were not significantly different from each other during high-water or low-water. Low-water mangrove porewater DOC concentrations averaged 14.7 ± 0.557 mg L^{-1}, 11.1 ± 1.032 mg L^{-1}, and 11.7 ± 0.777 mg L^{-1}, within the mangrove, transition zone, and saltgrass plots, respectively. Depth also significantly controlled concentrations of DOC in the porewater during the low-water season (Table 13). Values were highest within the top depth interval, then decreased sharply between 0-5 cm and 10-15 cm. Below 15 cm, values increased to roughly half the concentrations in the top depth interval and stayed constant throughout the rest of the depth profile.

Discussion

Carbon Dynamics

One of the prevailing foci of research into mangrove encroachment concerns the impact to soil C stores. In this study, unexpectedly, soil CO_2 production did not differ between vegetation types (Figure 25), coinciding with the null hypothesis (Figure 21, panel A). Studies have hypothesized that the structural differences between mangrove roots and the rhizomes of salt marsh plants will affect oxygenation of the soil, with mangroves hypothesized to exude more oxygen (Scholander and others 1955; Comeaux and others, 2012). In a study within a salt marsh in coastal Louisiana, Perry and Mendelssohn (2009) reported higher Eh values in *Avicennia* dominated plots, compared to *Spartina* dominated plots. This higher Eh from root exudation of O_2 has been generally believed to enhance soil CO_2 production in soils dominated by mangrove roots, as oxygen provides a terminal electron acceptor thermodynamically favored over sulfate

reduction (Perry and Mendelssohn 2009; Comeaux and others 2012; Kelleway and others 2017). Yet, very few studies have documented soil CO_2 efflux from *Avicennia*-dominated soils compared to saltmarsh-dominated soils, and they have reported conflicting results (Barreto and others 2018; Simpson and others 2018). In this study, soil CO_2 production was similar throughout vegetation types and salinity and inundation regimes, leading to the assumption that rate of soil organic matter decomposition is relatively stable across this ecotonal transition (i.e. the null hypothesis, Figure 21, panel A). This is surprising not only in relation to oxygen availability, but also when considering differences in microclimate, litter fall, belowground biomass, and other soil physicochemical differences that could occur between sites (Kelleway and others 2017). Though not measured within this study, mangrove cover has been documented to provide shade (Krauss and others 2008), which can lower the temperature of soils beneath mangroves compared to those with herbaceous salt marsh cover. Additionally, mangroves are woody species that contain higher ratios of recalcitrant C compounds, such as lignin, within leaf litter relative to salt marsh grasses, such as saltgrass (Bianchi and others 2013). These recalcitrant C compounds require more energy to be mineralized than labile, low molecular weight compounds, and thus are thought to decompose slower. Other studies have hypothesized that the proliferation of these high molecular weight compounds within mangrove plots might limit decomposition, and subsequently CO_2 production as well, which was not observed in this study. Instead, the similar rates of CO_2 production between vegetation types could reflect unique microbiota between the two vegetation types (i.e. Barreto and others, 2018), or the interaction of vegetation with present abiotic gradients. Although microbial community composition was not quantified in this study, MBC was similar across the ecotone during high water, and weakly correlated with CO_2 production during low-water (Figure 25). Finally, it is important to note the

CO_2 production rates reported in this study represent potential rates derived from bottle incubations. Although the rates of CO_2 produced during bottle incubations have been shown to closely mimic those found with *in-situ* studies (Breithaupt et al., in review) repeated *in-situ* measurements would be beneficial in confirming if CO_2 production is indeed unaltered by mangrove encroachment.

Generally, the mangrove-salt marsh ecotone literature has focused on quantifying changing stocks of C (Kelleway and others, 2017 and references therein). Some studies have reported no change in soil C stocks with regards to vegetation (Perry and Mendelssohn 2009; Henry and Twilley 2013; Doughty and others 2016), while others have asserted that mangrove soils contain higher concentrations of total C (Osland and others 2012; Bianchi and others 2013; Lewis and others 2014; Yando and others 2016; Simpson and others 2017), with implications for C sequestration in the face of climate change. This study takes this idea a step further, evaluating carbon dynamics not only in the two end member communities, but also within the transition zone were both species co-dominate. Surprisingly, our data conflicts with previous work, showing not only does the saltgrass contain roughly 65% more soil C than the mangrove plots, but the transition zone generally functions more similarly to the mangrove community, rather than as a true intermediate (supporting hypothesis F in Figure 21). The position of mangrove plots lower in the tidal frame could contribute to export of C in the form of leaf litter through tidal cycles, resulting in lower soil C than the saltgrass plots from the lack of litter being incorporated into the soil matrix (Bouillon and others 2008). Furthermore, following the freeze of 1989, mangroves died back within this region of central Florida, and as a result, the mangrove plots within this field study are not more than 29 years old (Dr. Paul Schmalzer, personal communication). The relatively young age of these trees could account for the small C

accumulation rates; with time, mangrove soil C content could surpass that of the saltgrass (Osland and others 2012).

Enzyme activities of BG, XY, and CB also offer some insight into the dynamics of C cycling within this system. The activity of soil extracellular enzymes is correlated to both the availability of substrates and the microbial need for energy sources (Tabatabai 2003). Specifically, BG and CB hydrolyze different forms of cellulose within wetland soils, resulting in either B-D-glucose or cellobiose, respectively (Dunn and others 2014). During high-water, both BG and CB expressed greater activity within the end members than in the transition zone (Figure 26, Figure 21). Under the evolutionary-economic hypothesis, enzyme activity is the inverse of availability (Allison and others 2011); for example, high activities of BG and CB within the mangrove and saltgrass plots relative to the transition indicate a depressed availability of cellulose within the end member soils. Meanwhile, the transition zone has an increased availability of cellulose, likely from the combined litterfall of mangrove leaves and herbaceous grasses. This low activity indicates that greater species richness and evenness in the transition zone alleviate the cellulose limitation. Hemicellulose, a more recalcitrant and less structurally stable form of C (Reddy and DeLaune 2008), is also degraded differentially across the ecotone. Xylosidase is indicative of the final stage of hydrolysis of hemicellulose into monomers such as xylan (Dunn and others 2014). The high XY activity within the saltgrass plots indicates a high demand (and thus low supply) of hemicellulose, while activities within the transition zone and mangrove plots demonstrate a low demand (and high supply) of hemicellulose (Figure 26, Figure 21). This is intuitive, as mangroves contain a higher proportion of recalcitrant compounds such as hemicellulose (Bianchi and others 2013), depressing the activity of XY within the mangrove and transition zone soils. Collectively, these C cycling enzymatic activities imply that

availability of cellulose for microbial respiration is highest in the transition zone, while availability of hemicellulose is greatest wherever mangroves are present. The presence of mangroves amplifies the availability, likely through increasing the quantity, of cellulose and hemicellulose substrates for microbial respiration within these soils. Except for the same changes in XY, this general trend was only present during high-water (Figure 26) and was likely obscured during the low-water season due to exceptionally high rates across the entire site from dry-down.

Nitrogen Dynamics

The different vegetation communities and physical characteristics along the transect also altered nitrogen dynamics and speciation. Though extractable NH_4^+ concentrations were highest within the saltgrass and transition zone plots (Figure 24), porewater NH_4^+ concentrations were greatest within the mangrove plots, following the tipping point hypothesis (Figure 21, panel F). Extractable NH_4^+ encompasses both porewater NH_4^+ and NH_4^+ ions adhered to the soil cation exchange complex (CEC) (DeLaune and others 2013). The high availability of porewater NH_4^+ within the mangrove plots could be mediated by salinity: exposure to high salinities can result in the replacement of NH_4^+ on the cation exchange complex with other mono- or divalent ions present in seawater (Steinmuller and Chambers, 2017). Comparatively, NH_4^+ within the saltgrass and transition zone plots, which experience a lower salinity, might still be adhered to the CEC and not released into the porewater. In addition to abiotic forcings such as salinity, available concentrations of NH_4^+ are also mediated by plant uptake (Brannon 1973). Rates of PMN indicate the transition zone and mangrove soils produce less NH_4^+ through the breakdown of organic matter than soils within the saltgrass plots (Figure 24). PMN is mediated by available

organic matter (which is greatest within the saltgrass plots), quality of organic matter, available NH_4^+ concentrations, and resident microbial communities (Roy and White 2013).

Differences in nitrate availability were observed between high and low-water, likely mediated by changes in soil redox potential. As soils dried down during the low-water season, nitrate availability increased as the system became more oxidized, promoting nitrification, the microbially-mediated oxidation of NH_4^+ to NO_3^- (Reddy and DeLaune 2008). The drop in water level during the low-water season not only catalyzed changes in speciation of N, but increased the activity of all enzymes, as well as CO_2 production.

<center>Phosphorus and Sulfur Cycling</center>

The abundance of total P within the saltgrass soils compared to the transition and mangrove soils may be related to the high content of organic matter within the saltgrass soils and changes in bulk density across the landscape gradient. When accounting for bulk density (transforming total P into units of density), differences in total P are no longer as apparent. The more tidally influenced mangrove site contributes a higher bulk density due to less volume for pore space and organic matter, while the saltgrass plots have a higher total P concentration from high organic matter content, effectively evening out the difference between plots. Alkaline phosphatase activity represents this difference in organic versus inorganically-bound P present within the vegetation communities (Figure 27). Depressed activity within the transition and mangrove sites indicate that there is plenty of P available for microbial processes, while high activity within the saltgrass site represents increased rates of breakdown of organically-bound P monoesters to satisfy microbial needs for P.

Sulfate is one of the most dominant ions within seawater. As the mangrove plots contained the highest salinity, followed by the transition zone plots, it follows that activity of AS

would be depressed within these two zones (Figure 27). The availability of sulfate is therefore lowest within the saltgrass plots, owing to their lower salinity, dampened inundation regime, and increased activity of AS. Aryl sulfatase liberates sulfate ions from plant-derived detritus to supply to growing vegetation. In a previous study at this site, it was observed that saltgrass emitted high rates of various sulfur compounds (H_2S, DMS, CS_2, and DMDS), and thus concluded that these high rates indicate that saltgrass might utilize sulfonium compounds within their osmoregulatory system (Cooper and others, 1986). Utilization of such sulfur-containing ions could promote the liberation of sulfate ions for further uptake by plants.

Conclusions

The encroachment of mangroves onto into saltgrass in coastal wetlands catalyzes biogeochemical change by altering long-term pools of nutrients and generally impacting indicators of C, N, and P cycling. Of all the hypotheses postulated, the majority of the data collected showed a tipping point in biogeochemical response where the transition zone soils were functionally similar to soils within the mangrove zone. More specifically, longer term pools (i.e. total soil C, N, P, organic matter content) within the transition zone were functionally equivalent to the mangrove zone (Figure 21, panel F), indicating that encroachment rapidly affects these long term pools. Enzyme activity, mineralization rates, and microbial biomass, all indicators of current biogeochemical cycling, appeared to either be more affected by seasonality and environmental variation, rather than encroachment. Based on the total nutrient pool response, it is likely that these short-term indicators will reach a 'tipping point', likely correlated to shifting ratios of mangrove: saltgrass dominance, where biogeochemical processing in the transition zone will function equivalently to the mangrove soils, with implications for macronutrient cycling within this system as a whole.

Though CO_2 production, a proxy for decomposition potential along the ecosystem gradient, did not change with vegetation communities, long-term pools of C (total C, organic matter) were lower within the mangrove zone. As mangrove encroachment continues to occur, this can alter the C balance within the system, potentially impacting the source/sink dynamics of this system. The differences observed within utilization of specific C compounds via measurements of enzyme activity indicate that C breakdown is occurring differently across the ecotone, these effects were not present between both seasons, and are relatively short-term indicators of biogeochemical change.

Regarding nutrient availability, seasonal differences affected speciation of N, while the biotic and abiotic environmental gradients impacted PMN rates, porewater NH_4^+ availability, and activity of AP. Encroachment of mangroves, coupled with a higher salinity and water level, increased the amount of bioavailable NH_4^+ within the soils while simultaneously decreasing rates of mineralization of N, though this changes seasonally. Alkaline phosphatase activity indicates the same trend, with decreased AP activity within the mangrove and transition zones indicating higher availability.

Another interesting facet of this study is the linkage between salinity, inundation, and encroachment of mangroves into saltmarsh. Previous studies have postulated that the landward transgression of mangroves is catalyzed by changes in salinity and inundation regimes, as mangroves can occupy a lower place in the tidal frame and withstand high salinities (McKee and others 2012). However, the majority of these assertions are anecdotal, and to our knowledge, this study is the first to link salinity and water level gradients, likely facilitated by regional sea level rise, to mangrove encroachment. Future work is needed to disentangle which biogeochemical parameters are more impacted by the biotic change (i.e., mangrove

encroachment) from those driven by the co-occurring abiotic gradients (i.e. salinity and water level).

CHAPTER SIX: HERBACEOUS ENCROACHMENT INTO A COASTAL MARSH INCREASES SOIL NUTRIENT CONTENT AND SUPPORTS HIGHER RATES OF BIOGEOCHEMICAL PROCESSING

Abstract

Vegetation transitions occur globally, altering ecosystem processing of organic matter and changing rates of soil biogeochemical cycling. In coastal marshes, more salt- and inundation-tolerant herbaceous species are encroaching on less tolerant species, concomitant with sea level rise. These species shifts could disrupt ecosystem services such as soil organic matter storage and the cycling of carbon (C), nitrogen (N), and phosphorus (P). To determine how these ecosystem processes were affected by encroachment, we characterized biogeochemical properties and functions along a transect of encroaching *Distichlis spicata L. Greene* (saltgrass) on *Spartina bakeri Merr.* (cordgrass), two herbaceous species. During both wet and dry season, nine soil cores were obtained from three community types: saltgrass end member, transition zone, and cordgrass end member. Total soil C, N, and organic matter were greatest within the saltgrass and transition zone. The saltgrass and transition zone soils also supported higher rates of enzyme activity and potentially mineralizable N and P than cordgrass soils during the dry season, and greater carbon dioxide production and microbial biomass C during the wet season. Generally, the transition zone functioned similarly to the saltgrass zone and the encroachment gradient coincided with a 33 cm elevation change. Seasonally, low extractable nutrient availability (nitrate and soluble reactive phosphorus) during the dry season was correlated with overall greater enzyme activity (N-acetyl-β-D-glucosidase, alkaline phosphatase, β-glucosidase, xylosidase, and cellobiosidase) and potentially mineralizable N and phosphorus (P) rates. This study demonstrates that shifts in dominant herbaceous species and

accompanying abiotic gradients alters biogeochemical processing of organic matter within

coastal marshes.

Introduction

Shifting abiotic factors associated with climate change are altering the spatial extent of

vegetation communities worldwide (Koch and Mooney 1996; Vitousek and others 1997). Each

plant species occupies a specific zone of tolerance in regards to environmental gradients, such as

temperature or salinity, where primary productivity is highest (i.e. Pennings and others; Bertness

1991; Pennings and Callaway 1992). Outside of that optimal zone, plant species are stressed,

and are uniquely vulnerable to being outcompeted by different vegetation types with more

suitable zones of tolerance. Altered global and local climate regimes mediate these vegetation

shifts, which have a variety of impacts on the affected ecosystems (Vitousek and others 1997).

For example, shrub encroachment into previously herbaceous communities has been shown to

alter the quality of organic matter within the soil (Berg and Bossata, 1985), change regional

productivity (Knapp and others 2008), create denuded interspaces of bare soil (Darrouzet-Nardi

and others 2006), and decrease regional biodiversity (Ratajczak and others 2012). Encroachment

can also alter the plant-soil interactions that dominate biogeochemical transformations.

Vegetation modifies the edaphic environment through rhizosphere interactions, seasonal

senescence of biomass, and root-associated microbiota, each of which can change

biogeochemical cycling (Ehrenfeld 2003).

Though coastal salt marshes occupy less than 0.03% of global land area, they sequester

roughly 244.7 g C m^{-2} y^{-1}, making them a critical component of the global carbon budget

(Ouyang and Lee 2014). Coastal wetlands also retain and cycle nutrients, regulating water

quality in the adjacent coastal ocean (Barbier and others 2011). Within coastal wetlands,

vegetation dominance is primarily mediated by factors influencing inundation (anaerobic conditions) and salinity (Pennings and others; Bertness 1991). Shifts in dominant species are often abrupt and catalyzed by minute differences in microtopography and/or climate (Osland and others 2016). For example, along the US coast, saltmarsh grasses (e.g., Spartina sp.) are outcompeting more brackish or freshwater marsh grasses, such as *Juncus roemerianus,* due to their higher salinity tolerance (Donnelly and Bertness 2001). These shifts in species dominance can alter biogeochemical processes, leading to ecosystem level implications.

In this study, we characterized both soil nutrient storage (total C, N, P, and organic matter) and biogeochemical activity (enzyme assays, potential mineralization rates, carbon dioxide production) across an herbaceous-to-herbaceous encroachment gradient of vegetative change in a coastal marsh. Specifically, we characterized the transition of *Distichlis spicata L. Greene* (saltgrass) encroaching into *Spartina bakeri Merr.* (cordgrass) within a subtropical coastal marsh. The transition zone (where both species co-occur) was included in the analysis to determine how rapidly encroachment alters biogeochemical processes. We anticipated that soil organic matter (and total C and N) would be highest within the saltgrass zone, followed by the transition zone, as invading vegetation has been documented to increase total nutrient storage (Liao and others 2008). We also expected the cordgrass-dominated zone to support higher CO_2 production, greater nutrient availability, and lower enzyme activity than both the transition and saltgrass-dominated zones.

Co-incidentally with a change in vegetation type, we anticipated the existence of a gradient of inundation and ambient salinity due to an elevation gradient, which could be viewed as 'low marsh' community encroaching into a previously 'high marsh' community (find ref for these terms). These abiotic variables could provide a mechanism for herbaceous encroachment

while simultaneously contributing to observed differences in biogeochemical characteristics, but such an investigation was not the impetus for this study. Instead, we sought to determine if the 'vegetation transition' (herein referring to both the vegetation shift and accompanying abiotic characteristics) results in altered biogeochemical cycling, with implications for changes in ecosystem services, such as carbon storage, at the landscape scale and applications for ecosystem modeling.

In addition to characterizing biogeochemical properties along an herbaceous-herbaceous vegetation transition, this study also leverages data from a similar study (Steinmuller et al., this issue) that investigates the same biogeochemical parameters along a woody-herbaceous transition, specifically *Avicennia germinans* (black mangrove) encroaching on saltgrass. The two sites are both within the Merritt Island National Wildlife Refuge, located approximately 13 km apart. Mangrove encroachment is the dominant form of vegetation change observed within coastal wetlands in this region and has received significant scientific attention (i.e. Doughty et al. 2016). However, dikes historically surrounding the study site investigated herein have prevented the transport and establishment of mangrove propagules, creating a unique opportunity to compare the biogeochemical effects of an herbaceous-herbaceous transition to that of a woody-herbaceous transition, both located in close proximity, using effect size comparisons.

Methods

Site Description and Soil Sampling

Three replicate transects were set up within an impoundment at the Merritt Island National Wildlife Refuge, a 567 km^2 area on the eastern coast of Florida, within management cell T-16 (Figure 28). Each transect consisted of three 2 m^2 plots: one within the saltgrass end member, one within the transition zone (co-occurrence of both species), and one within the

cordgrass end member (Figure 28) for a total of 9 plots. Historical aerial imagery (Figure 29)

shows the roughly 60 m change in the leading edge of the transition zone between 1991 and

2014 (Google Earth).

Soils at the site are within the Riomar/Turnbull series: fine, smectitic, nonacid

hyperthermic Typic Hydraquents (US Soil Survey 2018). Though historically surrounded by an

earthern dike (since the late 1950s – early 1960s; Brockmeyer et al. 2004), Hurricane Irma

(2017) destroyed the dikes around this wetland prior to the first sampling, effectively

hydrologically connecting the site with the adjacent Indian River Lagoon (IRL). A 251 km long

lagoon, the IRL is microtidal, with salinity between 29 – 40 ppt (USGS Monitoring Station at

Haulover Canal). Water levels at the site are regulated by the combination of tidal forcings,

precipitation, and wind energy related to seasonality. Wet season occurs during the late summer

and fall of each year, while dry season occurs between the late winter and early spring (Foster

and others 2017). Water level and salinity at the site were recorded from August 2017 to

February 2018 with U20 water level logger (Onset, Bourne, MA, USA) and a U24 high-salinity

conductivity logger (Onset, Bourne, MA, USA), each deployed in a well (1.5 inch PVC pipe

with 0.01 inch screen) located in the transition zone, but 1 m away from the soil sampling plot

(Figure 30). Plot elevation was determined by use of a Trimble Geo 7x (Trimble Inc., Sunnyvale,

CA) and LiDAR. Ambient surface water salinity was determined at each sampling time using a

YSI ProDSS (YSI Inc., Yellow Springs, OH, USA).

Sampling occurred during both wet season (November 2017) and dry season (March

2018). At each plot, 3 cores were taken to a depth of 30 cm via push-core and field extruded

into 3 10-cm intervals for a total of 27 cores. Samples were stored in polyethylene bags on ice

and transported to the laboratory, where they remained at 4 °C until the completion of sample analysis.

Soil Physicochemical Parameters

Following homogenization of each sample, a subsample was dried until constant weight within a gravimetric oven at 70 °C to determine soil moisture content. Bulk density was then calculated as dry soil weight per volume for each depth interval. Dried soils were ground (SPEX Sample Prep 8000M Mixer Mill, Metuchen, NJ) and organic matter content was determined via the loss-on-ignition method. Following ashing at 550° C for 3 hours in a muffle furnace, 50 mL of 1 M HCl was added to each sample. Samples were boiled for 30 minutes and the digestate was filtered through Whatman #41 filters for colorimetric analysis of total P (Andersen, 1976, with modifications) on an AQ2 Automated Discrete Analyzer (Seal Analytical, Mequon, WI; EPA method 365.1, Rev. 2). Dried, ground subsamples were also used to determine total soil C and N on a Vario Micro Cube CHNS Analyzer (Elementar Americas Inc., Mount Laurel, NJ). Total C, N, P, and organic matter content were only analyzed during dry season, as pilot data indicated no change in these soil nutrient pools with season.

Extractable Nutrients and Microbial Biomass

Within 24 hours of sampling, replicate samples of 2.5 g of field-moist soil were weighed into centrifuge tubes. Twenty-five (25) mL of 2 M KCl was added to one set of samples, which were shaken at 125 rpm for 1 hour, centrifuged at 5000 rpm for 10 minutes at 10 °C, and vacuum-filtered through Supor 0.45 μm filters.

Figure 28: Location of the study sites within a) the state of Florida, b) Kennedy Space Center/Merritt Island National Wildlife Refuge, and c) within cell T16 as designated by Brevard County Mosquito Control.
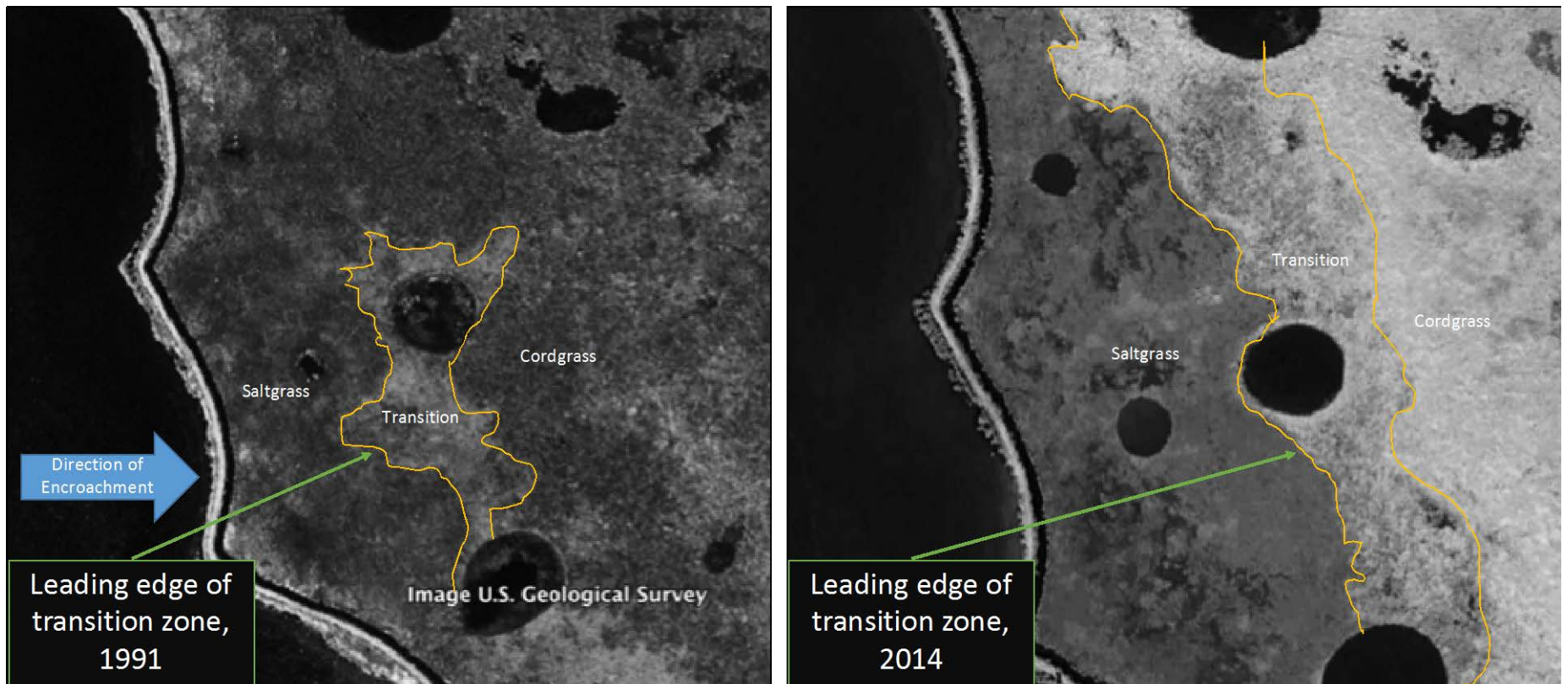
Figure 29: Edges of the transition zone as identified by historical aerial photography. Image on the left shows the leading edge of the transition between saltgrass and cordgrass in 1991, while the left image shows the same zone in 2014. The change in the edge of the transition zone between 1991 and 2014 is roughly 60m, as estimated through Google Earth. Approximate zone boundaries are highlighted.
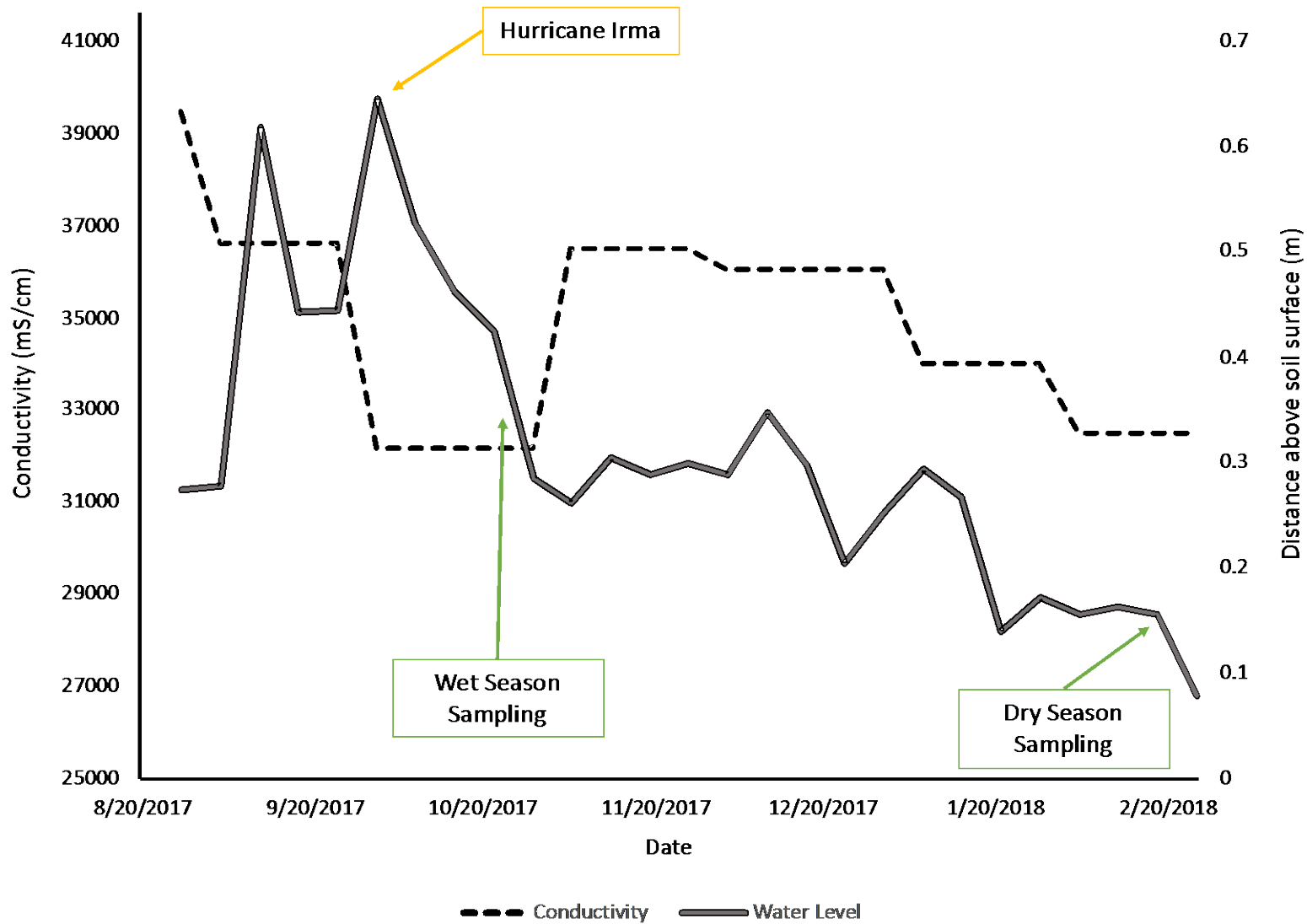
Figure 30: Weekly average water levels in distance above soil surface and monthly maximum conductivity (mS/cm) recorded from August 2017 to February 2018.

The filtered sample was acidified to a pH of <2 with double distilled H_2SO_4 and analyzed

colorimetrically on an AQ2 Automated Discrete Analyzer for ammonium (NH_4^+), nitrate (NO_3^-),

and soluble reactive phosphorus (SRP) (Seal Analytical, Mequon, WI; EPA methods 231-A Rev.

0, 210-A Rev. 1, and 204-A Rev. 0). The second set of samples were fumigated with chloroform

for 24 hours within a glass desiccator for determination of soil microbial biomass following

Vance and others (1987). Samples were then extracted as referenced above. Dissolved organic

C (DOC) content was determined for both the initial and fumigated samples via use of a

Shimadzu TOC-L Analyzer (Shimadzu Instruments, Kyoto, Japan) and microbial biomass was

calculated as the $DOC_{final} - DOC_{initial}$.

Greenhouse Gas Production and Potential Mineralization Rates

Seven grams of field-moist soil from each homogenized sample was weighed into glass

serum bottles. Bottles were capped with a rubber septa and aluminum crimp, evacuated to -75

mmHg, then purged with 99 % O_2-free N_2 gas for three minutes to instill an anaerobic

environment. Nitrogen-purged artificial seawater matching the surface water salinity at each plot

was injected into each bottle to create a slurry (1:2 of soil:water). Each bottle was placed in a

dark orbital shaker at 100 rpm and 25° C. Headspace was collected after 24, 72, 120, 168, and

240 hours and analyzed on a GC-2014 gas chromatograph (Shimadzu Instruments, Kyoto, Japan)

to determine CO_2 and methane production over time. In general, methane peaks were either low

or below detection, and thus will not be discussed. To determine the concentration of dissolved

inorganic C, soil pH was determined by creating a 1:5 slurry of soil to distilled, deionized water

and measured with an Accumet XL200 benchtop pH probe (ThermoFisher Scientific, Waltham,

MA, USA). Concentrations of CO_2 were calculated using Henry's Law and a rate determined

with a linear regression over time.

After the 10-day incubation period, 25 mL of 2 M KCl was added to each bottle. Bottles shook for 1 h at 125 rpm and 25 °C, then decanted and vacuum-filtered using Supor 0.45 μm membrane filters. Samples were acidified to a pH of <2 with double distilled H_2SO_4 and analyzed colorimetrically for NH_4^+ and SRP concentrations (Seal Analytical, Mequon, WI; EPA methods 231-A Rev. 0 and 204-A Rev. 0). The potential mineralization rates of both N and P were calculated as the difference in concentration divided by the 10 day incubation period.

Extracellular Enzyme Activity

Extracellular enzyme activity of N-acetyl-β-D-glucosidase (NAG), alkaline phosphatase (AP), β-glucosidase (BG), xylosidase (XY), and cellobiosidase (CB) were determined via fluorometric assays with MUF-linked substrates. A soil slurry was created by adding 39 mL of distilled, deionized water to 0.5 g of field moist soil. Slurries were shaken on an orbital shaker for 1 h at 25° C and 125 rpm, then pipetted into clear 96-well plates. Non-limiting substrates were added to each sample and measured both initially and after 24 hours on a BioTek Synergy HTX (BioTek Instruments Inc., Winooski, VT) at excitation/emission wavelengths of 360/460 nm to determine rates of enzyme activity.

Porewater Nutrients

Porewater equilibrators (polycarbonate base with evenly spaced 7 mL wells, covered with a 0.45 μm membrane, and driven into the soil to a depth of 35 cm) were assembled in an anaerobic underwater environment prior to deployment. Immediately following soil sample collection, equilibrators were deployed within an undisturbed region of each plot for 10 days. Upon retrieval, cells were extracted using a syringe and 0.45 μm syringe filters, consolidated into 5 cm intervals, and acidified with double distilled H_2SO_4 to a pH of <2. Samples were analyzed for porewater nutrient concentrations (NH_4^+, NO_3^-, SRP, and DOC) as described above.

Statistical Analysis

Statistical analysis was performed in R via RStudio (RStudio Inc., Boston, MA, USA). Data were transformed using a logarithmic transformation to meet the assumptions of normality, as determined via the Shapiro-Wilk test. Homogeneity of variance was determined using Levene's test. Initially, a t-test was performed to determine whether each parameter was significantly different between seasons. Data were then analyzed separately by season.

Data were analyzed via a linear mixed model using package 'lme4' (Bates and others, 2015), with fixed effects of depth and vegetation, and random effects of replicate core nested within transect. Model simplification was applied to determine the best model based on AIC scores. Based on model simplification results, we excluded the interaction of depth and vegetation community from the model. A Bonferroni correction was applied to the initial alpha value of 0.1 due to the number of model iterations, which decreased the alpha value to reject the null hypothesis to 0.0005. Following determination of significance within the linear model, least-square means tests were applied post-hoc to determine differences among vegetation types (and associated abiotic shifts) and depth intervals, separately.

Cohen's d was used to calculate the effect size of the vegetation change, using the means of each parameter within the end members of the vegetation change. Effect size was also calculated for parameters presented in a companion paper (Steinmuller et al., this issue), where the same biogeochemical properties were analyzed with the same study design along a woody-herbaceous vegetation gradient.

Table 16: Significance table for the linear model testing the additive effects of vegetation community type and depth and random effects of transect and replicate core. Significant p-values are denoted by underlined values. Note that no analysis was performed for wet season total soil C, N, P, and organic matter, as indicated by '-'. (n=27 for each season, $\alpha = 0.005$).

	Wet Season		Dry Season	
	Community	*Depth*	*Community*	*Depth*
Moisture Content	<0.0001	<0.0001	<0.0001	<0.0001
Bulk Density	<0.0001	<0.0001	<0.0001	<0.0001
Total C	-	-	<0.0001	<0.0001
Total N	-	-	<0.0001	<0.0001
Total P	-	-	0.4147	0.0850
Organic Matter	-	-	<0.0001	<0.0001
Ext. Nitrate	<0.0001	<0.0001	<0.0001	<0.0001
Ext. Ammonium	0.6787	0.0674	0.0003	<0.0001
Ext. SRP	0.0262	<0.0001	0.0095	<0.0001
Microbial Biomass C	0.00029	<0.0001	0.0248	<0.0001
NAG	<0.0001	<0.0001	0.0001	<0.0001
AP	<0.0001	<0.0001	<0.0001	<0.0001
BG	<0.0001	<0.0001	<0.0001	<0.0001
CB	<0.0001	<0.0001	<0.0001	<0.0001
XY	<0.0001	<0.0001	0.0041	<0.0001
AS	<0.0001	<0.0001	<0.0001	<0.0001
CO_2 Production	0.0001	<0.0001	<0.0001	<0.0001
PMN	0.0007	<0.0001	0.2775	<0.0001
PMP	<0.0001	<0.0001	0.0051	<0.0001
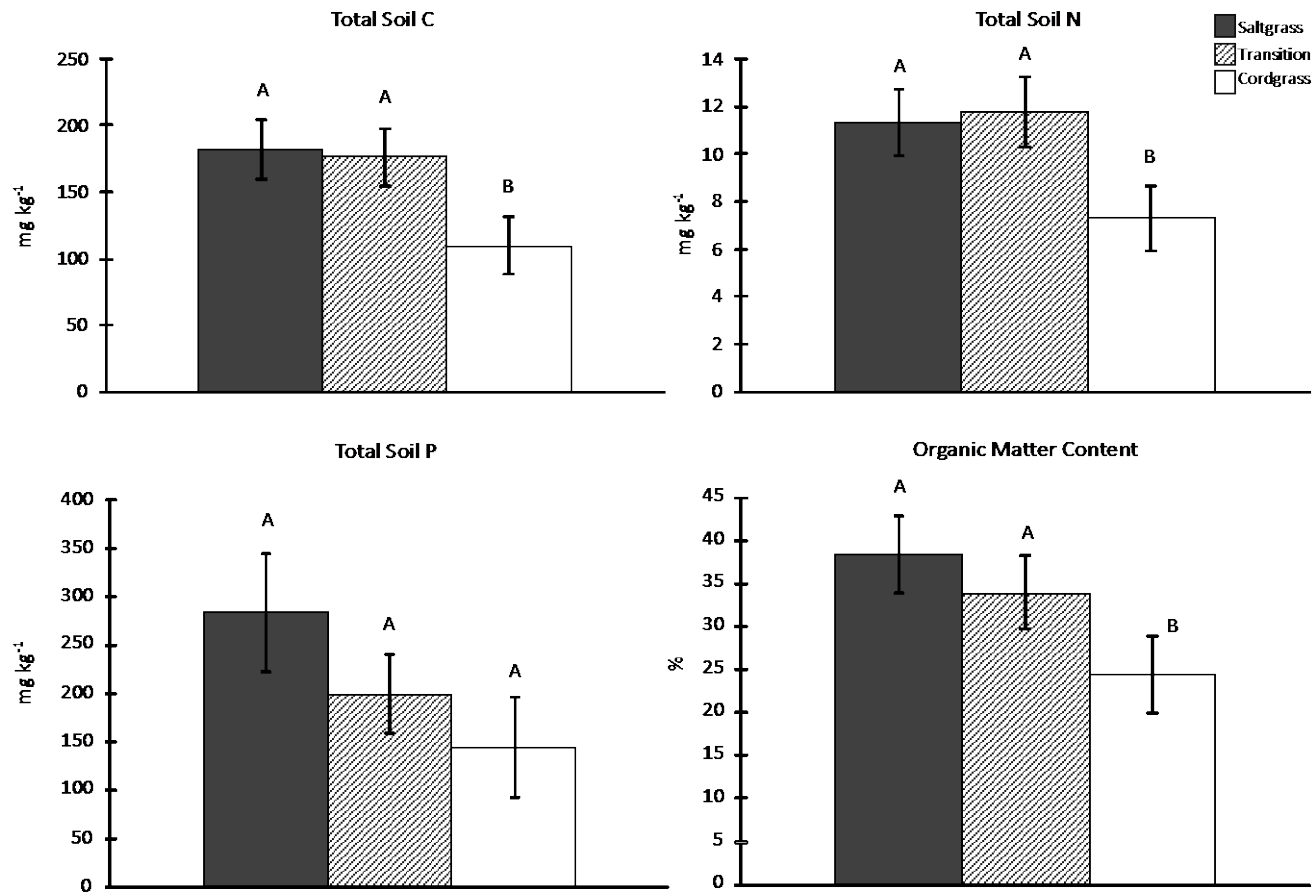
Figure 31: Total soil carbon, nitrogen, phosphorus, and percent organic matter within each vegetation community. Capital letters denote significant differences between vegetation communities. Statistics were conducted on log transformed data, while plotted data is not log transformed.

Results

Elevation and Salinity

Elevation was 18.4 ± 2.59 cm (NAVD88) within the saltgrass plots, 18.89 ± 3.14 cm within the transition zone, and 51.1 ± 2.52 cm within the cordgrass plots. Dry season salinities were 19.3, 17.7, and 15.2 within the saltgrass, transition, and cordgrass, respectively. This trend was the same during wet season, though salinities were slightly lower.

Soil Physicochemical Properties

During both seasons, soil moisture content was highest in saltgrass plots (71 ± 2.8 % and 69 ± 2.2 % for wet and dry seasons, respectively) and lowest in the cordgrass plots (54 ± 4.9 % and 52 ± 4.3 %, respectively) and always decreased with depth (Table 16). During wet season, moisture content was positively correlated to extractable NH_4^+ and SRP concentrations, PMN and PMP rates, CO_2 production, MBC, and all enzyme activity (Supplementary Tables 3 and 4). Bulk density was also significantly different among vegetation communities during both seasons (Table 12), being highest within the cordgrass plots, and lowest within the saltgrass plots. Bulk density increased with depth and was negatively correlated to all parameters during wet season (Supplementary Tables 3 and 4). Total soil C, N, and organic matter content were highest within the saltgrass and transition zone plots and decreased with depth in all plots (Table 16, Figure 31). Total P was not affected by either vegetation community or depth (Table 16, Figure 31).

Extractable and Porewater Nutrients

Extractable NO_3^- concentrations were roughly 70x higher during dry season, compared to wet season, and were influenced by vegetation community and depth only during the dry season sampling (Table 16). During dry season, extractable NO_3^- concentrations decreased from 0-10 to 20-30 cm and were higher within the transition and saltgrass plots (18.4 ± 4.87 mg kg^{-1}), compared to cordgrass plots (4.80 ± 0.942 mg kg^{-1}) (Table 16). Dry season extractable NO_3^-

concentrations were positively correlated to extractable SRP, PMP rates, CO_2 production, MBC, and all enzyme activity (Supplementary Tables 3 and 4). Extractable NH_4^+ concentrations were negatively correlated to extractable NO_3^- concentrations (Supplementary Tables 3 and 4).

Extractable NH_4^+ concentrations were roughly 6.6x higher during the wet season, relative to dry season, but did not differ with vegetation community (Table 16, Figure 32). Depth did have a significant effect, ranging from 37.7 ± 5.36 mg kg^{-1} at 0-10 cm to 31.2 ± 5.28 mg kg^{-1} at 20-30 cm during wet season. In contrast, dry season extractable NH_4^+ concentrations averaged 1.62 ± 0.714 mg kg^{-1} at 0-10 cm to 8.92 ± 1.48 mg kg^{-1} at 20-30. Wet season extractable NH_4^+ concentrations were positively correlated to extractable SRP, PMN and PMP rates, CO_2 production, MBC, and all enzyme activity (Supplementary Tables 3 and 4). However, during dry season, extractable NH_4^+ concentrations were negatively correlated to extractable SRP, PMP rates, MBC, CO_2 production, and all enzyme activity.

Concentrations of extractable SRP during wet season were roughly 18.5x higher than dry season concentrations. Extractable SRP concentrations differed significantly with vegetation community during wet season (greater in saltgrass plots, 0.885 ± 0.148 mg kg^{-1}, than cordgrass plots, 0.591 ± 0.105 mg kg^{-1}) and decreased with depth during both seasons (Table 16, Figure 32). While wet season extractable SRP concentrations were significantly correlated to PMN and PMP rates, CO_2 production, MBC, and all enzyme activity; dry season concentrations were significantly correlated to only PMP rates, MBC, CO_2 production, AP activity, BG activity, and AS activity (Supplementary Tables 3 and 4).

There was no effect of either vegetation community or depth on porewater DOC (both seasons), though dry season concentrations were approximately 2x less than wet season concentrations. Porewater NH_4^+ increased with depth during dry season, while porewater SRP

increased with depth during both seasons. Porewater SRP was the only nutrient affected by vegetation, with greatest concentrations within the saltgrass zone, followed by the cordgrass zone, then the transition zone during dry season. However, during wet season, porewater SRP concentrations were greatest within the cordgrass and lowest within the saltgrass. Porewater NO_3^- values were consistently below detection.

Microbial Biomass and CO_2 Production

Wet season MBC concentrations were 2.3x higher than MBC concentrations in dry season, with concentrations ranging from 4998 ± 541 mg kg^{-1} (wet season) and 2354 ± 243 mg kg^{-1} (dry season) within the saltgrass plots, to 3793 ± 632 mg kg^{-1} (wet season) and 1280 ± 249 mg kg^{-1} (dry season) in the cordgrass plots (Table 16, Figure 33). Concentrations of MBC decreased with depth during both seasons and were correlated to CO_2 production and all enzyme activity (Supplementary Tables 3 and 4).

Carbon dioxide production during both seasons decreased with depth (Table 16, Figure 33), though production rates were 1.4x higher during the wet season. During wet season, CO_2 production within saltgrass plots averaged 2.68 ± 0.626 mg CO_2-C kg^{-1} hr^{-1} and cordgrass plots averaged 1.41 ± 0.419 mg CO_2-C kg^{-1} hr^{-1} (Table 16), but there was no effect during the dry season. Carbon dioxide production was correlated to all enzymatic activity during both seasons (Supplementary Tables 3 and 4).

Extracellular Enzyme Activity and Potentially Mineralizable N and P Rates

All extracellular enzyme activities (AP, NAG, BG, CB, XY, AS) were greater during wet season than dry season and decreased with increasing depth (Table 16; Figures 32, 33, 38).
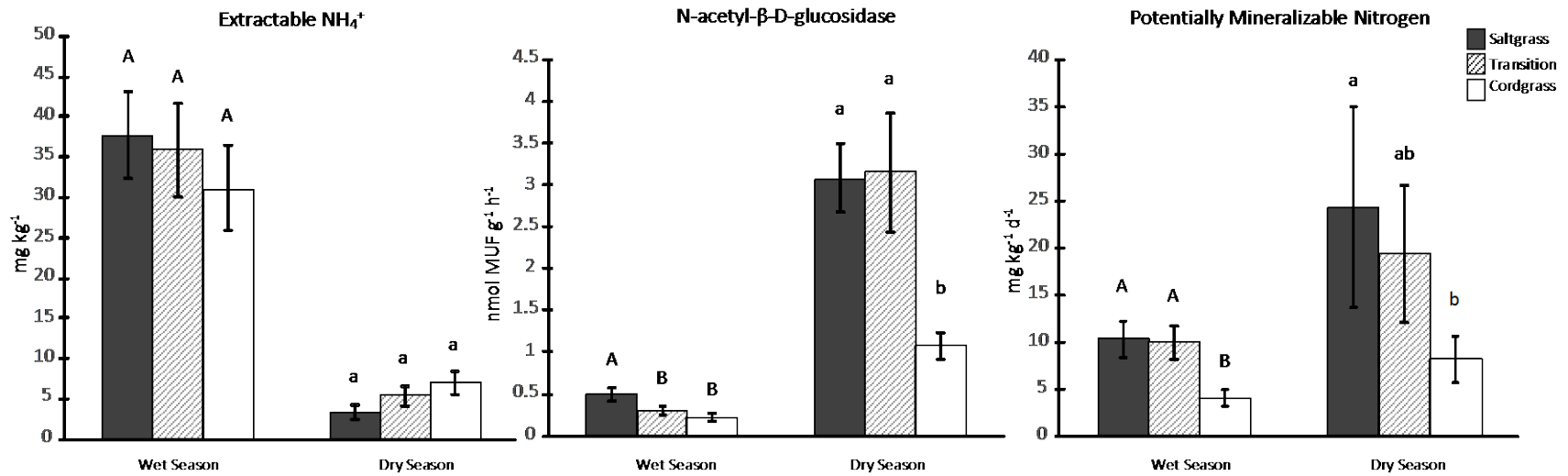
Figure 32: Soil extractable ammonium, N-acetyl-β-D-glucosidase (NAG) activity, and potentially mineralizable nitrogen (PMN) rates within each vegetation community at both high and dry season. Capital letters denote significant differences between vegetation communities during the wet season, while lowercase letters denote significant differences between vegetation communities during the dry season.
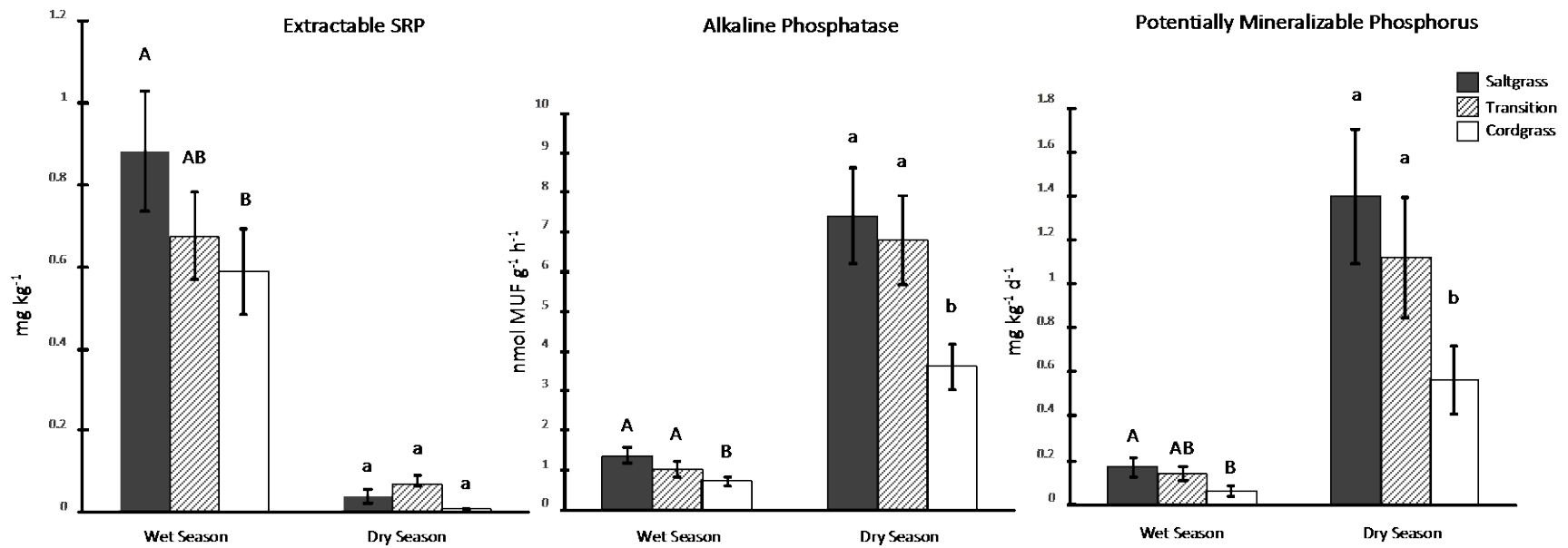
Figure 33: Soil extractable SRP concentrations, alkaline phosphatase activity, and potentially mineralizable phosphorus rates within each vegetation community at both high and dry season. Capital letters denote significant differences between vegetation communities during the wet season, while lowercase letters denote significant differences between vegetation communities during the dry season.
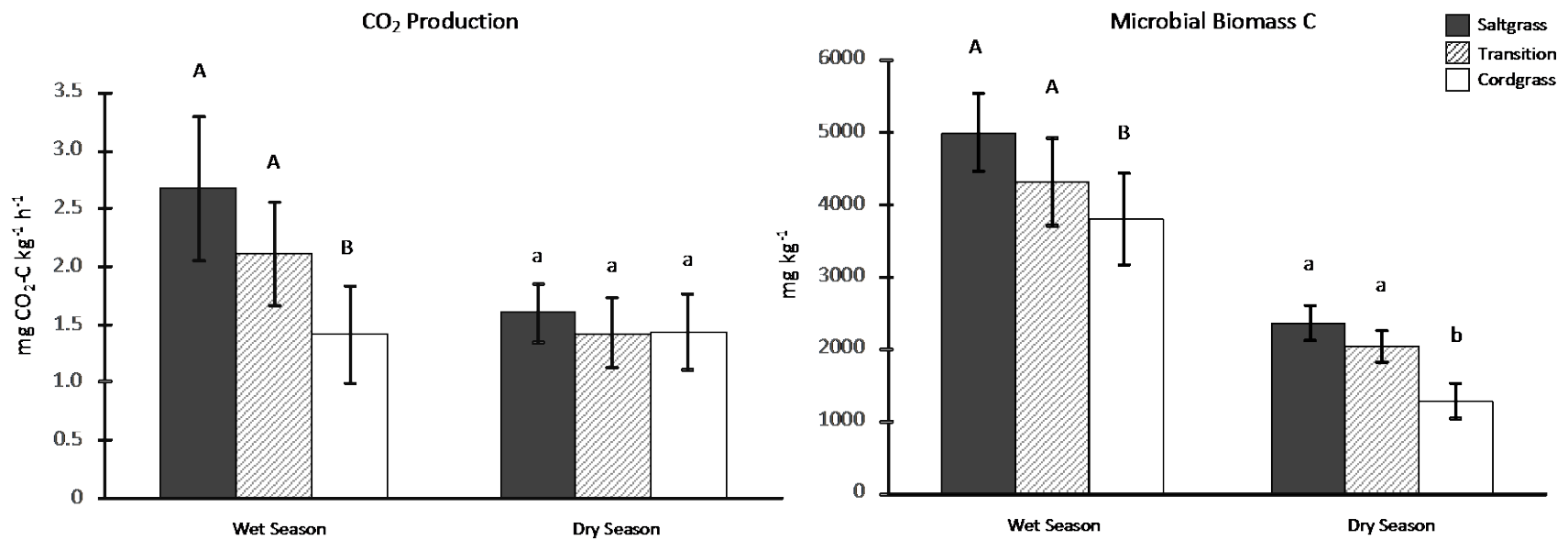
Figure 34: Soil CO_2 production and microbial biomass carbon concentrations within each vegetation community at both high and dry season. Capital letters denote significant differences between vegetation communities during the wet season, while lowercase letters denote significant differences between vegetation communities during the dry season.
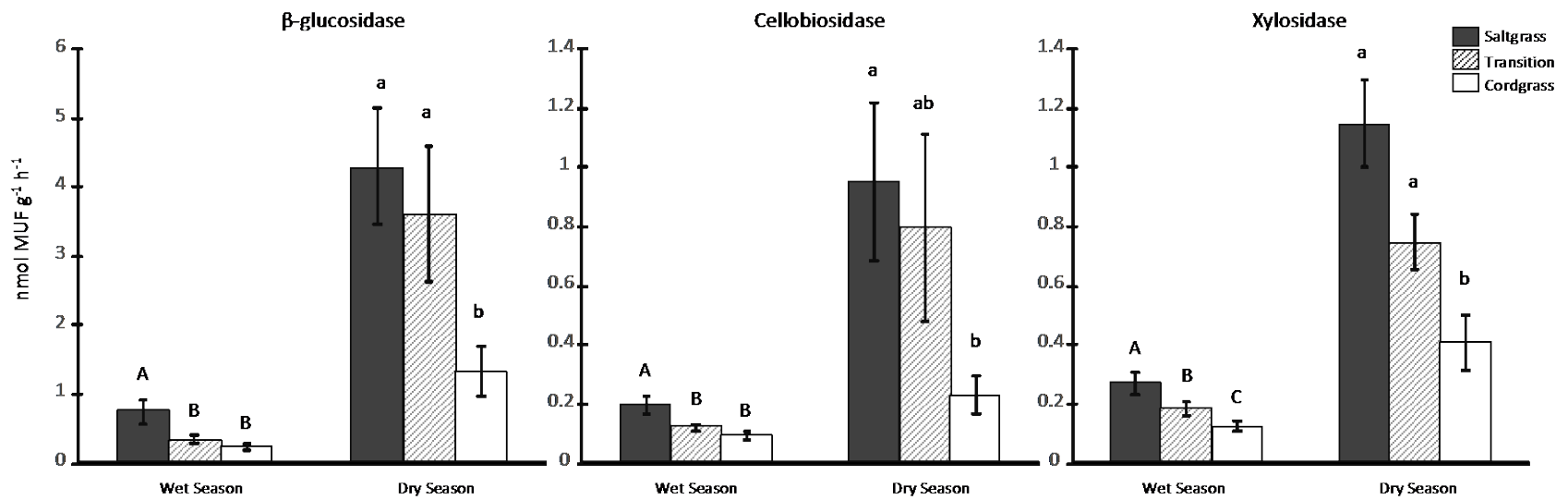
Figure 35: Activity of soil carbon-degrading enzymes (BG, CB, XY) within each vegetation community at both high and dry season. Capital letters denote significant differences between vegetation communities during the wet season, while lowercase letters denote significant differences between vegetation communities during the dry season.

Consistently, enzyme activity was greatest within the saltgrass plots, followed by the transition zone, and lowest within the cordgrass plots. All enzyme activities were significantly correlated to each other during both seasons (Supplementary Tables 3 and 4).

During dry season, PMN and PMP rates were roughly 2x and 8x higher than during wet season, respectively. The saltgrass plots had the highest PMN and PMP rates during both seasons, followed by the transition zone and then the cordgrass plots. Both PMN and PMP decreased with depth.

Discussion
Abiotic Gradients

The region of marsh dominated by saltgrass coincided with a micro-topographical elevation difference of approximately -33 cm, relative to the cordgrass community. This elevation difference contributed to higher surface water salinity and soil moisture content within the saltgrass plots, reflecting a lower position within the tidal range and a greater marine influence. As a result, soils within the saltgrass and transition zone plots remained saturated during the dry season, while the cordgrass soils experienced dry-down (~20 cm, Figure 30). Although the present experimental design cannot elucidate the causal relationship between vegetation shifts and abiotic gradients, the co-variation suggests continued sea level rise will likely favor further encroachment of saltgrass into areas presently dominated by cordgrass. As such, understanding the differences in biogeochemical properties between these two vegetation communities (as well as the accompanying abiotic gradients) is crucial to quantifying potential changes in C, N, and P storage and cycling across the coastal landscape.

Seasonality

Both the seasonal changes in water levels and the greater marine influence acting on the saltgrass and transition plots, due to their lower elevation, contributed to observed differences in extractable and porewater nutrient concentrations, soil enzyme activity, N and P mineralization, and microbial biomass C content. Increased concentrations of both porewater and extractable SRP, NH_4^+, and DOC during the wet season are likely driven by exchange with the adjacent lagoon (Brockmeyer and others 1996). The influx of coastal lagoon waters appears to have provided inorganic nutrients and labile C substrates to microbial communities, thereby decreasing enzyme activity and mineralization rates of N and P, relative to the dry season (Figures 32, 33, 35). Enzyme activity is regulated by microbial need for substrates cleaved from larger organic compounds and, under the evolutionary-economic principle of enzyme activity, it becomes less efficient for microbes to continue production of extracellular enzymes in the presence of the required organic substrates (Skujiņš and Burns 1976; Allison and others 2011). Similarly, mineralization rates are regulated by demand for inorganic nutrients and decrease in response to increased availability (Robertson and Groffman 2007). For example, the abundance of extractable SRP (which includes porewater SRP) during the wet season caused a decrease in both enzyme activity and P mineralization rates, while low concentrations of SRP within the dry season supported higher enzyme activity and P mineralization rates. This trend was not limited to P; both N and C enzymes exhibited the same relationship (Figures 32, 33, 35). The availability of inorganic nutrients supplied by the lagoon could also have bolstered microbial biomass C during the wet season by allowing the community to switch from mediating catabolic reactions (such as mineralization) to inputting energy into microbial anabolism and growth (Robertson and Groffman 2007; Reddy and DeLaune 2008, Figure 33).

Soil Nutrient Storage

Soils within the saltgrass plots stored 37% more total C and 34% more total N than soils within the cordgrass plots, which may be related to abiotic factors (e.g., lower elevation) and/or biotic factors (e.g., the unique morphology, productivity rates, and litter quality of the dominant plant species; Figure 31). The location of the saltgrass plots lower within the tidal frame is expected to limit decomposition by reducing the availability of terminal electron acceptors through the longer and deeper tidal flooding (Reddy and DeLaune 2008). However, soils within the saltgrass plots supported higher rates of CO_2 production and C-degrading enzyme activity than within the cordgrass soils. Both of these measurements imply higher rates of C cycling within the saltgrass zone, which is in opposition to an increase in C storage. This paradox could be an effect of, a) differences in primary production between species (i.e. Choi and others 2001), b) saltgrass litter being more labile (i.e. lower C:N ratio) than cordgrass litter, or c) an influx of labile DOC from the lagoon supporting higher rates of C turnover within the saltgrass, while still enhancing C storage. Although we cannot tease apart this mechanism with the data collected, we did observe a minute difference in C:N ratios, 16.13 and 15.27 within the saltgrass and cordgrass, respectively, suggesting saltgrass litter may be of higher quality. Additionally, annual production of saltgrass and a similar species of cordgrass (*Spartina alterniflora*) within coastal marshes in Louisiana has been reported to be 3237 g m^{-2} and 2658 g m^{-2}, respectively, which illustrates a potential difference in primary productivity between the two species, if *S. bakeri* functions similarly to *S. alterniflora* (Hopkinson and others, 1980). Regardless of the mechanism facilitating simultaneously higher C storage and C cycling within the saltgrass and transition zone soils, it is evident that encroachment of saltgrass is presently enhancing the burial of both C and N, with implications for landscape-scale C and nutrient budgets.

Nutrient Cycling

Saltgrass plots had greater enzyme activity and mineralization rates than cordgrass plots during both seasons. If the combination of water level and nutrient supply from the water column solely controlled enzyme activity and mineralization rates within this system, then the less-inundated cordgrass plots would exhibit the highest enzyme activity and mineralization rates, as low water level facilitates increased breakdown of organic matter and low nutrient availability enhances microbial need for enzymatic cleavage (McLatchey and Reddy 1998; Allison and others 2011). Instead, the observed higher rates of enzyme activity and mineralization within the saltgrass soils suggest the presence of a vegetation effect on these processes. In terrestrial systems, soil microbial community structure has been documented to be dependent both on the associated species of vegetation (Berg and Smalla 2009) and changes in vegetation dominance (Kourtev and others 2002), suggesting the intrinsic properties of saltgrass and its associated microbiome could account for the increased rates of organic matter processing observed within the saltgrass plots.

Soil NAG, AP, and PMP rates within the transition zone sites were similar to rates expressed by the saltgrass soils, and greater than rates within the cordgrass soils during both seasons. This similarity between the saltgrass and the transition zone indicates that rather than the transition zone functioning as an intermediate as the vegetation community composition would suggest, biogeochemical processing within the transition zone is functionally similar to that of the saltgrass zone. This has important management implications, as it suggests altered biogeochemical functioning in an ecosystem prior to the visible shift in plant species. However, these relationships were mediated by season. Specifically, during the dry season BG, CB, and XY, which are indicators of microbial need for cellulose, cellobiose, and xylose, respectively,

were similar between the transition and saltgrass plots (Eivazi and Tabatabai 1988; Deng and Tabatabai 1994). However, during the wet season, the transition zone soils become more functionally similar to the cordgrass soils in terms of C-degrading enzyme activity, exhibiting a lower need for labile C substrates than the saltgrass. This shift indicates that both season and vegetation type interactively regulate differences in availability and microbial demand for these C substrates between species.

Interestingly, all measured enzyme activity rates within this study were roughly 30-50% lower than observed enzyme activity within a proximal saltmarsh, where saltgrass is being encroached upon, rather than acting as the encroaching species (Steinmuller and others, this issue). In contrast, PMN rates in this study were slightly higher than where saltgrass is being encroached upon (Steinmuller and others, this issue). As extractable ammonium concentrations were similar between the two studies, the higher PMN rates observed here could be caused by larger aboveground biomass and/or a greater proportion of fine roots when saltgrass is the encroaching species, rather than the species that is being encroached upon (Ehrenfeld 2003). These differences in soil biogeochemical processes (i.e. enzyme activity and potential mineralization rates) between encroaching saltgrass and saltgrass experiencing encroachment indicate that, to some extent, the biogeochemical effects of encroachment are dependent on the local ecological context, rather than being universal species-specific responses, similar to trends shown within exotic plant invasions (Ehrenfeld 2003).

Comparisons to Mangrove Encroachment

Many coastal marshes are also experiencing the encroachment of woody species, such as the black mangrove (Stevens and others 2006, Giri and others 2011; Montagna and others 2011; Armitage and others 2015; Doughty and others 2016). Steinmuller and others (this issue)

151

reported changes in nutrient cycling along a separate ecological gradient of encroaching black mangroves within a proximal coastal wetland. The combination of these two studies presents a unique opportunity to compare the two vegetation transition types (woody-herbaceous and herbaceous-herbaceous) at sites that are spatially related and face similar drivers. Effect size (calculated as Cohen's d) facilitates a comparison of these two sites: larger effect sizes indicate larger implications for ecosystem response to the vegetation transition and abiotic changes.

The average effect size for the woody-herbaceous transition was 0.7, compared to 0.5, for the herbaceous-herbaceous transition, both categorized as a 'medium effect' (Table 17, Cohen 1988). The minimal difference between the effect sizes observed in these two types of transitions may be surprising considering woody species have such dramatically different physiology (Camacho-B and others 1974), metabolic functioning, biomass allocation, and interaction with the edaphic environment than herbaceous species. Moreover, woody encroachment in coastal wetlands has received far more research attention (e.g., 1,397 papers between 1998-2018) than herbaceous encroachment (357 papers over the same timescale, based on a Web of Science search). Despite the preferential study of mangrove encroachment, this study suggests both types of encroachment (woody-herbaceous and herbaceous-herbaceous) exhibit medium-to-high-effects on biogeochemical properties and processes. Furthermore, mangrove encroachment is geographically confined to predominantly subtropical regions, while herbaceous encroachment is the dominant process throughout temperate coastal wetlands, suggesting the implications of herbaceous-herbaceous coastal marsh encroachment warrants further study.

Table 17: Effect size (Cohen's d) of the vegetation transition (and concomitant abiotic changes) within both the woody-herbaceous transition (data from Steinmuller et al. (this issue) and the herbaceous – herbaceous transition (this paper). ect sizes characterized as trivial (<0.2) are highlighted in grey, small effect sizes (0.2-0.49) are highlighted in yellow, medium effect sizes (0.5-0.79) are in green, and large effect sizes (0.8+) are in blue.

Parameter	Woody – Herbaceous Transition	Herbaceous - Herbaceous Transition
TC	1.8	0.6
TN	1.6	0.5
TP	0.7	0.4
OM	1.8	0.6
Ext. Nitrate	0.6	0.5
Ext. Ammonium	0.3	0.1
Ext. SRP	0.4	0.3
PMN Rate	0.7	0.4
PMP Rate	0.2	0.5
MBC	0.7	0.4
CO_2 Rate	0.1	0.3
NAG	0.3	0.7
AP	0.6	0.5
BG	0.1	0.6
XY	0.6	0.8
CB	0.2	0.5
Average	**0.7**	**0.5**

Further examination of the differences in effect size between the two sites clearly indicates soil nutrient pools with slow turnover rates (total soil C, N, P, and organic matter content) within the woody-herbaceous transition appear to be most affected by encroachment (Table 17). These total nutrient pools provide electron donors to support microbial respiration and plant growth, contribute to elevation gains, and are responsible for the critical ecosystem services such as sequestration of C (Reddy and DeLaune 2008). Altering these total soil nutrient pools could quickly disrupt trends in biogeochemical processing and nutrient storage on an

ecosystem level. In contrast, the highest effect sizes within the herbaceous-herbaceous transition were observed within the enzyme activities (NAG, AP, BG, XY, and CB), which are indicators of current nutrient availability and lability and reflect soil organic matter pools with shorter residence times. Therefore, as vegetation transitions continue within coastal wetlands, it appears that the largest effects within woody-herbaceous transitions will be to critical stocks of soil nutrients, while short-term pools of labile nutrients cycled by enzymatic activity will be most affected within herbaceous-herbaceous transitions; both results will impact the C storage and ecological functioning of the system as a whole. More studies encompassing different regions and climatic drivers need to be conducted to further understand the effects of both woody-herbaceous and herbaceous-herbaceous encroachment on biogeochemical processing in coastal wetlands, and to disentangle the effects of vegetation encroachment from sea level rise and other abiotic gradients.

Conclusions

Biogeochemical functioning is highly dependent on seasonal water levels within this coastal marsh. Both the influx of nutrients and presence of a water column during the wet season generally dampened rates of soil microbial processing of organic matter (enzyme activity and N and P mineralization), while these rates increased during the dry season. The encroachment of saltgrass into this cordgrass-dominated coastal marsh enhanced both total soil nutrient storage and the rate of biogeochemical processing of organic matter. Soil C and N content within the saltgrass marsh was higher than within the cordgrass zones, as were accompanying measures of C loss (i.e. CO_2 production) and organic matter processing (i.e. enzyme activity and mineralization of inorganic N and P). Together, these parameters imply that while C storage might increase with saltgrass encroachment, the quantity and quality of C substrates is also

increasing, resulting in a concomitant increase in the release of greenhouses gases (i.e., CO_2) and the rate of organic matter turnover.

Leveraging effect size between this study and Steinmuller et al. (this issue) demonstrates that though woody-herbaceous encroachment has a larger effect size than herbaceous-herbaceous encroachment, the difference between the two is small. Encroachment has a larger effect on total soil nutrients with a slow turnover time (i.e. total soil nutrients) within the woody-herbaceous site, while at the herbaceous-herbaceous site, short-term biogeochemical indicators (i.e. enzyme activity) were the most affected. While encroachment will continue to alter biogeochemical processing at each site, the woody-herbaceous site is likely to experience slower changes while the herbaceous-herbaceous site will experience rapid disruptions in rates of biogeochemical cycling. More studies investigating the consequences of herbaceous encroachment are critical to understanding both the biogeochemical and ecosystem-level effects of this process on a regional-scale, which can then be leveraged into creating predictions for climate change scenarios using global patterns. As sea level rise accelerates, these vegetation transitions are expected to become more prevalent, further demonstrating the need for characterizing the effects of encroachment.

CHAPTER SEVEN: SUMMARY

The combination of land ice melting and thermal expansion of the oceans, caused by increased anthropogenic carbon dioxide emissions within the atmosphere, is contributing to increases in global sea level. Currently, the eustatic sea level rise (SLR) rate is 3.0 ± 0.4 mm yr^{-1}, but is forecasted to reach rates as high as 16 mm yr^{-1} by the year 2100 under the most extreme radiative forcing scenarios (IPCC, 2013). These rates of SLR threaten the 40% of the global population that resides within 100 km of coastlines around the world, the accompanying infrastructure, and natural coastal environments. Coastal wetlands, which rank as one of the most productive ecosystem types in the world, are uniquely vulnerable to increases in sea level, as they occupy the low-lying coastal plain that encompasses the transition between aquatic and terrestrial systems. Increases in urban development and drainage of natural wetland systems is already decreasing the extent of coastal wetlands worldwide. The addition of SLR as a stressor is predicted to result in a net loss of 22% of coastal wetlands globally by 2100 (Nicholls et al. 1999). Coastal wetlands perform and facilitate critical ecosystem services, including providing habitat for wetland fauna, mediating hydrologic flux and storage, serving as a buffer to storm surge, regulating water quality, and sequestering carbon (C) (Barbier et al. 2011). These services can be disrupted or eliminated entirely as coastal wetlands respond to SLR.

Previous studies suggest that coastal wetlands respond to sea level rise by following one of three trajectories: vertical accretion, landward transgression, or wetland submergence (Kirwan and Megonigal, 2013). The latter two trajectories eventually lead to either wetland loss or transitions that impact the ability of wetlands to perform crucial ecosystem functions. Coastal wetlands, though their position in the landscape and co-occurrence of aerobic and anaerobic environments, are biogeochemical hotspots that facilitate key biogeochemical transformations (McClain et al. 2003). As such, it is critical to understand how wetland loss (through submergence) and transitions (i.e. landward transgression) impact biogeochemical functioning within coastal wetlands and potentially impact both adjacent coastal zones

156

and climate feedback loops. Through five separate goals, this dissertation assessed the biogeochemical impacts of SLR- induced transitions within coastal wetlands.

Chapter 2:

The effects of SLR on coastal wetlands are not limited to direct occurrence on the coastal fringe and include processes like saltwater intrusion and/or incursion. As SLR occurs, tidally-influenced freshwater (and brackish) wetlands can experience increases in salinity and inundation as more seawater is pushed further into the tidal frame. The high ionic strength of seawater has been documented to, within hours, prompt releases of inorganic nutrients from freshwater wetland soils (Seitzinger et al. 1991; Rysgaard et al. 1999; Weston et al. 2006; Jun et al. 2013; Ardon et al. 2013). Additionally, the influx of sulfate from seawater has been demonstrated to decrease microbial respiration through methanogenesis and increase respiration through sulfate reduction, contributing to an increase in carbon dioxide production from these wetlands (Weston et al. 2006; Chambers et al. 2011; Weston et al. 2011; Marton et al. 2012; Chambers et al. 2014). Despite the many experimental studies conducted to determine the impacts of increased salinities on freshwater wetland soils, a knowledge gap still existed in a) understanding how soil type mediates these effects, and b) quantifying flux of nutrients liberated into the surrounding water column. Through experimental manipulation of salinity levels on three different wetland soil types, this dissertation addressed that knowledge gap. Results indicated that soil type mediated flux of nutrients into the surrounding water, with organic soils contributing more NH_4^+ and SRP than mineral soils. Porewater NH_4^+ flux was also mediated by salinity level, with 8x and 5x higher concentrations within the 15 ppt treatment and 5 ppt treatments than within the control treatments. Findings also indicated a lag period of roughly 1 week between initial liberation of NH_4^+ (increases in the porewater) and export into the surrounding water. Together, **these results indicate that saltwater incursion within tidally-influenced freshwater wetlands could release stores of nutrients from freshwater wetland soils and export these nutrients into the adjacent coastal zone, contributing to coastal hypoxia.**

<u>Chapter 3:</u>

The rate of relative SLR in coastal Louisiana is roughly 13 mm yr^{-1}, which is a function of both eustatic sea level rise, coastal erosion, and tectonic downwarping (Church et al. 2013). These high rates result in increases in wetland submergence, particularly within Barataria Bay, LA, where wetlands (through a combination of processes) are being lost at rates of roughly 25.9 km^2 yr^{-1} (Penland et al. 2000). As these highly organic wetlands are lost through submergence and erosion, approximately 1-2 m of accumulated coastal peat soils are also lost through disarticulation of the soil structure. These organic peat soils can have three potential fates: a) reburial within the bay soils, b) export into the coastal ocean, and c) microbial mineralization. Chapter 3 addressed this bacterial mineralization component by assessing the potential mineralization rates of these organic soils, down to a depth of 1m at three separate sites.

Soils were subjected to one of two treatments, an anaerobic (to mimic an intact marsh) treatment or an aerobic (to mimic a submerging marsh) treatment and production of CO_2 was evaluated as well as other biogeochemical parameters. Within the aerobic treatment, CO_2 production was 66% greater than within the anaerobic treatment. Interestingly, CO_2 production and total C content also increased with depth, especially between 40-100 cm. The difference in CO_2 production between treatments (the expected mineralization effect) was roughly 4x greater at 90-100 cm than at the surface. **Results from this study suggest that as soils are disarticulated and exposed to oxygenated seawater through wetland submergence and erosion, there is a potential for a 66% increase in CO_2 emissions, relative to anaerobic conditions.** Specifically, if 25% of the organic C within the 1 m depth profile was mineralized, the result would be an annual release of approximately 8-11 Gg of C from this area of Barataria Bay alone.

<u>Chapter 4:</u>

The fate of organic matter disarticulated and lost through wetland submergence is partially dependent on the 'quality', or the elemental stoichiometry and molecular complexity, of the organic

matter itself. Following the paradigm of selective preservation, the soil organic matter that is stored within wetland soils should decrease in quality (i.e. increase in molecular complexity) with increasing depth (Sollins et al. 1996). As labile organic material is preferentially degraded, the soil organic matter that is buried should consist of highly degraded, refractory organic material. However, following the findings of the previous chapter, CO_2 production increased with depth, which would be contrary to this paradigm. Objective three evaluated the potential degradability of soil organic matter within the same study site (Barataria Bay, LA) to a depth of 150 cm by a combination of chemical fractionation of organic material, assessing stable isotope signatures, evaluating both total and bioavailable nutrient stores, and quantifying abundance of various microbial genes.

Combining total C content with $\delta^{13}C$ profiles allowed for the inference that the soil profile represented different depositional periods, alternating between clay layers and different marsh types. Contrary to the established paradigm of selective preservation, labile fractions only decreased 10% along the entire depth profile, while refractory portions increased 7%. This decreasing labile: refractory ratio, coupled with no change in C:N ratios and the increasing degree of decomposition ($\delta^{15}N$) indicate that **limited decomposition has taken place on stored soil organic matter, and thus the release of these stores through submergence would input easily degradable organic material into the water column where mineralization can take place and increase regional CO_2 emissions**. **These results provide evidence to begin a further investigation into the nature of soil organic matter stabilization and decomposition paradigms within wetland soils**. Furthermore, stores of NH_4^+ and SRP at depth were approximately 7x and 11x concentrations at the surface, representing **a store of bioavailable nutrients that could be released with wetland submergence and contribute to eutrophication and hypoxia within the coastal zone**.

Chapters 5 and 6:

Landward transgression occurs in coastal wetlands with a lack of adjacent upland development and moderate rates of relative sea level rise that exceed local accretion rates, and are often accompanied by shifting vegetation patterns. As vegetation dominance within the coastal plain is mediated by tolerance to environmental stressors such as salinity and inundation, SLR can cause vegetation communities to gradually migrate upslope. Similarly, more salt- and inundation- tolerance species can encroach along the coastal fringe. The combination of vegetative shifts and an altered physicochemical environment within these coastal wetlands can impact nutrient cycling and C storage within the region by disrupting key biogeochemical transformations. A seasonal survey of key biogeochemical indicators along a transect of mangrove encroachment into saltmarsh (Chapter 5) and herbaceous encroachment into herbaceous marsh (Chapter 6) was conducted to determine how these indicators shift in response to changes in species dominance.

Along the mangrove-salt marsh ecotone, **soil biogeochemical indicators were found to shift in advance of full mangrove dominance**, as the transition zone (co-occurring species) functioned similarly to the mangrove zones. Unexpectedly, **soil nutrient content was greater within the saltgrass zones than within mangrove zones**, and **soil CO_2 production did not change with vegetation type**. In contrast, the **herbaceous encroachment of saltgrass into previously cordgrass-dominated marsh enhanced soil C and N content**, **and encroachment accelerated soil C cycling and C storage**. Within both systems, **vegetation shifts were found to co-occur with shifts in inundation in salinity**.

Future Directions

Together, conclusions from these five studies represent a holistic investigation of how biogeochemical transformations are altered within coastal systems experiencing SLR-induced transitions. Through both experimental and field-based studies, this dissertation fills critical knowledge gaps within the scientific literature concerning how coastal wetland function will be impacted by SLR. To further

understand the effects of SLR on key biogeochemical transformations within coastal wetland systems, I recommend the following research objectives:

- Scaling up the experimental study conducted in chapter 1 to include assessing the long-term impacts of increased salinity on different freshwater wetland soil types on nutrient dynamics, as well as:

  o Understanding the effects to microbial community composition and expression of various genes required for decomposition,

  o Incorporating an understanding of how pulsing events (i.e. king tides, storm surge) can affect biogeochemical processing and microbial community structure in the short term,

  o Assessing these objectives within a field-based study that incorporates vegetation,

- Investigating the molecular complexity of soil organic matter and decomposition processes within wetland soils and leveraging a new paradigm to explain how decomposition and stabilization of organic matter occurs within wetland systems,

- Disentangling the combination of salinity, inundation, and vegetation shifts on biogeochemical transformations with different coastal wetland types.

APPENDIX: SUPPLEMENTARY TABLES

Supplementary Table 1: Correlation matrices for both high water samplings. For each matrix, n=81, α = 0.05, critical value = 0.217. Cells with a dash are not statistically significant.

HIGH WATER	pH	Moisture Content	Organic Matter	Total C	Total N	Total P	Ext. NO_3^-	Ext. NH_4^+	Ext. SRP	PMN Rate	PMP Rate	MBC	CO_2 Production	NAG	AP	BG	XY	CB
Moisture Content	-																	
Organic Matter	-0.34	0.89																
Total C	-0.42	0.86	0.96															
Total N	-0.39	0.86	0.96	0.99														
Total P	-	0.82	0.86	0.81	0.83													
Ext. NO_3^-	-	0.42	0.35	0.37	0.33	0.32												
Ext. NH_4^+	0.42	-	-	-	-	-	-											
Ext. SRP	-	0.49	0.51	0.46	0.47	0.57	-	0.36										
PMN Rate	-0.24	0.51	0.54	0.54	0.56	0.49	-	-	0.32									
PMP Rate	-	0.38	0.45	0.43	0.43	0.50	0.26	-	0.29	0.45								
MBC	-	-	-	-	-	-	-	-	-	-	-							
CO_2 Production	-	0.45	0.43	0.41	0.42	0.58	-	-	0.35	0.45	0.66	-						
NAG	-	0.44	0.37	0.32	0.35	0.52	0.34	0.48	0.59	0.37	0.32	-	0.38					
AP	-	0.63	0.58	0.56	0.56	0.53	0.35	-	0.45	0.33	0.28	-	0.31	0.55				
BG	-	0.49	0.50	0.44	0.46	0.68	-	-	0.59	0.39	0.47	-	0.54	0.75	0.54			
XY	-	0.79	0.81	0.74	0.75	0.83	0.24	-	0.67	0.55	0.52	-	0.56	0.64	0.66	0.72		
CB	-	0.54	0.51	0.38	0.39	0.63	-	-	0.59	0.37	0.39	-	0.42	0.66	0.58	0.79	0.74	
AS	-	0.73	0.69	0.62	0.63	0.76	0.30	0.24	0.62	0.43	0.48	-	0.59	0.70	0.73	0.80	0.84	0.74

Supplementary Table 2: Correlation matrices for both low water samplings. For each matrix, n=81, $\alpha = 0.05$, critical value = 0.217. Cells with a dash are not statistically significant.

LOW WATER	pH	Moisture Content	Organic Matter	Total C	Total N	Total P	Ext. NO_3^-	Ext. NH_4^+	Ext. SRP	PMN	PMP	MBC	CO_2 Production	NAG	AP	BG	XY	CB
Moisture Content	-0.39																	
Organic Matter	-0.45	0.78																
Total C	-0.42	0.77	0.99															
Total N	-0.36	0.73	0.94	0.95														
Total P	-0.25	0.62	0.84	0.81	0.84													
Ext. NO_3^-	-0.38	0.38	0.59	0.61	0.61	0.57												
Ext. NH_4^+	-	0.22	-	-	-	-	0.22											
Ext. SRP	-0.44	0.54	0.65	0.64	0.63	0.60	0.60	-										
PMN Rate	-0.38	0.56	0.70	0.70	0.70	0.78	0.69	-	0.66									
PMP Rate	-	0.30	0.38	0.50	0.47	0.53	0.54	0.30	0.42	0.68								
MBC	-	0.45	0.47	0.46	0.30	0.34	0.46	0.57	0.34	0.40	0.39							
CO_2 Production	-0.37	0.51	0.64	0.63	0.64	0.66	0.56	-	0.60	0.72	0.47	0.29						
NAG	-0.43	0.61	0.60	0.59	0.60	0.59	0.44	-	0.61	0.59	0.45	0.32	0.56					
AP	-0.47	0.73	0.71	0.70	0.69	0.57	0.30	-	0.47	0.55	0.22	0.27	0.48	0.72				
BG	-0.39	0.51	0.53	0.53	0.54	0.58	0.49	-	0.56	0.70	0.60	0.36	0.54	0.87	0.59			
XY	-0.43	0.69	0.75	0.75	0.75	0.65	0.65	-	0.64	0.72	0.46	0.45	0.56	0.83	0.75	0.80		
CB	-0.29	0.55	0.54	0.54	0.55	0.55	0.47	0.26	0.50	0.67	0.59	0.47	0.47	0.82	0.57	0.95	0.82	
AS	-0.39	0.79	0.79	0.79	0.79	0.73	0.50	-	0.63	0.73	0.43	0.42	0.63	0.83	0.83	0.79	0.87	0.80

Supplementary Table 3: Correlation matrix for wet season sampling, where degrees of freedom = 80, alpha = 0.01, and critical value = 0.283. Bold values indicate positive correlations while italicized values indicate negative correlations. – indicates non-significant correlation. Note that the TC, TN, TP, and OM were only analyzed during dry season, but applied to both tables as pilot data indicated no change in long-term soil nutrient pools between seasons.

WET SEASON	Moisture Content	Bulk Density	Ext. Nitrate	Ext. NH$_4^+$	Ext. SRP	PMN Rate	PMP Rate	MBC	CO$_2$ Rate	NAG	AP	BG	XY	CB	TC	TN	OM
Bulk Density	*-0.98*																
Ext. Nitrate	-	-															
Ext. Ammonium	**0.79**	*-0.71*	-														
Ext. SRP	**0.77**	*-0.69*	-	**0.84**													
PMN Rate	**0.63**	*-0.57*	-	**0.73**	**0.74**												
PMP Rate	**0.56**	*-0.49*	-	**0.79**	**0.71**	**0.93**											
MBC	**0.84**	*-0.77*	-	**0.78**	**0.82**	**0.64**	**0.59**										
CO$_2$ Rate	**0.60**	*-0.52*	-	**0.77**	**0.73**	**0.72**	**0.74**	**0.65**									
NAG	**0.70**	*-0.63*	-	**0.75**	**0.87**	**0.72**	**0.74**	**0.79**	**0.75**								
AP	**0.71**	*-0.63*	-	**0.81**	**0.85**	**0.75**	**0.78**	**0.74**	**0.79**	**0.93**							
BG	**0.52**	*-0.46*	-	**0.66**	**0.78**	**0.67**	**0.72**	**0.67**	**0.60**	**0.93**	**0.84**						
XY	**0.73**	*-0.66*	-	**0.75**	**0.83**	**0.73**	**0.73**	**0.78**	**0.72**	**0.96**	**0.91**	**0.88**					
CB	**0.70**	*-0.61*	-	**0.78**	**0.86**	**0.75**	**0.78**	**0.78**	**0.73**	**0.96**	**0.92**	**0.92**	**0.96**				
Total N	**0.89**	*-0.82*	-	**0.84**	**0.88**	**0.74**	**0.69**	**0.86**	**0.70**	**0.77**	**0.76**	**0.61**	**0.78**	**0.76**			
Total C	**0.89**	*-0.82*	-	**0.81**	**0.87**	**0.73**	**0.66**	**0.86**	**0.68**	**0.77**	**0.75**	**0.60**	**0.78**	**0.76**	**0.99**		
Organic Matter	**0.62**	*-0.61*	-	**0.52**	**0.71**	**0.49**	**0.44**	**0.54**	**0.49**	**0.61**	**0.60**	**0.49**	**0.59**	**0.54**	**0.67**	**0.69**	
Total P	-	-	-	**0.34**	**0.31**	**0.28**	**0.41**	-	**0.32**	**0.37**	**0.40**	**0.37**	**0.36**	**0.38**	-	-	**0.32**

Supplementary Table 4: Correlation matrix for dry season sampling, where degrees of freedom = 80, alpha = 0.01, and critical value = 0.283. Bold values indicate positive correlations while italicized values indicate negative correlations. – indicates non-significant correlation. Note that the TC, TN, TP, and OM were only analyzed during dry season, but applied to both tables as pilot data indicated no change in long-term soil nutrient pools between seasons.

DRY SEASON	Moisture Content	Bulk Density	Ext. Nitrate	Ext. NH4+	Ext. SRP	PMN Rate	PMP Rate	MBC	CO2 Rate	NAG	AP	BG	XY	CB	TC	TN	OM
Bulk Density	*-0.98*																
Ext. Nitrate	**0.45**	*-0.42*															
Ext. Ammonium	*-0.50*	**0.49**	*-0.44*														
Ext. SRP	-	-	**0.76**	*-0.32*													
PMN Rate	**0.31**	-	-	-													
PMP Rate	**0.59**	*-0.54*	**0.74**	*-0.43*	**0.48**												
MBC	**0.81**	*-0.77*	**0.57**	*-0.45*	**0.29**	-	**0.71**										
CO2 Rate	**0.52**	*-0.49*	**0.54**	*-0.29*	**0.40**	-	**0.63**	**0.55**									
NAG	**0.57**	*-0.51*	**0.34**	*-0.32*	-	-	**0.61**	**0.58**	**0.37**								
AP	**0.68**	*-0.61*	**0.63**	*-0.44*	**0.35**	-	**0.82**	**0.70**	**0.60**	**0.77**							
BG	**0.54**	*-0.49*	**0.54**	*-0.39*	**0.34**	-	**0.78**	**0.63**	**0.47**	**0.85**	**0.85**						
XY	**0.60**	*-0.58*	**0.32**	-	-	-	**0.41**	**0.64**	**0.38**	**0.63**	**0.56**	**0.59**					
CB	**0.39**	*-0.35*	**0.42**	*-0.29*	-	-	**0.63**	**0.50**	**0.35**	**0.81**	**0.74**	**0.93**	**0.54**				
Total N	**0.79**	*-0.77*	**0.67**	*-0.48*	**0.49**	-	**0.72**	**0.81**	**0.65**	**0.52**	**0.67**	**0.62**	**0.57**	**0.48**			
Total C	**0.79**	*-0.77*	**0.66**	*-0.48*	**0.49**	-	**0.71**	**0.80**	**0.64**	**0.52**	**0.65**	**0.61**	**0.60**	**0.47**	**0.99**		
Organic Matter	**0.68**	*-0.68*	**0.68**	*-0.42*	**0.49**	-	**0.64**	**0.69**	**0.59**	**0.35**	**0.56**	**0.48**	**0.50**	**0.31**	**0.83**	**0.84**	
Total P	-	-	-	-	-	-	**0.41**	**0.28**	**0.39**	-	**0.28**	**0.30**	-	-	-	-	**0.32**

LIST OF REFERENCES

Amthor, J.S., Huston, M.A., 1998. Terrestrial Ecosystem Responses to Global Change: A Research Strategy. ORNL Oak Ridge National Laboratory (US).

Andersen JM (1976) An ignition method for determination of total phosphorus in lake sediments. Water Res 10:329–331. doi: 10.1016/0043-1354(76)90175-5

Ardón M, Helton AM, Bernhardt ES (2016) Drought and saltwater incursion synergistically reduce dissolved organic carbon export from coastal freshwater wetlands. Biogeochemistry 127:411–426. doi: 10.1007/s10533-016-0189-5

Ardón M, Morse JL, Colman BP, Bernhardt ES (2013) Drought-induced saltwater incursion leads to increased wetland nitrogen export. Glob Chang Biol 19:2976–85. doi: 10.1111/gcb.12287

Baldwin DS, Rees GN, Mitchell AM, et al (2006) The Short-Term Effects of Salinization on Anaerobic Nutrient Cycling and Microbial Community Structure in Sediment from a Freshwater Wetland. Wetlands 26:455–464.

Bartlett KB, Bartlett DS, Harriss RC, Sebacher DI (1987) Methane emissions along a salt marsh salinity gradient. Biogeochemistry 4:183–202. doi: 10.1007/BF02187365

Baumann, R.H., Day, J.W.J., Miller, C.A., 1984. Mississippi deltaic wetland survival-sedimentation versus coastal submergence. Science (80-.). 224, 1093–1095.

Bedford, B. L., Walbridge, M. R. and Aldous, A. (1999), Patterns in nutrient availability and plant diversity of temperate North American wetlands. Ecology, 80: 2151–2169. doi:10.1890/0012-9658

Beltman B, Rouwenhorst TG, Van Kerkhoven MB, et al (2000) Internal eutrophication in peat soils through competition between chloride and sulphate with phosphate for binding sites. Biogeochemistry 50:183–194. doi: 10.1023/A:1006374018558

Bianchi, T.S., Dimarco, S.F., Allison, M.A., Chapman, P., Cowan, J.H., Hetland, R.D., Morse, J.W., Rowe, G., 2008. Controlling Hypoxia on the U.S. Louisiana Shelf: Beyond the Nutrient-Centric View. Eos, Trans. Am. Geophys. Union 89, 236–237. doi:10.1029/2008EO260005

Blume, E., Bischoff, M., Reichert, J.M., Moorman, T., Konopka, A., Turco, R.F., 2002. Surface and subsurface microbial biomass, community structure and metabolic activity as a function of soil depth and season. Appl. Soil Ecol. 20, 171–181.

Boon P, Mitchell A (1995) Methanogenesis in the sediments of an Australian freshwater wetland: Comparison with aerobic decay, and factors controlling methanogenesis. FEMS Microbiology Ecology 18:175-190. doi: 10.1111/j.1574-6941.1995.tb00175.x

Boström B, Andersen JM, Fleischer S, Jansson M (1988) Exchange of Phosphorus Across the Sediment-Water Interface. In: Persson G, Jansson M (eds) Phosphorus in Freshwater Ecosystems: Proceedings of a Symposium held in Uppsala, Sweden, 25--28 September 1985. Springer Netherlands, Dordrecht, pp 229–244

Brady NC, Weil RR (2010) Elements of the Nature and Properties of Soils. Pearson Education.

Bridgham, S.D., Updegraff, K., Pastor, J., 1998. Carbon, nitrogen, and phosphorus mineralization in northern wetlands. Ecology 79, 1545–1561.

Brinson, M.M., Christian, R.R., Blum, L.K., Estuaries, S., Odum, W.E., Symposium, M., Blum, L.K., 2018. Multiple States in the Sea-Level Induced Transition from Terrestrial Forest to Estuary Linked references are available on JSTOR for this article : Multiple States in the Sea-Level Induced Transition From Terrestrial 18, 648–659.

Brix, H., 1987. Treatment of wastewater in the rhizosphere of wetland plants–the root-zone method. Water Sci. Technol. 19, 107–118.

Capone, Douglas G., and Ronald P. Kiene. "Comparison of microbial dynamics in marine and freshwater sediments: Contrasts in anaerobic carbon catabolism." Limnology and Oceanography 33.4 (1988): 725-749.

Chambers LG, Davis SE, Troxler T, et al (2014) Biogeochemical effects of simulated sea level rise on carbon loss in an Everglades mangrove peat soil. Hydrobiologia 726:195–211. doi: 10.1007/s10750-013-1764-6

Chambers LG, Osborne TZ, Reddy KR (2013) Effect of salinity-altering pulsing events on soil organic carbon loss along an intertidal wetland gradient : a laboratory experiment. Biogeochemistry 363–383. doi: 10.1007/s10533-013-9841-5

Chambers LG, Reddy KR, Osborne TZ (2011) Short-Term Response of Carbon Cycling to Salinity Pulses in a Freshwater Wetland. Soil Sci Soc Am J. doi: 10.2136/sssaj2011.0026

Church J A, Clark PU, Cazenave a., et al (2013) Sea level change. Clim Chang 2013 Phys Sci Basis Contrib Work Gr I to Fifth Assess Rep Intergov Panel Clim Chang 1137–1216. doi: 10.1017/CBO9781107415315.026

Church, J.A., Clark, P.U., Cazenave, A., Gregory, J.M., Jevrejeva, S., Levermann, A., Merrifield, M.A., Milne, G.A., Nerem, R.S., Nunn, P.D., 2013. Sea level change. PM Cambridge University Press.

Conner, W., Day, J.W., 1987. The ecology of Barataria Basin, Louisiana: an estuarine profile.

DeBusk, W.F., Reddy, K.R., 1998. Turnover of detrital organic carbon in a nutrient-impacted Everglades marsh. Soil Sci. Soc. Am. J. 62, 1460–1468.

Delaune, R.D., 1986. The use of 613C signature of C-3 and C-4 plants in determining past depositional enviornments in rapidly accreting marshes of the Mississippi River 59, 315–320.

DeLaune, R.D., Lindau, C.W., 1987. δ13C signature of organic carbon in estuarine bottom sediment as an indicator of carbon export from adjacent marshes. Biogeochemistry 4, 225–230. doi:10.1007/BF02187368

DeLaune, R.D., Pezeshki, S.R., 2003. The role of soil organic carbon in maintaining surface elevation in rapidly subsiding US Gulf of Mexico coastal marshes. Water, Air, Soil Pollut. Focus 3, 167–179.

Delaune, R.D., Reddy, C.N., Patrick, W.H., 1981. Accumulation of Plant Nutrients and Heavy Metals through Sedimentation Processes and Accretion in a Louisiana Salt Marsh 4, 328–334.

DeLaune, R.D., White, J.R., 2012. Will coastal wetlands continue to sequester carbon in response to an increase in global sea level?: A case study of the rapidly subsiding Mississippi river deltaic plain. Clim. Change 110, 297–314. doi:10.1007/s10584-011-0089-6

Fierer, N., Schimel, J.P., Holden, P.A., 2003. Variations in microbial community composition through two soil depth profiles. Soil Biol. Biochem. 35, 167–176.

Gale, P.M., Gilmour, J.T., 1988. Net Mineralization of Carbon and Nitrogen Under Aerobic and Anaerobic Conditions. Soil Sci. Soc. Am. J. 52, 1006–1010. doi:10.2136/sssaj1988.03615995005200040019x

Gardner LR, Michener WK, Blood ER, et al (1991) Ecological impact of Hurricane Hugo—Salinization of a coastal forest. J Coast Res Special Is:301–317. doi: 10.2307/25735423

Gardner, L.M., White, J.R., 2010. Denitrification enzyme activity as an indicator of nitrate movement through a diversion wetland. Soil Sci. Soc. Am. J. 74, 1037–1047.

German, D.P., Weintraub, M.N., Grandy, A.S., Lauber, C.L., Rinkes, Z.L., Allison, S.D., 2011. Optimization of hydrolytic and oxidative enzyme methods for ecosystem studies. Soil Biol. Biochem. 43, 1387–1397. doi:https://doi.org/10.1016/j.soilbio.2011.03.017

Gribsholt B, Kristensen E (2002) Impact of sampling methods on sulfate reduction rates and dissolved organic carbon (DOC) concentrations in vegetated salt marsh sediments. Wetl Ecol Manag 10:371–379. doi: 10.1023/A:1020940314010

Harvey, J.W., Germann, P.F., Odum, W.E., 1987. Geomorphological control of subsurface hydrology in the creekbank zone of tidal marshes. Estuar. Coast. Shelf Sci. 25, 677–691. doi:https://doi.org/10.1016/0272-7714(87)90015-1

Hatton, R.S., Delaune, R.D., Patrick, W.H.J., 1983. Sedimentation, accretion, and subsidence in marshes of Barataria Basin, Louisiana. Limnol. Oceanogr. 28, 494–502. doi:10.4319/lo.1983.28.3.0494

Hemminga MA, Buth GJC (1991) Decomposition in salt marsh ecosystems of the S.W. Netherlands: the effects of biotic and abiotic factors. Vegetatio 92:73–83. doi: 10.1007/BF00047133

Herbert ER, Boon P, Burgin AJ, et al (2015) A global perspective on wetland salinization: ecological consequences of a growing threat to freshwater wetlands. Ecosphere 6:art206. doi: 10.1890/ES14-00534.1

Huettel, M., Ziebis, W., Forster, S., Luther, G.W., 1998. Advective Transport Affecting Metal and Nutrient Distributions and Interfacial Fluxes in Permeable Sediments. Geochim. Cosmochim. Acta 62, 613–631. doi:https://doi.org/10.1016/S0016-7037(97)00371-2

Hussein, A.H., 2009. Modeling of Sea-Level Rise and Deforestation in Submerging Coastal Ultisols of Chesapeake Bay. Soil Sci. Soc. Am. J. 73, 185–196. doi:10.2136/sssaj2006.0436

IPCC, 2014: Climate Change 2014: Synthesis Report. Contribution of Working Groups I, II, and III to the Fifth Assessment Report of the Intergovernmental Panel on Climate Change [Core Writing Team, R.K. Pachauri and L.A. Meyer (eds.)]. IPCC, Geneva, Switzerland, 151 pp.

Jun M, Altor AE, Craft CB (2013) Effects of Increased Salinity and Inundation on Inorganic Nitrogen Exchange and Phosphorus Sorption by Tidal Freshwater Floodplain Forest Soils, Georgia (USA). Estuaries and Coasts 36:508–518. doi: 10.1007/s12237-012-9499-6

Kelleway, J.J., Cavanaugh, K., Rogers, K., Feller, I.C., Ens, E., Doughty, C., Saintilan, N., 2017. Review of the ecosystem service implications of mangrove encroachment into salt marshes. Glob. Chang. Biol. 23, 3967–3983. doi:10.1111/gcb.13727

Kirwan, M.L., Megonigal, J.P., 2013. Tidal wetland stability in the face of human impacts and sea-level rise. Nature 504, 53.

Lamers LPM, Falla S-J, Samborska EM, et al (2002) Factors controlling the extent of eutrophication and toxicity in sulfate-polluted freshwater wetlands. Limnol Oceanogr 47:585–593. doi: 10.4319/lo.2002.47.2.0585

Levine, B.M., White, J.R., DeLaune, R.D., 2017. Impacts of the long-term presence of buried crude oil on salt marsh soil denitrification in Barataria Bay, Louisiana. Ecol. Eng. 99, 454–461.

Mackie, E.A.V., Leng, M.J., Lloyd, J.M., Arrowsmith, C., 2005. Bulk organic δ13C and C/N ratios as palaeosalinity indicators within a Scottish isolation basin. J. Quat. Sci. 20, 303–312. doi:10.1002/jqs.919

Maltby, E., 1988. Cotton Strip Assay: An Index of Decomposition in Soils 129–130.

Mann, C.J., Wetzel, R.G., 1995. Dissolved organic carbon and its utilization in a riverine wetland ecosystem. Biogeochemistry 31, 99–120.

Marton JM, Herbert ER, Craft CB (2012) Effects of salinity on denitrification and greenhouse gas production from laboratory-incubated tidal forest soils. Wetlands 32:347–357. doi: 10.1007/s13157-012-0270-3

Marton, J.M., Roberts, B.J., 2014. Spatial variability of phosphorus sorption dynamics in Louisiana salt marshes. J. Geophys. Res. Biogeosciences 119, 451–465.

McLatchey, G.P., Reddy, K.R., 1998. Regulation of Organic Matter Decomposition and Nutrient Release in a Wetland Soil. J. Environmenal Qual. doi:10.2134/jeq1998.00472425002700050036x

Melillo, J.M., Aber, J.D., Linkins, A.E., Ricca, A., Fry, B., Nadelhoffer, K.J., 1989. Carbon and nitrogen dynamics along the decay continuum: plant litter to soil organic matter. Plant Soil 115, 189–198.

Mendelssohn, I.A., Sorrell, B.K., Brix, H., Schierup, H.H., Lorenzen, B., Maltby, E., 1999. Controls on soil cellulose decomposition along a salinity gradient in a Phragmites australis wetland in Denmark. Aquat. Bot. 64, 381–398. doi:10.1016/S0304-3770(99)00065-0

Michener WK, Blood ER, Bildstein KL, et al (1997) Climate Change , Hurricanes and Tropical Storms , and Rising Sea Level in Coastal Wetlands. Ecol Appl 7:770–801. doi: 10.1890/1051-0761

Morrissey EM, Gillespie JL, Morina JC, Franklin RB (2014) Salinity affects microbial activity and soil organic matter content in tidal wetlands. Glob Chang Biol 20:1351–1362. doi: 10.1111/gcb.12431

Neubauer SC, Franklin RB, Berrier DJ (2013) Saltwater intrusion into tidal freshwater marshes alters the biogeochemical processing of organic carbon. Biogeosciences 10:8171–8183. doi: 10.5194/bg-10-8171-2013

Nicholls RJ, Hoozemans FMJ, Marchand M (1999) Increasing flood risk and wetland losses due to global sea-level rise: Regional and global analyses. Glob Environ Chang. doi: 10.1016/S0959-3780(99)00019-9

Noe GB, Krauss KW, Lockaby BG, et al (2013) The effect of increasing salinity and forest mortality on soil nitrogen and phosphorus mineralization in tidal freshwater forested wetlands. Biogeochemistry 114:225–244. doi: 10.1007/s10533-012-9805-1

Nyman, J. a. A., Delaune, R.D.D., Patrick, W.H.H., 1990. Wetland soil formation in the rapidly subsiding Mississippi River delatic plain- mineral and organic-matter relationships. Estuar. Coast. Shelf Sci. 31, 57–69. doi:10.1016/0272-7714(90)90028-P

Odum, E.P., 1968. Energy flow in ecosystems: a historical review. Am. Zool. 8, 11–18.

Osgood, D.T., 2000. Subsurface hydrology and nutrient export from barrier island marshes at different tidal ranges. Wetl. Ecol. Manag. 8, 133–146. doi:10.1023/A:1008488317880

Ouyang, X., Lee, S.Y., 2014. Updated estimates of carbon accumulation rates in coastal marsh sediments. Biogeosciences 11, 5057–5071. doi:10.5194/bg-11-5057-2014

Penland, S., Wayne, L., Britsch, D., Williams, S.J., Beall, A.D., Butterworth, V., 2000. Process Classification of Coastal Land Loss between 1932 and 1990 in the Mississippi River Delta Plain, Southeastern Louisiana USGS, 1.

Pietroski, J.P., White, J.R., DeLaune, R.D., Wang, J.J., Dodla, S.K., 2015. Fresh and weathered crude oil effects on potential denitrification rates of coastal marsh soil. Chemosphere 134, 120–126.

Poffenbarger HJ, Needelman BA, Megonigal JP (2011) Salinity influence on methane emissions from tidal marshes. Wetlands 31:831–842. doi: 10.1007/s13157-011-0197-0

Rakocinski, C.F., Baltz, D.M., Fleeger, J.W., 1992. Correspondence between environmental gradients and the community structure of marsh-edge fishes in a Louisiana estuary. Mar. Ecol. Prog. Ser. 135–148.

Reddy KR, DeLaune RD (2008) Biogeochemistry of Wetlands: Science and Applications. CRC Press

Reddy KR, Kadlec RH, Flaig E, Gale PM (1999) Phosphorus retention in streams and wetlands: a review. Crit Rev Environ Sci Technol 29:83–146. doi: 10.1080/10643389991259182

Reddy, K.R., DeLaune, R.D., 2008. Biogeochemistry of Wetlands: Science and Applications. CRC Press.

Reddy, K.R., Kadlec, R.H., Flaig, E., Gale, P.M., 1999. Phosphorus retention in streams and wetlands: a review. Crit. Rev. Environ. Sci. Technol. 29, 83–146. doi:10.1080/10643389991259182

Reddy, K.R., Patrick, W.H., Lindau, C.W., 1989. Nitrification-denitrification at the plant root-sediment interface in wetlands. Limnol. Oceanogr. 34, 1004–1013.

Roden EE, Wetzel RG (1996) Organic carbon oxidation and suppression of methane production by microbial Fe(III) oxide reduction in vegetated and unvegetated freshwater wetland sediments. Limnol Oceanogr 41:1733–1748. doi: 10.4319/lo.1996.41.8.1733

Roy ED, White JR (2013) Measurements of Nitrogen Mineralization Potential in Wetland Soils. In: Methods in Biogeochemistry of Wetlands. Soil Science Society of America, Madison, WI, pp 465–471

Rysgaard S, Thastum P, Dalsgaard T, et al (1999) Effects of Salinity on NH4+ Adsorption Capacity, Nitrification and Denitrification in Danish Estuarine Sediments. Estuaries 22:21–30. doi: 10.2307/1352923

Schipper, L. a, Mcleod, M., Scott, N., Clarkson, B., Smith, J., Campbell, D., 2002. Subsidence rates and carbon loss in peat soils following conversion to pasture in the Waikato Region , New Zealand. Soil Use Manag. 18, 91–93. doi:10.1079/SUM2001106

Schipper, L.A., Reddy, K.R., 1995. In Situ Determination of Detrital Breakdown in Wetland Soil-Floodwater Profile. Soil Sci. Soc. Am. J. 1437, 565–568. doi:10.1126/science.1146511

Seitzinger SP, Gardner WS, Spratt a K (1991) The effects of salinity on ammomium sorption in aquatic sediments- Implications for benthic nutrient recycling. Estuaries 14:167–174. doi: 10.2307/1351690

Sholkovitz, E.R. 1976. Flocculation of dissolved organic and inorganic matter during the mixing of river water and sea water. Geochim Cosmochim Acta 40:931-845.

Smith, C.J., De Laune, R.D., 1983. Nitrogen loss from freshwater and saline estuarine sediments. J. Environ. Qual. 12, 514–518.

Stevenson, F.J., Cole, M.A., 1999. Cycles of soils: carbon, nitrogen, phosphorus, sulfur, micronutrients. John Wiley & Sons.

Stumm, Werner, and James J. Morgan. Aquatic Chemistry: Chemical Equilibria and Rates in Natural Waters. New York: Wiley, 1996.

Sundareshwar P V., Morris JT (1999) Phosphorus sorption characteristics of intertidal marsh sediments along an estuarine salinity gradient. Limnol Oceanogr 44:1693–1701. doi: 10.4319/lo.1999.44.7.1693

Taillefert, M., Neuhuber, S., Bristow, G., 2007. The effect of tidal forcing on biogeochemical processes in intertidal salt marsh sediments. Geochem. Trans. 8, 6.

Tiedje, J.M., 1982. Denitrification. Methods Soil Anal. Part 2. Chem. Microbiol. Prop. 1011–1026.

Turner, R. E., and R. L. Allen (1982). "Bottom water oxygen concentration in the Mississippi River Delta Bight." Contributions in Marine Science 25: 161-172.

Turner, R.E., Rabalais, N.N., 1991. Changes in Mississippi River water quality this century. Bioscience 41, 140–147.

Updegraff, K., Pastor, J., Bridgham, S.D., Johnston, C.A., 1995. Environmental and substrate controls over carbon and nitrogen mineralization in northern wetlands. Ecol. Appl. 5, 151–163.

US Environmental Protection Agency, 1993. Methods for the determination of inorganic substances in environmental samples. EPA/600/R-93/100. Washington, DC.

van Dijk G, Smolders AJP, Loeb R, et al (2015) Salinization of coastal freshwater wetlands; effects of constant versus fluctuating salinity on sediment biogeochemistry. Biogeochemistry 126:71–84. doi: 10.1007/s10533-015-0140-1

Vance ED, Brookes PC, Jenkinson DS (1987) An extraction method for measuring soil microbial biomass C. Soil Biol Biochem 19:703–707. doi: 10.1016/0038-0717(87)90052-6

Vance, E.D., Brookes, P.C., Jenkinson, D.S., 1987. An extraction method for measuring soil microbial biomass C. Soil Biol. Biochem. 19, 703–707.

Webster, J.R., Benfield, E.F., 1986. Vascular Plant Breakdown in Freshwater Ecosystems. Annu. Rev. Ecol. Syst. 17, 567–594.

Weston NB, Dixon RE, Joye S (2006) Ramifications of increased salinity in tidal freshwater sediments: Geochemistry and microbial pathways of organic matter mineralization. J Geophys Res 111:14. doi: G01009 10.1029/2005jg000071

Weston NB, Neubauer SC, Velinsky DJ, Vile MA (2014) Net ecosystem carbon exchange and the greenhouse gas balance of tidal marshes along an estuarine salinity gradient. Biogeochemistry 163–189. doi: 10.1007/s10533-014-9989-7

Weston NB, Vile M A., Neubauer SC, Velinsky DJ (2011) Accelerated microbial organic matter mineralization following salt-water intrusion into tidal freshwater marsh soils. Biogeochemistry 102:135–151. doi: 10.1007/s10533-010-9427-4

White, J.R., DeLaune, R.D., Li, C.Y., Bentley, S.J., 2009. Sediment Methyl and Total Mercury Concentrations Along the Georgia and Louisiana Inner Shelf, USA. Anal. Lett. 42, 1219–1231. doi:10.1080/00032710902901947